

# Steenrod square for virtual links toward Khovanov-Lipshitz-Sarkar stable homotopy type for virtual links

Louis H. Kauffman and Eiji Ogasa

**Abstract.** We define a second Steenrod square for virtual links, which is stronger than Khovanov homology for virtual links, toward constructing Khovanov-Lipshitz-Sarkar stable homotopy type for virtual links. This induces the first meaningful nontrivial example of the second Steenrod square operator on the Khovanov homology for links in a 3-manifold other than  $S^3$ .

## CONTENTS

<b>Part 1. Introduction</b>	2
1. Main result	2
2. Making a CW complex from a given chain complex	3
3. Strategy of the construction of CW complexes for virtual links	6
<b>Part 2. Review of Khovanov homology for virtual links</b>	6
4. Virtual knots and virtual links	6
5. Khovanov homology for virtual links	10
6. An example of Khovanov basis of the Khovanov chain complex for a virtual link diagram	31
<b>Part 3. Khovanov-Lipshitz-Sarkar CW complexes and the second Steenrod square for virtual links</b>	31
7. Framed flow category: framings, modulis, and CW complexes	31
8. The ladybug configuration for classical link diagrams	33
9. Ladybug configurations and quasi-ladybug configurations for virtual link diagrams	38
10. Why is it more difficult to define Khovanov-Lipshitz-Sarkar stable homotopy type for virtual links than for classical links?	43
11. Our strategy of the construction of the second Steenrod square for virtual links	46
12. 0-dimensional modulis and framings	49
13. 1-dimensional modulis and framings	49
14. 2-dimensional modulis and framings	50
15. 3-dimensional modulis and framings	55
16. Review of the first Steenrod square operator $Sq^1$	57
17. Review of the second Steenrod square operator $Sq^2$	58
18. The second Steenrod square operator for virtual links	59
19. Our second Steenrod square does not depend on modulis or framings	62

20. Reidemeister moves do not change our second Steenrod square	65
21. Sub CW complexes	68
22. Open problems	75
References	80

## Part 1. Introduction

### 1. MAIN RESULT

In this paper we define a second Steenrod square operator acting on Khovanov homology for virtual links. This induces the first meaningful nontrivial example of the second Steenrod square operator on the Khovanov homology for links in a 3-manifold other than  $S^3$  (see §22). Our work extends the work of Lipshitz and Sarkar [29, 31] and Seed [53] (See the part above Theorem 5.1 and Theorem 5.1 in §5). It also raises many new questions about extending more fully their work on Khovanov-Lipshitz-Sarkar stable homotopy type. The list of contents for the paper given above shows the structure of this paper. In §4 we review the basics of virtual knot theory. In this paper we consider Khovanov homology for virtual links defined by Manturov [37]. We review its definition in §5, which is self-contained. See the part below Theorem 5.1 for other versions of Khovanov homology for virtual links. In §22 we explain why virtual knot theory is important for research on the Jones polynomial, Khovanov homology, and Khovanov homotopy, and describe key relationships of virtual knot theory with problems in low dimensional topology.

We state our main theorem, which follows from “Theorem 20.1 with Definition 21.2”, Theorem 21.3, and Theorem 21.4.

**Main Theorem 1.1.** (1) *We define the second Steenrod square operator for virtual links.*  
(2) *If  $L$  is a classical link diagram, our second Steenrod square is the same as the second Steenrod square in the case of classical links which is defined in [31].*  
(3) *In the case of non-classical, virtual links, the second Steenrod square is stronger than Khovanov homology. That is, there is a pair of non-classical, virtual links that have different second Steenrod square operators while they have the same Khovanov homology.*

The paper consists of two main parts. Part 2 is a review and technical definition of Khovanov homology of links and virtual links. If the reader is already familiar with these theories, this part will be useful for reference. It is important for the reader to understand that single-cycle resmoothings can occur in virtual link theory and that these lead to the differences between classical and virtual Khovanov homology. Part 3 consists in the work needed to prove the main results of the paper and uses the constructions in Part 2.

## 2. MAKING A CW COMPLEX FROM A GIVEN CHAIN COMPLEX

We will make a CW complex from a Khovanov chain complex for a given virtual link diagram. However we begin by discussing chain complexes that are not necessarily a Khovanov chain complex for classical links or virtual links.

Suppose that we are given a chain complex whose basis is a set  $\{g_i\}$ , where  $\{i\}$  is a finite set. Note that the given chain complex is not necessarily a Khovanov chain complex for classical links or virtual links. Is there a CW complex whose chain complex is the given chain complex? The answer is positive. The proof is easy (See [39, Theorem in Exercise 4, section 39, page 231]). However, there may be more than one CW complex whose chain complex is the given one. We want to give a specific stable homotopy type to a given chain complex. It is an important step in our procedure. We summarize our idea below.

**Example 2.1.** Both the one point union  $S^2 \vee S^4$  and  $\mathbb{C}P^2$  have a natural CW decomposition (the base point)  $\cup e^2 \cup e^4$ . Both have the same chain complex and different stable homotopy types.

If we specify maps to  $\partial e^4$  to the 2-skeleton (the base point)  $\cup e^2$  as follows, we determine which the resulting 4-skeleton is  $S^2 \vee S^4$  or  $\mathbb{C}P^2$ . Take the trivial knot  $S^1$  in the 3-sphere  $\partial e^4$ .

(1) We give a framing on the normal bundle of  $S^1$  in  $\partial e^4$  so that the framing extends to an embedded disc that bounds  $S^1$ .

(2) We give it as follows; A framing consists locally of two orthonormal vectors (arrows). Let the normal frame to the circle so that the original circle and either circle traced by one of the arrows makes the Hopf link.

Use the Pontrjagin-Thom construction associated with (1) and (2). Then the condition (1) defines  $S^2 \vee S^4$ , and the condition (2) induces  $\mathbb{C}P^2$ . Recall a relation between the Hopf fibration and the Pontrjagin-Thom construction associated with (2).

The circle  $S^1$  in  $\partial e^4$  is an example of moduli. The term moduli is defined in LS and framed moduli are the basis for constructing CW complexes by Lipshitz and Sarkar (See [29, §3.3 and §4] and [31, §3.3]). We direct the reader to LS for the full definition of moduli and point out that the term is related to equivalence classes of points in the flow related to a Morse singularity. The flow concept is generalized in [29] to a flow category. We give the definition of flow category below and again direct the reader to [29] for the details. The examples we have cited are useful for understanding the general principle of the framed moduli. Those normal framings on  $S^1$  in the conditions (1) and (2) are

examples of framings on moduli. The method of moduli and framings is obtained by generalizing the Pontrjagin-Thom construction.

Note that, for any given CW complex, in each cell, we can define moduli and framings. We construct as follows.

**Construction 2.2.** We are given a chain complex and a basis. The basis is a poset by the differential. We attach the lowest dimensional cell to the base point. Note that if it is 0-dimensional cell, the attaching map is the empty. From lower dimensional cells to higher dimensional cells, step by step, we attach each cell to the lower dimensional skeleton as follows. When we attach each cell  $e$ , we define a moduli  $\mathcal{M}$  in  $\partial e$  and a framing on  $\mathcal{M}$ . So  $\partial\mathcal{M} \cap (\text{the lower dimensional skeleton})$  has been framed. We must define the framing on  $\mathcal{M}$  so that the given framing on  $\partial\mathcal{M}$  extends to  $\mathcal{M}$ .

In other words, we define moduli and framings in lower dimensional cells to those in higher dimensional ones.

Construction 2.2 does not complete for any basis of any chain complex. We show an example below. We use [29, Definition 3.12.(M-2)] crucially, so we cite it here.

**Definition 3.12 of [29].** A *flow category* is a pair  $(\mathcal{C}, \text{gr})$  where  $\mathcal{C}$  is a category with finitely many objects  $\text{Ob} = \text{Ob}(\mathcal{C})$  and  $\text{gr} : \text{Ob} \rightarrow \mathbb{Z}$  is a function, called the grading, satisfying the following additional conditions:

- (M-1)  $\text{Hom}(x, x) = \{\text{Id}\}$  for all  $x \in \text{Ob}$ , and for distinct  $x, y \in \text{Ob}$ ,  $\text{Hom}(x, y)$  is a compact  $(\text{gr}(x) - \text{gr}(y) - 1)$ -dimensional  $\langle \text{gr}(x) - \text{gr}(y) - 1 \rangle$ -manifold (with the understanding that negative dimensional manifolds are empty).
- (M-2) For distinct  $x, y, z \in \text{Ob}$  with  $\text{gr}(z) - \text{gr}(y) = m$ , the composition map

$$\circ : \text{Hom}(z, y) \times \text{Hom}(x, z) \rightarrow \text{Hom}(x, y)$$

is an embedding into  $\partial_m \text{Hom}(x, y)$ . Furthermore,

$$\circ^{-1}(\partial_i \text{Hom}(x, y)) = \begin{cases} \partial_i \text{Hom}(z, y) \times \text{Hom}(x, z) & \text{for } i < m \\ \text{Hom}(z, y) \times \partial_{i-m} \text{Hom}(x, z) & \text{for } i > m \end{cases}$$

- (M-3) For distinct  $x, y \in \text{Ob}$ ,  $\circ$  induces a diffeomorphism

$$(3.1) \quad \partial_i \text{Hom}(x, y) \cong \bigcup_{z \text{ gr}(z)=\text{gr}(y)+i} \text{Hom}(z, y) \times \text{Hom}(x, z).$$

Therefore, if  $\mathcal{D}$  is the diagram whose vertices are the spaces

$$\text{Hom}(z_m, y) \times \text{Hom}(z_{m-1}, z_m) \times \cdots \times \text{Hom}(x, z_1)$$

for  $m \geq 1$  and distinct  $z_1, \dots, z_m \in \text{Ob} - \{x, y\}$ , and whose arrows correspond to composing a single adjacent pair of Hom's, then

$$\partial \text{Hom}(x, y) \cong \cup_i \partial_i \text{Hom}(x, y) \cong \text{colim} \mathcal{D}.$$

Given objects  $x, y$  in a flow category  $\mathcal{C}$ , define the *moduli space from  $x$  to  $y$*  to be

$$\mathcal{M}(x, y) = \begin{cases} \phi & \text{if } x=y \\ \text{Hom}(x, y) & \text{otherwise.} \end{cases}$$

Given a flow category  $\mathcal{C}$  and an integer  $n$ , let  $\mathcal{C}[n]$  be the flow category obtained from  $\mathcal{C}$  by increasing the grading of each object by  $n$ .

**Example 2.3.** Take a CW decomposition (the base point)  $\cup e^2 \cup e^4$  of  $\mathbb{C}P^2$ . Consider a question whether we can attach a 5-cell  $e^5$  to  $\mathbb{C}P^2$  so that  $H_4(\mathbb{C}P^2 \cup e^5) = 0$ . The answer is negative because  $\pi_4 \mathbb{C}P^2 = 0$ . We show an alternative proof by using modulis and framings and Definition 3.12.(M-2). We use reductio ad absurdum. We assume that we can attach  $e^5$  to  $\mathbb{C}P^2$  so that  $H_4(\mathbb{C}P^2 \cup e^5) = 0$ . Then there is a moduli  $\mathcal{M}(e^5, e^2)$  in  $e^5$ . By Definition 3.12.(M-2),  $\partial \mathcal{M}(e^5, e^2) = \mathcal{M}(e^5, e^4) \times \mathcal{M}(e^4, e^2)$ . Since  $H_4(\mathbb{C}P^2 \cup e^5) = 0$ ,  $\mathcal{M}(e^5, e^4)$  is one point and the framing on the point is determined by the differential.  $\mathcal{M}(e^4, e^2)$  is a circle and the framing on the circle defined as in the above condition (2). The framing on  $\partial \mathcal{M}(e^5, e^2)$  is induced from that on  $\mathcal{M}(e^5, e^4)$  and that on  $\mathcal{M}(e^4, e^2)$  (See [29, Definition 3.18]). This framing on  $\partial \mathcal{M}(e^5, e^2)$  cannot extend to  $\mathcal{M}(e^5, e^2)$ . We arrived at a contradiction.

We can realize Construction 2.2 if a given chain complex has the following property.

**Property 2.4.** Suppose that we are given a basis of a chain complex. Each basis element is represented by a cell. Suppose that we can attach a cell  $e$  to the lower dimensional skeleton. Then we have a moduli  $\mathcal{M}$  in  $\partial e$ .

We have the following important property: Not all sub-modulis in  $\partial \mathcal{M}$  have been framed in the lower dimensional skeleton  $X$ . Furthermore we can extend the framing on  $\partial \mathcal{M}$  that has been framed in  $X$ , to  $\mathcal{M}$ .

Khovanov chain complexes for classical links always have Property 2.4 (See [29, Proposition 4.12 and Definition 5.5]). In this paper we will prove that a partial case of the virtual case has Property 2.4. So Property 2.4 is a key of our construction of Khovanov partial CW complex. Note that there are many chain complexes that satisfy Property 2.4 and that are not a Khovanov chain complex for classical or virtual links. Note that Example 2.3 does not satisfy Property 2.4.

### 3. STRATEGY OF THE CONSTRUCTION OF CW COMPLEXES FOR VIRTUAL LINKS

Lipshitz and Sarkar [29] defined moduli for all  $P(e, g)$ , where  $e$  and  $g$  run over all basis elements, and introduced framings on them, and constructed a stable homotopy type of a CW complex for a given classical link.

In the virtual case, it is very complicated to construct a moduli  $P(e, g)$  for a pair  $e$  and  $g$  such that the difference of the homological gradings is greater than four. The reason is that the property of coefficients in the virtual case (Definition 5.21) is different from the classical case (see also §10). In this paper we show an explicit way to assign to the moduli space when the difference  $\text{gr}_h \mathbf{x} - \text{gr}_h \mathbf{y}$  of the homological gradings is no greater than four. We construct a CW complex which consists of only  $(m - 1)$ -cells,  $m$ -cells,  $(m + 1)$ -cells,  $(m + 2)$ -cells, and  $(m + 3)$ -cells, where  $m$  is any integer, for the dual Khovanov chain complex in this case by using these moduli spaces. We prove that the second Steenrod square of the CW complex is invariant under any Reidemeister move although we do not prove whether the stable homotopy type of the CW complex is invariant under any Reidemeister move.

**Remark 3.1.** In Lipshitz and Sarkar's paper [29, §5.4] it is important how one assigns a moduli to the ladybug configuration. (We review the ladybug configuration in §8 and §9.). Lipshitz and Sarkar consider all ladybug configurations in a given classical link diagram and show that they can make the specific choice either the the right or the left pair. That is, all ladybug configurations are chosen to have the same pair. In our paper, we consider the following situation: Each ladybug configuration in a given virtual link diagram may have different pairs. We consider all cases. Therefore we may consider more than one set of moduli for one Khovanov chain complex. Note that classical link diagrams are virtual link diagrams. We discuss both the condition that Lipshitz and Sarkar[29] discussed and the condition that they did not discuss. Thus, in the case of classical links, we also handle moduli that they did not handle, but our second Steenrod square on a classical link is the same as theirs.

## Part 2. Review of Khovanov homology for virtual links

### 4. VIRTUAL KNOTS AND VIRTUAL LINKS

We work in the smooth category. Let  $L = \{L_1, \dots, L_m\}$  be a 1-dimensional submanifold of a connected 3-manifold  $M$ , where  $L_k$  denotes a connected component. Then  $L$  is called an  $m$ -component link in  $M$ . In this paper we only discuss 1-dimensional links, so we say link, not 1-dimensional link nor 1-link. Any 1-component link  $L$  in  $M$  is called a *knot* in  $M$ . If  $M$  is the 3-sphere  $S^3$ , any link (respectively, knot)  $L$  in  $M$  is called a *classical link* (respectively, *classical knot*).

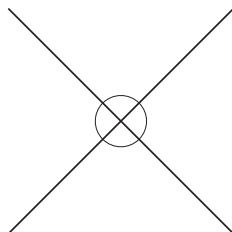


FIGURE 4.1. **Virtual crossing point**

The theory of *virtual knots* was introduced in [15, 16, 17] as a generalization of classical knot theory, and studies the embeddings of circles in thickened oriented closed surfaces modulo isotopies and orientation preserving diffeomorphisms plus one-handle stabilization of the surfaces.

By a one-handle stabilization, we mean a surgery on the surface that is performed on a curve in the complement of the link embedding and that either increases or decreases the genus of the surface. The reader should note that knots and links in thickened surfaces can be represented by diagrams on the surface in the same sense as link diagrams drawn in the plane or on the two-sphere. From this point of view, a one handle stabilization is obtained by cutting the surface along a curve in the complement of the link diagram and capping the two new boundary curves with disks, or taking two points on the surface in the link diagram complement and cutting out two disks, and then adding a tube between them. The main point about handle stabilization is that it allows the virtual knot to be eventually placed in a least genus surface in which it can be represented. A theorem of Kuperberg [26] asserts that such minimal representations are topologically unique.

Virtual knot theory has a diagrammatic formulation. A *virtual knot* can be represented by a *virtual knot diagram* in  $\mathbb{R}^2$  (respectively,  $S^2$ ) containing a finite number of real crossings, and *virtual crossings* indicated by a small circle placed around the crossing point as shown in Figure 4.1. A virtual crossing is a combinatorial structure that shows how the diagram for the virtual knot is connected, and allows the reconstruction of a surface in which the knot has a diagram, up to handle stabilization.

The moves on virtual knot diagrams in  $\mathbb{R}^2$  are generated by the usual Reidemeister moves plus the *detour move*. The detour move allows a segment with a consecutive sequence of virtual crossings to be excised and replaced by any other such a segment with a consecutive virtual crossings, as shown in Figure 4.2.

Virtual 1-knot diagrams  $\alpha$  and  $\beta$  are changed into each other by a sequence of the usual Reidemeister moves and detour moves if and only if  $\alpha$  and  $\beta$  are changed into each

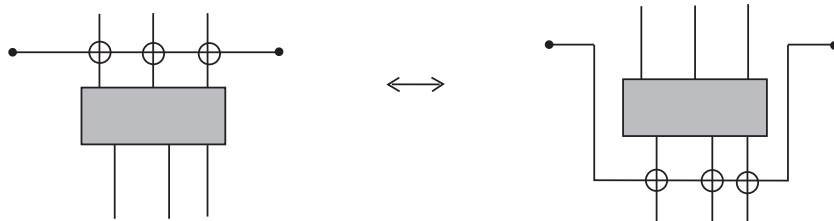


FIGURE 4.2. An example of detour moves

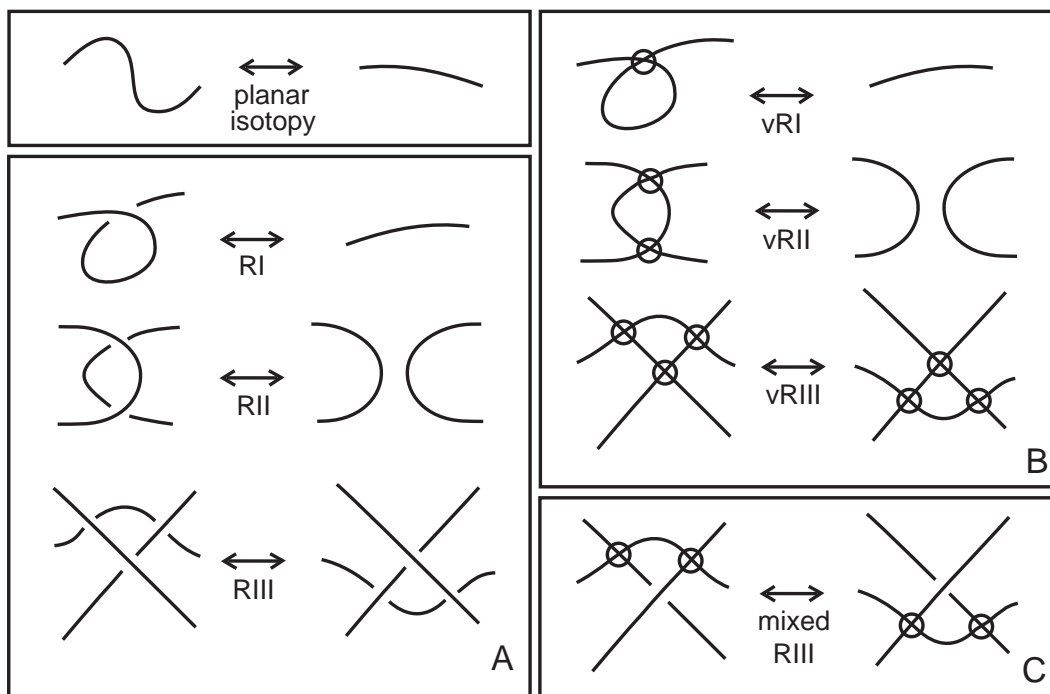


FIGURE 4.3. All Reidemeister moves

other by a sequence of all Reidemeister moves drawn in Figure 4.3.

Virtual knot and link diagrams that can be related to each other by a finite sequence of the Reidemeister and detour moves are said to be *virtually equivalent* or *virtually isotopic*.

The virtual isotopy class of a virtual knot diagram is called a *virtual knot*.

There is a one-to-one correspondence between the topological and the diagrammatic approach to virtual knot theory. The following theorem providing the transition between



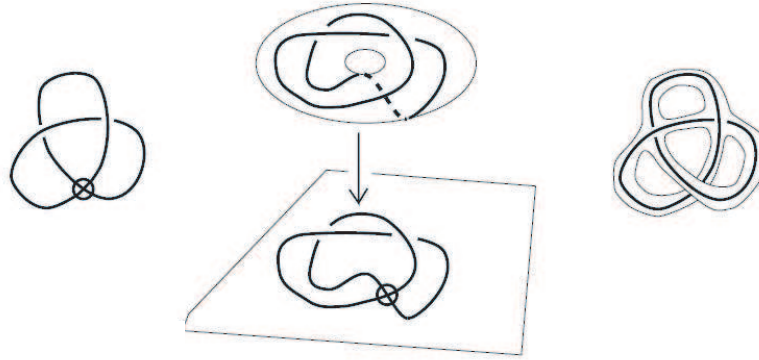


FIGURE 4.4. How to make a representing surface from the tubular neighborhood of a virtual knot diagram in  $\mathbb{R}^2$

the two approaches is proved by abstract knot diagrams, see [15, 16, 17].

**Theorem 4.1.** ([15, 16, 17]) *Two virtual link diagrams are virtually isotopic if and only if their surface embeddings are equivalent up to isotopy in the thickened surfaces, orientation preserving diffeomorphisms of the surfaces, and the addition/removal of empty handles.*

**Remark.** A handle is said to be *empty* if the knot diagram does not thread through the handle. One way to say this more precisely is to model the addition of and removal of handles via the location of surgery curves in the surface that do not intersect the knot diagram. Here, an oriented surface with a link diagram using only classical crossings appears. This surface is called a *representing surface*. In Figure 4.4 we show an example of a way to make a representing surface from a virtual knot diagram. Take the tubular neighborhood of a virtual knot diagram in  $\mathbb{R}^2$ . Near a virtual crossing point, double the tubular neighborhood. Near a classical crossing point, keep the tubular neighborhood and the classical crossing point. Thus we obtain a compact representing surface with non-vacuous boundary. We may start with a representing surface that is oriented and

not closed, and then embed the surface in a closed oriented surface to obtain a new representing surface. Taking representations of virtual knots up to such cutting (removal of exterior of neighborhood of the diagram in a given surface) and re-embedding, plus isotopy in the given surfaces, corresponds to a unique diagrammatic virtual knot type.

The presence of the single cycle zero map in the virtual Khovanov chain complex and the properties of the coefficients in the virtual Khovanov chain complex take us out of the cube complex method for defining a framed flow category. For this reason we use a truncated homotopy type for this paper.

## 5. KHOVANOV HOMOLOGY FOR VIRTUAL LINKS

In this section we give a detailed version of the Manturov method for defining Khovanov homology for virtual links. The reader interested in this definition should examine previous papers by Manturov [37] and by Dye, Kaestner and Kauffman [6] and also by Nikonov [40]. The definition has a necessary complexity due to the presence of single cycle resmoothings in the Kauffman states of virtual link diagrams. In the papers mentioned there are different motivating points of view given for the definitions. Here we use these ideas and give a strict definition that will require some work on the part of the reader to absorb. The advantage of this definition is that it permits specific formulas for the coefficients in the boundary formulas for the chain complex and it has some other advantages that are of a technical nature. The reader already familiar with Khovanov homology for virtual links should review what he knows before reading this section.

We begin by reviewing the case of classical links. Let  $\mathcal{L}$  be a classical link. Let  $L$  be a classical link diagram which represents  $\mathcal{L}$ . In [23] Khovanov defined a chain complex for  $L$ , and proved that the homology defined by the chain complex is an invariant of the link type of  $\mathcal{L}$ . We call this chain complex the *Khovanov chain complex*, and this homology *Khovanov homology*. Khovanov proved that the Jones polynomial of any classical link  $L$  is a graded Euler characteristic of the Khovanov homology of  $L$ . In [5] Bar-Natan reformulated the definition of Khovanov homology, and proved, by direct calculation, that Khovanov homology is stronger than the Jones polynomial.

The differential on each element in the Khovanov chain complex increases the degree of the element. This is not an ordinary convention but this terminology has been used for a long time. So we adopt this notation in this paper. Furthermore we define the following notations. We use the dual of the Khovanov chain complex in this paper. The differential on it decreases the degree. We call this chain complex the *dual Khovanov chain complex*. We call the homology defined by the dual Khovanov chain complex, the

*homology of the dual Khovanov chain complex.* We use often the terminologies, “chain complex”, “chain homotopy”, and “homological”, in both the case of Khovanov chain complexes and the case of the dual Khovanov chain complexes.

Lipshitz and Sarkar [29] introduced a stable homotopy type of CW complexes for each classical link, and proved that the stable homotopy type is a topological invariant of classical links. We call it *Khovanov-Lipshitz-Sakar stable homotopy type* for classical links. Stable homotopy types of CW complexes have Steenrod squares. Seed [53] proved the following fact by making a computer program according to Lipshitz and Sarkar’s method in [31].

**Theorem 5.1.** ([53].) *The second Steenrod square for classical links is stronger than Khovanov homology for classical links. That is, there are classical links  $K_1$  and  $K_2$  such that the Khovanov homology of  $K_1$  is the same as that of  $K_2$ , but the second Steenrod square of  $K_1$  is different from that of  $K_2$ . Therefore Khovanov-Lipshitz-Sakar stable homotopy type for classical links is stronger than Khovanov homology for classical links.*

We start the discussion on the case of virtual links now. Manturov defined Khovanov homology for virtual links in [37] (arXiv 2006). Rushworth [50] and Tubbenhauer [54] defined it in different methods. See also Viro [55]. Dye, Kaestner, and Kauffman [6] made an alternative definition of [37]. Nikonov [40] described an alternative definition of [6, 37].

We review the definition of Khovanov chain complexes and that of Khovanov homology for virtual links defined by Manturov [37]. In this paper, Khovanov homology for virtual links means Manturov’s Khovanov homology for virtual links. Our exposition below of virtual Khovanov homology is self-contained.

In this paper we will generalize the result about the Steenrod square operator on Khovanov homology for classical links in [30] to the virtual link case, by extending many results and methods in [29, 30]. So we first explain the mode of definition for Khovanov chain complexes and Khovanov homology for virtual links in the fashion of [29, section two].

**Definition 5.2.** *A resolution configuration  $D$  is a pair  $(Z(D), A(D))$ , where  $Z(D)$  is a set of pairwise-disjoint immersed circles in  $S^2$ , and  $A(D)$  is a totally ordered collection of disjoint arcs embedded in  $S^2$ , with  $A(D) \cap Z(D) = \partial A(D)$ . We call the number of arcs in  $A(D)$  the *index* of the resolution configuration  $D$ , and denote it by  $\text{ind}(D)$ . We sometimes abuse notation and write  $Z(D)$  to mean  $\cup_{Z \in Z(D)} Z$  and  $A(D)$  to mean  $\cup_{A \in A(D)} A$ . Occasionally, we will describe the total order on  $A(D)$  by numbering the arcs: a lower numbered arc precedes a higher numbered one.*

We sometimes call an element of  $Z(D)$ , an immersed circle, a circle, a loop or a component of  $D$ .

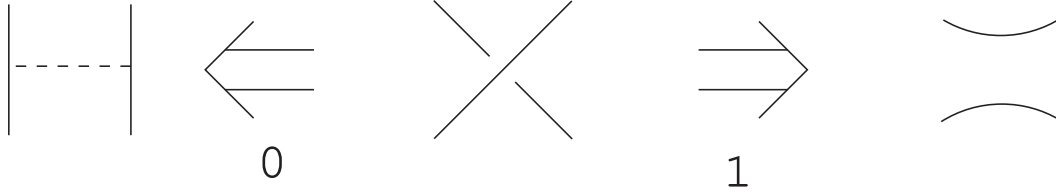


FIGURE 5.1. The 0- and 1-resolutions

Note that resolution configurations are the same as what many people call *Kauffman states*, which Kauffman first introduced in [14]. (The ways to draw arcs in both papers are different.)

**Definition 5.3.** Given a virtual link diagram  $L$  with  $n$  classical crossings, an ordering of the crossings in  $L$ , and a *vector*  $v \in \{0, 1\}^n$  there is an *associated resolution configuration*  $D_L(v)$  obtained by taking the resolution of  $L$  corresponding to  $v$  (that is, taking the 0-resolution at the  $i$ -th crossing if  $v_i = 0$ , and the 1-resolution otherwise) and then placing arcs corresponding to each of the crossings labeled by 0's in  $v$  (that is, at the  $i$ -th crossing if  $v_i = 0$ ). See Figure 5.1.

Therefore,  $n\text{-ind}(D_L(v)) = |v| = \sum v_i^2 = \sum v_i$ , the (Manhattan) norm of  $v$ . We use  $\text{Ind}$  as defined in Definition 5.2.

Note that the 0-(respectively, 1-)resolution is the same as the  $A$ -(respectively,  $B$ -)type split in [14].

Compare Definitions 5.2 and 5.3 with [29, Definitions 2.1 and 2.2]. In the case of classical link diagrams,  $Z(D)$  consists in only embedded circles, but in the case of virtual link diagrams,  $Z(D)$  consists in immersed circles whose singular points are virtual crossing points. The dotted arc in Figure 5.1 corresponds to the 0-smoothing, while the 1-smoothing is undotted. This corresponds to the red arc in [29, Figure 2.1.a].

It is important that we do not carry out a resolution on any virtual crossing.

**Definition 5.4.** ([29, Definition 2.3].) Given resolution configurations  $D$  and  $E$  there is a new resolution configuration  $D - E$  defined by

$$Z(D - E) = Z(D) - Z(E) \quad A(D - E) = \{A \in A(D) \mid \forall Z \in Z(E) : \partial A \cap Z = \emptyset\}.$$

Let  $D \cap E = D - (D - E)$ .

Note that  $Z(D \cap E) = Z(E \cap D)$  and  $A(D \cap E) = A(E \cap D)$ ; however, the total orders on  $A(D \cap E)$  and  $A(E \cap D)$  could be different.

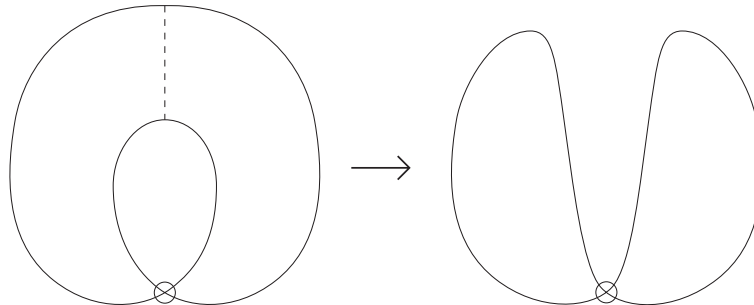


FIGURE 5.2. A single cycle surgery

**Definition 5.5.** ([29, Definition 2.4].) The *core*  $c(D)$  of a resolution configuration  $D$  is the resolution configuration obtained from  $D$  by deleting all the circles in  $Z(D)$  that are disjoint from all the arcs in  $A(D)$ . A resolution configuration  $D$  is called *basic* if  $D = c(D)$ , that is, if every circle in  $Z(D)$  intersects an arc in  $A(D)$ .

**Definition 5.6.** Let  $D$  be a resolution configuration. Suppose that, when we carry out a surgery along one arc of  $A(D)$  on an immersed circle of  $Z(D)$ , the number of the elements of  $Z(D)$  is not changed. Then we call this surgery *single cycle surgery*. See Figure 5.2 for an example.

Khovanov homology of virtual links is independent of orientations of virtual links but we use orientations of virtual links when we define it.

**Definition 5.7.** ([40]) Let  $D$  be a (unoriented) virtual link diagram and  $\mathcal{X}(D)$  be the set of classical crossings of  $D$ . For any crossing  $c \in \mathcal{X}(D)$  we choose one of the two *source-sink orientations* [10] (see Fig. 5.3). Denote the choice of source-link orientation at each classical crossing by  $\lambda$  and call it a *local source-sink structure* (LSSS) of the diagram  $D$ . Denote the set of all local source-sink structures by  $\Lambda(D)$ .

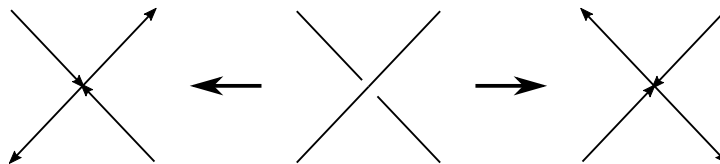


FIGURE 5.3. Source-sink orientations

If the diagram  $D$  is oriented, one can define the *canonical source-sink structure* [6] as shown in Fig. 5.4.

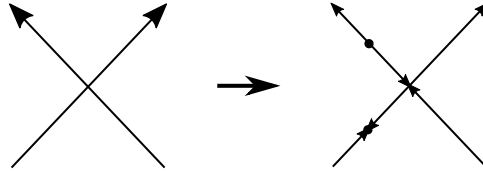


FIGURE 5.4. Canonical source-sink orientation. The cut loci mark the places where the local source-sink orientation changes to the orientation of the link

**Remark 5.8.** ([40]) Source-sink structure can be used to define (local) orientation of Kauffman states of the diagram, see Fig. 5.5.

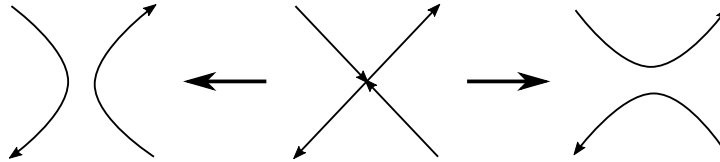


FIGURE 5.5. Local orientation of smoothed components

Any LSSS  $\lambda$  has the *opposite LSSS*  $-\lambda$  that is obtained by the *global change of orientation*, i.e. when one switches the source-sink structure at every classical crossing of  $D$ .

**Definition 5.9. The cut locus.** Let  $C$  be an immersed circle in  $Z(D)$ . Take all arrows drawn in Figure 5.5, in  $C$ . See an example in Figure 5.6.  $C$  is a union of arrows and immersed curved segments as follows: Any immersed curved segment is the image of an immersion  $f$  of the closed interval  $[0, 1]$ .  $f(0) \neq f(1)$ . Immersed curved segments may intersect other ones at virtual crossings. Put a point in  $f((0, 1))$  only if both of  $f(0)$  and  $f(1)$  touch arrowtails (respectively, arrowheads). Don't put the point at any virtual crossing point. We call this point the *cut locus*. Note that the cut locus point is always at the boundary between opposite local orientations induced by the arrows.

**Remark.** It is trivial that, after a surgery along one arc of a resolution configuration, the placements of cut loci do not change in  $S^2$ .

By Figure 5.4, we have the following.

**Proposition 5.10.** *We can put all cut loci near classical crossing points.*

By the method to give sink source orientations, we have the following.

**Proposition 5.11.** *There is no cut locus in an arbitrary classical link diagram.*

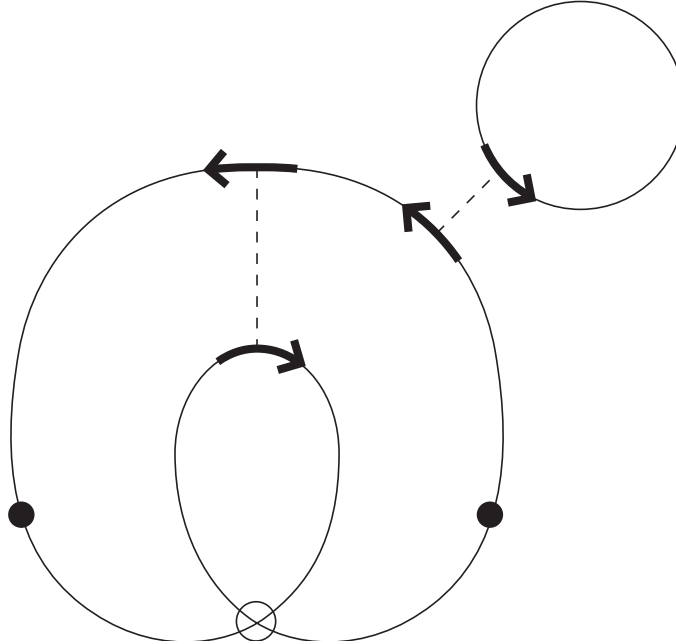


FIGURE 5.6. Cut loci

**Theorem 5.12.** *The number of cut loci in any immersed loop  $C$  in  $Z(D)$  is even.*

**Proof of Theorem 5.12.** Let  $n$  be a nonnegative integer. There are  $n$  arrows in  $C$  if and only if there are  $n$  immersed curved segments in  $C$ . If there is a set of two arrows and one immersed curved segment in  $C$  as drawn in Figure 5.7, there is no cut locus in this immersed curved segment. If there is a set as drawn in Figure 5.7, change it into one arrow whose orientation of the arrow is the same as the two ones in Figure 5.7. Repeat this procedure. If each immersed curved segment in the result includes a cut locus, then stop the procedure.

*Claim.* The number of immersed curved segments in the result of the process in Figure 5.7. is even. *Reason.* If the number of arrows in the result is odd, there is at least one set of the type in Figure 5.7. The immersed curved segment in the set does not include a cut locus by the definition. We arrived at a contradiction. Therefore the number of immersed curved segments in  $C$  is even, and the number of cut loci in  $C$  is even. This completes the proof of Theorem 5.12.  $\square$

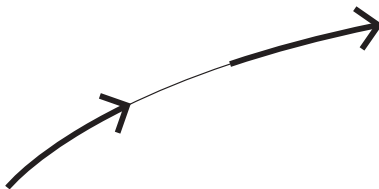


FIGURE 5.7. An example that the orientations of two arrowheads are the same. The immersed curved segment touches both arrows. In this figure, the immersed curved segment is drawn as an embedding, but it is not always embedding.

**Definition 5.13.** Let  $D$  be a resolution configuration. We notate a star in each immersed circle in  $Z(D)$  so that it does not touch an arrow, a cut locus, nor a virtual crossing, as indicated below, and call it a *starting star*.

Let  $E$  be a resolution configuration that we obtain from  $D$  by a surgery along one arc of  $E$ . Let  $S$  be an immersed circle in  $Z(D) \cap Z(E)$ . Note that the place of  $S$  in  $S^2$  before this surgery is the same as that after it. We put the starting star in the same place in  $S$  of  $E$  as in that of  $D$ . See Figure 5.8.

**Remark.** In Figures 5.8, circles may not be embedded circles, but we draw them as embedded ones abstractly.

**Definition 5.14.** ([29, Definition 2.9]). A *labeled resolution configuration* is a pair  $(D, x)$  of a resolution configuration  $D$  and a labeling  $x$  of each element of  $Z(D)$  by either  $x_+$  or  $x_-$ .

Note that labeled resolution configurations are the same as what many people call *enhanced Kauffman states* or *enhanced states*. Some people use  $v_+$  (respectively,  $v_-$ ) for  $x_+$  (respectively,  $x_-$ ).

**Definition 5.15.** ([29, Definition 2.10]). There is a partial order  $\prec$  on labeled resolution configurations defined as follows. We declare that  $(E, y) \prec (D, x)$  if:

- (1) The labelings  $x$  and  $y$  induce the same labeling on  $D \cap E = E \cap D$ .
- (2)  $D$  is obtained from  $E$  by surgering along a single arc of  $A(E)$ . In particular, either:
  - (a)  $Z(E - D)$  contains exactly one circle, say  $Z_i$ , and  $Z(D - E)$  contains exactly two circles, say  $Z_j$  and  $Z_k$ , or
  - (b)  $Z(E - D)$  contains exactly two circles, say  $Z_i$  and  $Z_j$ , and  $Z(D - E)$  contains exactly one circle, say  $Z_k$ .



Consider this  $\delta$  map.

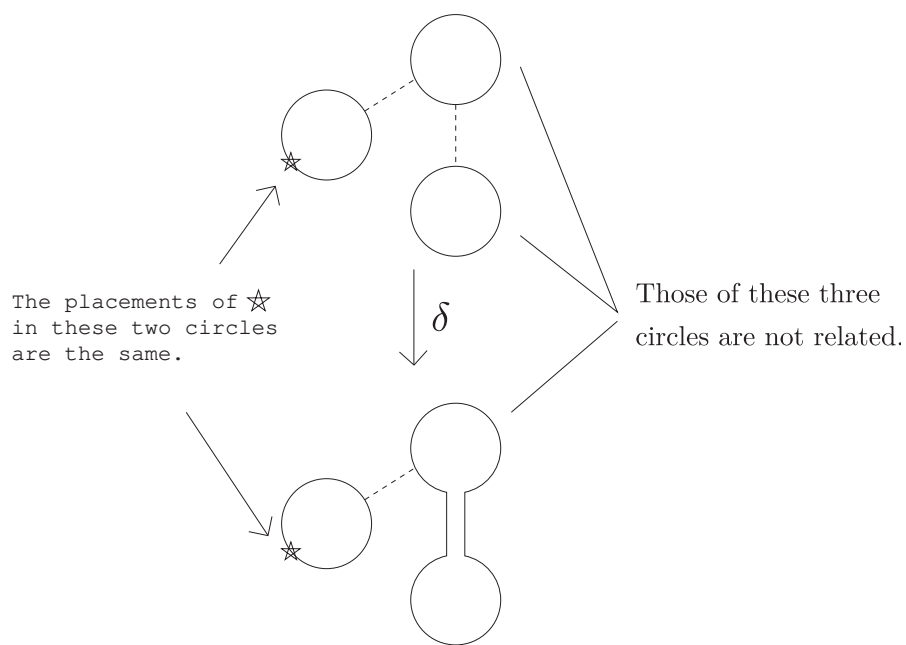
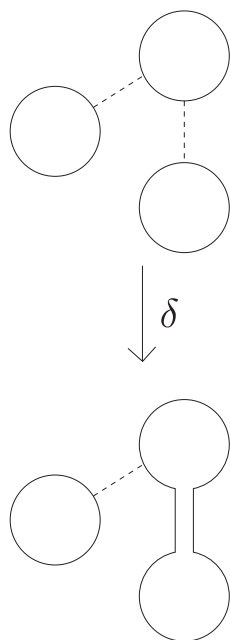


FIGURE 5.8. In this figure, circles may not be embedded circles, but we draw (not necessarily embedded) immersed circles as embedded ones abstractly.

- (3) In Case (2a), either  $y(Z_i) = x(Z_j) = x(Z_k) = x_-$  or  $y(Z_i) = x_+$  and  $\{x(Z_j), x(Z_k)\} = \{x_+, x_-\}$ .  
 In Case (2b), either  $y(Z_i) = y(Z_j) = x(Z_k) = x_+$  or  $\{y(Z_i), y(Z_j)\} = \{x_-, x_+\}$  and  $x(Z_k) = x_-$ .

Note that no surgery in Definition 5.15 is a single cycle surgery although we now consider virtual links.

See [29, §2] for  $s(D)$ .

**Definition 5.16.** ([29, Definition 2.11].) A *decorated resolution configuration* is a triple  $(D, x, y)$  where  $D$  is a resolution configuration and  $x$  (respectively,  $y$ ) is a labeling of each component of  $Z(s(D))$  (respectively,  $Z(D)$ ) by an element of  $x_+, x_-$ . If we do not have  $(D, y) \preceq (s(D), x)$ , we say that  $(D, x, y)$  is empty.

Associated to a decorated resolution configuration  $(D, x, y)$  is the *poset*  $P(D, x, y)$  consisting of all labeled resolution configurations  $(E, z)$  with  $(D, y) \preceq (E, z) \preceq (s(D), x)$ . We say that  $P(D, x, y)$  is the poset of a decorated resolution configuration  $(D, x, y)$ .

**Remark.** In [29, Definition 2.11], if we write  $(D, x, y)$ , then  $(D, x, y)$  is not empty. We define a term, “empty decorated resolution configuration” for convenience. If  $(D, x, y)$  is empty,  $P(D, x, y)$  is the empty set.

**Definition 5.17.** (A part of Definition 2.15 in [29].) For labeled resolution configurations, *homological grading*  $gr_h$  and a *quantum grading*  $gr_q$ , defined as follows:

$$\begin{aligned} gr_h((DL(u), x)) &= -n_- + |u|, \\ gr_q((DL(u), x)) &= n_+ - 2n_- + |u| \\ &\quad + \#\{Z \in Z(DL(u)) \mid x(Z) = x_+\} - \#\{Z \in Z(DL(u)) \mid x(Z) = x_-\}. \end{aligned}$$

Here  $n_+$  denotes the number of positive crossings in  $L$ ; and  $n_- = n - n_+$  denotes the number of negative crossings.

**Remark 5.18.** If  $L$  has only one component, when we define  $n, n_+, n_-, gr_h$ , and  $gr_q$ , we do not need to use the orientation of  $L$ . If  $L$  has greater than one component, we use that of  $L$  when we define  $n_+$  and  $n_-$ . Note that, if we change the orientation of  $L$  into the opposite one, then neither  $n_+$  nor  $n_-$  changes.

Each of  $gr_h(D, x)$  and  $gr_q(D, x)$  is independent of which orientation we give  $Z(D)$ , and is independent of which we choose  $L$  or  $-L$ . Here, let  $-L$  be a link made from  $L$  by reversing the orientation of  $L$ .

**Fact 5.19.** Assume that a single cycle surgery changes a (non-labeled) resolution configuration  $D_L(u)$  into  $D_L(v)$ . Let  $A_i$  (respectively,  $A_j$ ) be a labeled resolution configuration defined on  $D_L(u)$  (respectively,  $D_L(v)$ ). Then  $A_i$  and  $A_j$  have different quantum gradings.

**Proof of Fact 5.19.** Recall the definition of quantum gradings,  $gr_q((DL(u), x))$ , above. Since  $n_+$  and  $n_-$  are determined by a given virtual link diagram, a single cycle surgery

does not change  $n_+ - 2n_-$ . By the definition of a (single cycle) surgery and that of  $| \cdot |$ , a single cycle surgery changes the parity of  $|u|$ . Since a single cycle surgery does not change the number of immersed circles in a labelled resolution configuration, a single cycle surgery does not change the parity of  $\#\{Z \in Z(DL(u)) | x(Z) = x_+\} - \#\{Z \in Z(DL(u)) | x(Z) = x_-\}$ . Therefore a single cycle surgery always changes a quantum grading  $\text{gr}_q((DL(u), x))$ .  $\square$

We define the integral ( $\mathbb{Z}$ -coefficient) Khovanov chain complex for  $L$  in Definition 5.21 after we state the conditions with which it should satisfy.

We define the Khovanov chain complex to be generated by all labeled resolution configurations made from a virtual link diagram  $L$ . Let  $\{A_i\}_{i \in \Lambda}$  be the set of all labeled resolution configurations made from  $L$ . Note that  $\Lambda$  is a finite set. We will define

$$\delta A_i = \sum_{j \in \Lambda} c[A_i; A_j] \cdot A_j.$$

Here,  $c[A_i; A_j]$  is an integer coefficient. We only have to define  $c[A_i; A_j]$ , which should have the following properties.

(1) If  $A_i$  and  $A_j$  have different quantum gradings, then  $c[A_i; A_j] = 0$ . Note: This condition holds in the case of Khovanov homology for classical links. If  $A_i$  and  $A_j$  are given as in Fact 5.19 above, then we want to define  $c[A_i; A_j] = 0$ . We will explain why we want this condition in Remark 5.23.

(2) If (the homological grading  $A_i$ ) + 1  $\neq$  (that of  $A_j$ ), then  $c[A_i; A_j] = 0$ .

(3) Suppose that (the homological grading  $A_i$ ) + 1 = (that of  $A_j$ ), and that (the quantum grading  $A_i$ ) = (that of  $A_j$ ). Then  $c[A_i; A_j]$  may not be zero.

We change notations, and continue to explain how we define virtual Khovanov homology. Let  $\alpha$  and  $\beta$  be enhanced Kaffman states. Let  $\alpha^{\text{no}}$  (respectively,  $\beta^{\text{no}}$ ) be a (non-enhanced) Kaffman state under  $\alpha$  (respectively,  $\beta$ ).

We define the coefficient  $[\alpha : \beta]$  of  $\beta$  in  $\delta\alpha$  to be nonzero only if  $\alpha$  and  $\beta$  satisfy the following condition (\*).

(\*)  $\beta$  is obtained from  $\alpha$  by a single multiplication or a single co-multiplication drawn in Figure 5.17.

Furthermore we define  $[\alpha : \beta]$  in the case of (\*) to be +1 or -1. We explain how we define it.

We define  $[\alpha : \beta]$  to be a product,  $\mathcal{O}(\alpha^{\text{no}}, \beta^{\text{no}})\mathcal{P}(\alpha, \beta)$ , of  $\mathcal{O}(\alpha^{\text{no}}, \beta^{\text{no}})$  and  $\mathcal{P}(\alpha, \beta)$ .

$\mathcal{P}(\alpha, \beta)$  depends on labelings in general.  $\mathcal{P}(\alpha, \beta)$  is defined by using cut loci and starting stars as below.

$\mathcal{O}(\alpha^{\text{no}}, \beta^{\text{no}})$  is independent of labelings.  $\mathcal{O}(\alpha^{\text{no}}, \beta^{\text{no}})$  is defined by using local and global orders of loops in Kauffman states below.

**Definition 5.20. Global and local orders of loops in Kauffman states, and the sign  $\mathcal{O}(\ , \ )$ .**

(1) Let  $D$  be a diagram of a virtual link and  $\mathcal{X}(D)$  be the set of the classical crossings of  $D$ . Denote the set of Kauffman states of the diagram  $D$  by  $S(D) = \{s: \mathcal{X}(D) \rightarrow \{0, 1\}\}$ . Let  $\Gamma(s)$  be the sets of components, circles, or loops, of Kauffman states. Fix an arbitrary order  $\sigma_s: \{1, 2, \dots, |\Gamma(s)|\} \rightarrow \Gamma(s)$  of the components for all Kauffman states  $D_s, s \in S(D)$ . This order is called a *global order* of  $D_s$ .

(2) At each crossing we choose one of the incoming edges in the source-sink orientation as shown in Fig. 5.9. We mark the distinguished edge with a box. The choice of the edges for all classical crossings will be denoted by  $o = \{o_c\}_{c \in \mathcal{X}(D)}$  and called an *oriented direction system* on the LSSS  $\lambda$ .

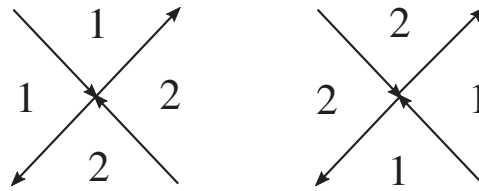


FIGURE 5.9. Directions of a source-sink orientation. It is associated with Figure 5.3.

If  $\lambda$  is a canonical LSSS of the oriented diagram  $D$ , we can consider the *canonical oriented direction system* choosing the incoming edges as shown in Fig. 5.10.

The *oriented direction* or local order  $o_c^s$  in a crossing  $c$  defines a local ordering of the components in Kauffman states which pass by  $c$ : Here,  $s$  defines an enhanced Kauffman state. See Fig. 5.11. We can consider the local order as a family of maps  $o_c^s: \{1, 2\} \rightarrow \Gamma(s)$ ,  $c \in \mathcal{X}(D)$ ,  $x \in S(D)$  (the images of 1 and 2 may coincide).

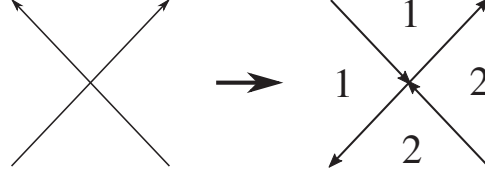


FIGURE 5.10. Canonical oriented direction system. It is related to Figure 5.4.

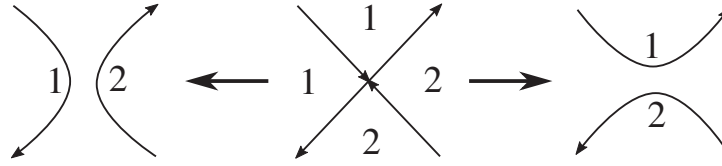


FIGURE 5.11. Local ordering of component induced by an oriented direction

For any crossing  $c \in \mathcal{X}(D)$ , state  $s \in S(D)$ , global order  $\sigma_s$  and oriented direction system  $o_c^s$  we define two new orders:

- an order  $\sigma_s \setminus c$  on the set  $\Gamma(s) \setminus c = \Gamma(s) \setminus \text{im } o_c^s$  consisting of the components in  $D_s$  which don't pass by the crossing  $c$ . The order  $\sigma_s \setminus c$  is the restriction of  $\sigma_s$  to this set. Formally, let  $j_1 = \min \sigma_s^{-1}(\text{im } o_c^s)$  and  $j_2 = \max \sigma_s^{-1}(\text{im } o_c^s)$  be the indices of the component which pass by  $c$  in the order  $\sigma_s$ . Then  $j_1 \leq j_2$ , they may coincide. We define

$$(5.1) \quad (\sigma_s \setminus c)(i) = \begin{cases} \sigma_s(i), & i < j_1, \\ \sigma_s(i+1), & j_1 \leq i < j_2 - 1, \\ \sigma_s(i+2), & i \geq j_2 - 1. \end{cases}$$

- an order  $\sigma_s \triangleleft (o, c)$  on the set  $\Gamma(s)$ . Informally, we start the numbering of the components of  $D_s$  with those that pass the crossing  $c$ , and enumerate them in the order  $o_c^s$ . The other components are ordered according  $\sigma_s$ . Let us give the explicit formulas. Let  $n_s(c)$  be the number of component of  $D_s$  which pass by the crossing  $c$ . Then

$$(5.2) \quad (\sigma_s \triangleleft (o, c))(i) = \begin{cases} o_c^s(i), & i \leq n_s(c), \\ (\sigma_s \setminus c)(i - n_s(c)), & i > n_s(c). \end{cases}$$

Given two orders  $\sigma_1, \sigma_2: \{1, \dots, |Z|\} \rightarrow Z$  on a finite set  $Z$ , we define the sign  $\epsilon(\sigma_1, \sigma_2)$  as the sign of the permutation  $\sigma_1^{-1} \circ \sigma_2$  on the set  $\{1, \dots, |Z|\}$ .

Now we can define  $\text{sign}(s, s')$  of the differential  $\partial_{s \rightarrow s'}$  as follows

$$(5.3) \quad \text{sign}(s, s') = \epsilon(\sigma_s, \sigma_s \triangleleft (o, c)) \cdot \epsilon(\sigma_s \setminus c, \sigma_{s'} \setminus c) \cdot \epsilon(\sigma_{s'}, \sigma_{s'} \triangleleft (o, c)).$$

If  $s$  (respectively,  $s'$ ) defines an enhanced Kauffman state  $\alpha$  (respectively,  $\beta$ ), we write  $\text{sign}(s, s')$  by  $\mathcal{O}(\alpha, \beta)$ .

**Definition 5.21.** (1) **The differential  $\delta$ .** Given an oriented virtual link diagram  $L$  with  $n$  crossings, an ordering of the crossings in  $L$  and global and local orders of loops, or circles, in each Kauffman state, the *Khovanov chain* complex is defined as follows. The Khovanov chain group  $KC(L)$  is the  $\mathbb{Z}$ -module freely generated by labeled resolution configurations of the form  $(DL(u), x)$  for  $u \in \{0, 1\}^n$ . The differential preserves the quantum grading, increases the homological grading by 1, and is defined as follows.

$$\delta(D_L(v), y) = \sum_{\text{all } (D_L(u), x) \text{ as below}} \mathcal{O}((D_L(v)), (D_L(u))) (-1)^\zeta.$$

Here,  $(D_L(u), x)$  satisfies the condition  $|u| = |v| + 1$ ,  $(D_L(v), y) \prec (D_L(u), x)$ . The number  $\zeta = \zeta((D_L(u), x), (D_L(v), y))$  is defined for a pair  $(D_L(u), x)$  and  $(D_L(v), y)$  in Definition 5.21.(3) by using the number  $\xi$  defined in Definition 5.21.(2).

Here is an out line of how to define  $\xi$  and  $\zeta$ . We count the parity of cut loci traversed between a surgered point and a star, on a loop. If the loop is labeled by  $x_-$  and if the parity on it is odd, we multiply  $-1$  (once) in the coefficient. If the loop is labelled by  $x_+$ , we do not multiply  $-1$ .

The number  $\mathcal{O}((D_L(v)), (D_L(u)))$  is defined above.

The numbers  $\mathcal{O}((D_L(v)), (D_L(u)))$  and  $(-1)^{\zeta((D_L(u), x), (D_L(v), y))}$  are  $+1$  or  $-1$ . The product  $\mathcal{O}((D_L(v)), (D_L(u))) (-1)^{\zeta((D_L(u), x), (D_L(v), y))}$  is a coefficient.

Recall the above notation  $\mathcal{P}(\quad, \quad)$ : We define  $\mathcal{P}((D_L(u), x), (D_L(v), y))$  to be  $(-1)^{\zeta((D_L(u), x), (D_L(v), y))}$ .

**Remark 5.22.** The reader should note the following facts, before reading the definitions below.

Let  $\alpha$  and  $\beta$  be two enhanced Kauffman states of a classical link diagram. Let  $\alpha^{\text{no}}$  (respectively,  $\beta^{\text{no}}$ ) be a (non-enhanced) Kauffman state under  $\alpha$  (respectively,  $\beta$ ) Let  $\mathcal{A}(\alpha^{\text{no}}, \beta^{\text{no}})$  be an integer defined for  $\alpha^{\text{no}}$  and  $\beta^{\text{no}}$ , which is the same one as  $(-1)^{s_0(C_{u,v})}$  in [29, Definition 2.15]: Each (non-enhanced) Kauffman state is characterized by each vector  $w = (w_1, \dots, w_n)$ , where  $w_* \in \{0, 1\}$  (See Definition 2.2.). Let  $\alpha$  (respectively,  $\beta$ ) be characterized by  $u$  (respectively,  $v$ ). We define  $s_0(C_{u,v}) \in \mathbb{Z}_2$  as follows: if  $u = (\epsilon_1, \dots, \epsilon_{i-1}, 1, \epsilon_{i+1}, \dots, \epsilon_n)$  and  $v = (\epsilon_1, \dots, \epsilon_{i-1}, 0, \epsilon_{i+1}, \dots, \epsilon_n)$ , then  $s_0(C_{u,v}) = (\epsilon_1 + \dots + \epsilon_{i-1})$ ; see also [29, Definition 2.15].

In Khovanov's original case, the case of classical links in  $S^3$ , we define the coefficient of  $\beta$  in  $\delta\alpha$  to be  $\mathcal{A}(\alpha^{\text{no}}, \beta^{\text{no}})$ .

The issue is as follows. See Figure 6.3. See also [6, Figure 13 and the explanation about it]. Call the left upper Kauffman state with a labeling  $x_+$ ,  $A$  as in Figure 6.4. If

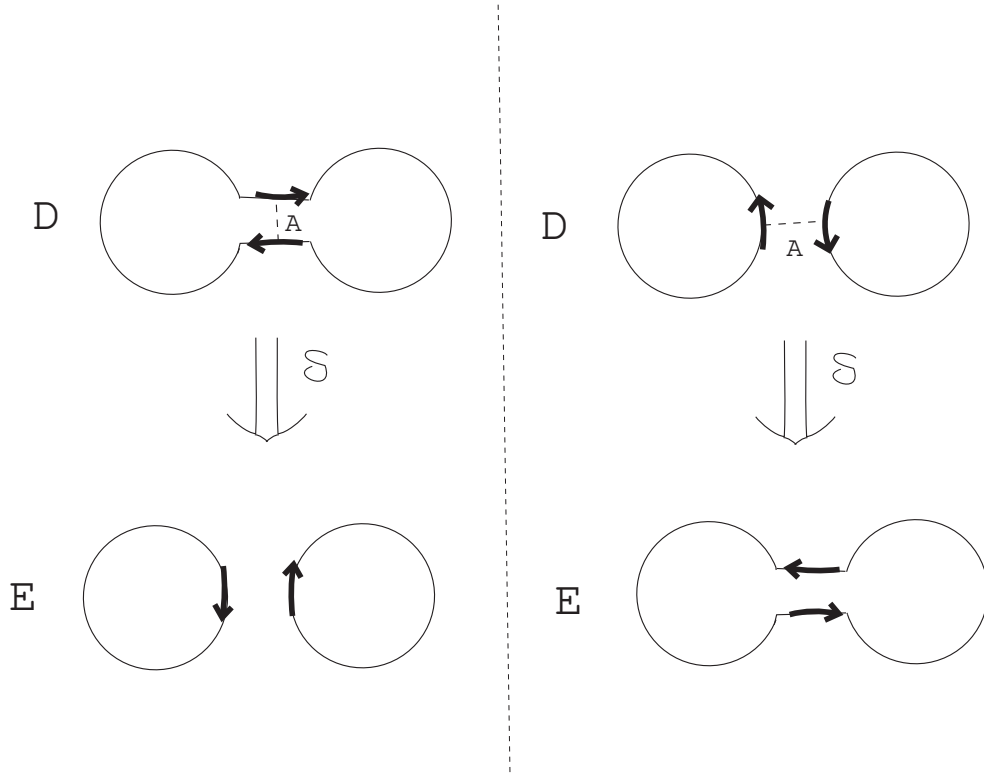


FIGURE 5.12. A multiplication surgery and a co-multiplication surgery

we define the coefficient of  $\beta$  in  $\delta\alpha$  by using  $\mathcal{A}(\alpha^{\text{no}}, \beta^{\text{no}})$  as in the case of classical links, we have  $\delta^2 A \neq 0$ . So we introduce  $\mathcal{O}(\alpha^{\text{no}}, \beta^{\text{no}})$  and  $\mathcal{P}(\alpha, \beta)$ , and settle this issue.

See Theorem 5.28 on a relation among  $\mathcal{A}(\alpha^{\text{no}}, \beta^{\text{no}})$ ,  $\mathcal{O}(\alpha^{\text{no}}, \beta^{\text{no}})$  and  $\mathcal{P}(\alpha, \beta)$ .

**Definition 5.21.(2) The number  $\xi$ .** We define the coefficient in Definition 5.21.(1) to be nonzero only if  $(D_L(u), x)$  is obtained from  $(D_L(v), y)$  by one multiplication surgery or one co-multiplication surgery. We define a number  $\xi$  before we introduce a number  $\zeta$ . These numbers are obtained by appropriate counts of the parity of cut points on a path or paths between the site of the algebraic operation (multiplication or co-multiplication) and the starting stars on the loops of the state configuration.

See Figure 5.12. Kauffman states  $D$  and  $E$  are the same in the part other than Figure 5.12: We carry out a surgery along an arc  $A$ .  $(D_L(u), x)$  and  $(D_L(v), y)$  are different only in the part like Figure 5.12.

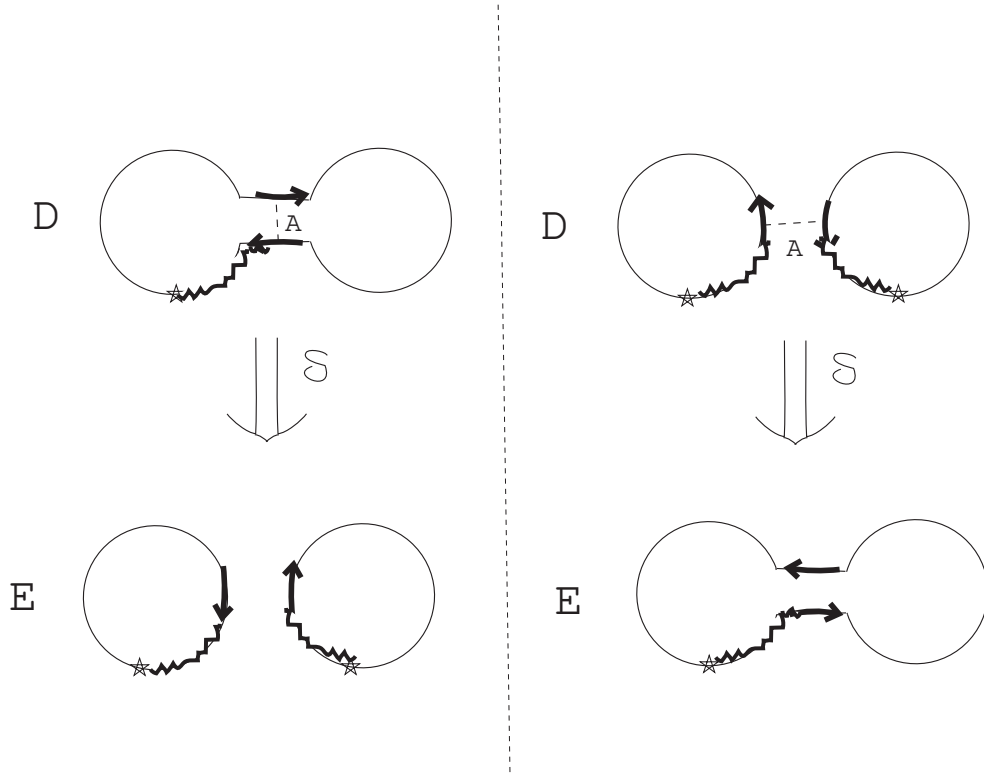


FIGURE 5.13. A multiplication surgery and a co-multiplication surgery

In Figure 5.12, we put arrows at two foots of an arc where we carry out surgery according to Figures 5.4 and 5.5. We also put arrows the points in Kauffman states after a surgery according to Figures 5.4 and 5.5.

Since we do not consider a single cycle surgery here, there are three loops related to this surgery. We define a number  $\xi$  for each loop in  $D$  (respectively,  $E$ ) and the arc  $A$  in Figure 5.12. There are two cases.

We count cut loci in each the waved curve of Figure 5.13. More precisely, we do as follows.

**Case 1.** The case where the loop includes only one arrow: Each of two loops in the left lower  $E$  of Figure 5.13, and Each of two loops in the right upper  $D$  of Figure 5.13.

See an example in Figure 5.14. See  $X$  and  $Y$  in Figure 5.14.

Let  $\xi$  be 0 (respectively, 1) if the number of the cut loci in  $X$  is even (respectively, odd). Note the following: By Theorem 5.12, the parity of the number of cut loci in



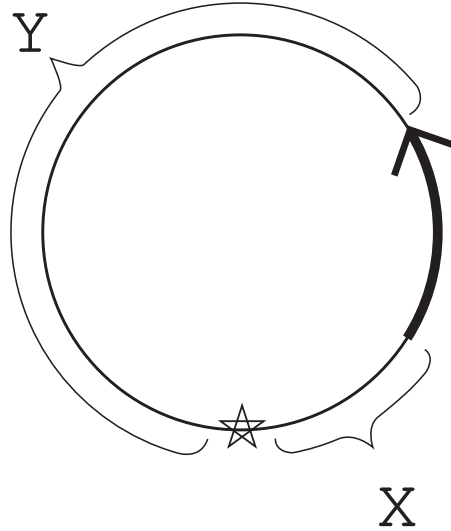


FIGURE 5.14. A figure associated with the definition of  $\xi$  in Definition 5.21.(2).

both immersed curved segments,  $X$  and  $Y$ , are the same. If we change  $X$  into  $Y$  in the definition of  $\xi$ , the value of  $\xi$  is the same.

**Case 2.** The case where the loop includes the two arrows: A unique loop in the left upper  $D$  of Figure 5.13, and a unique loop in the right lower  $E$  of Figure 5.13.

See four cases in Figure 5.15.

The case of Figure 5.15.(1) and that of Figure 5.15.(2) occur if and only if the surgery is a single cycle surgery. We do not need these cases now. In the case of Figure 5.15.(3) and that of Figure 5.15.(4), let  $\xi$  be 0 (respectively, 1) if the number of the cut loci in  $X$  is even (respectively, odd). Note the following: Each of  $Z$  in Figure 5.15.(3) and  $Z$  in Figure 5.15.(4) is an immersed circle before (respectively, after) this surgery. Hence the number of cut loci in  $Z$  is even by Theorem 5.12. Furthermore, by Theorem 5.12, the sum of the number of cut loci in  $X$ , that in  $Y$ , and that in  $Z$  is even. Therefore the parity of the number of cut loci in  $X$  and that in  $Y$  are the same. If we change  $X$  into  $Y$  in the definition of  $\xi$ , the value of  $\xi$  is the same.

Note that, when we consider classical links, then  $\xi = 0$  in all cases.

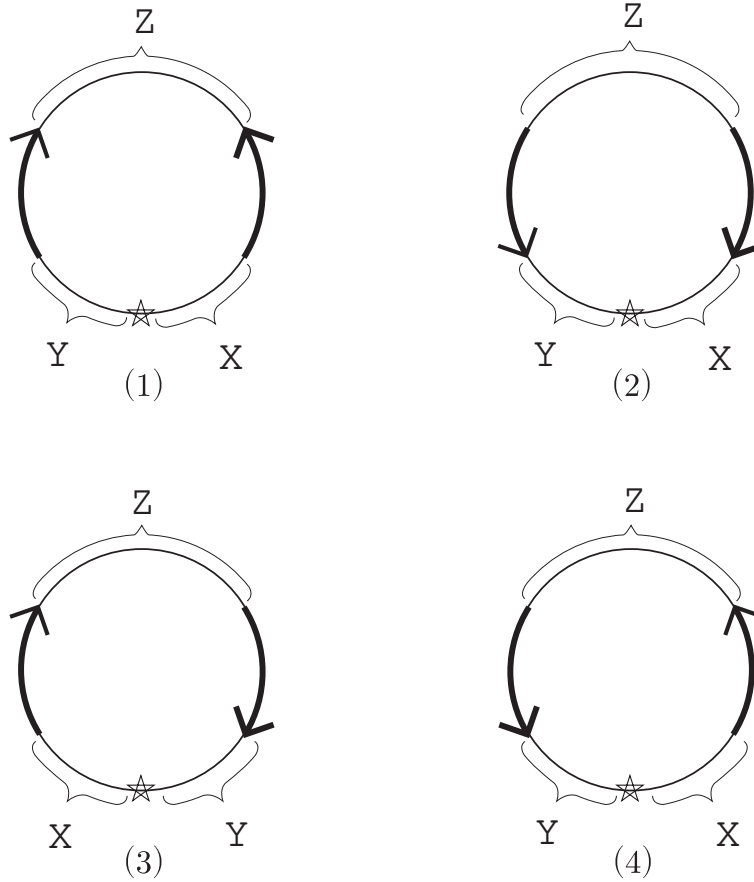


FIGURE 5.15. Figures associated with the definition of  $\xi$  in Definition 5.21.(2).

**Remark 5.23.** In the case of Figure 5.15.(1) and (2),  $Z$  does not make an immersed circle before (respectively, after) this surgery, because it is a single cycle surgery. See Figure 5.16 for an example. Hence we cannot claim that the parity of the number of cut loci in  $Z$  is zero, unlike the case of Figure 5.15.(3) and (4). Therefore we can not conclude that the parity of the number of cut loci in  $X$  is equivalent to that in  $Y$ , unlike the case of Figure 5.15.(3) and (4). We cannot determine which we choose that of  $X$  or that of  $Y$ . One way of settling this situation is defining the coefficient in the differential associated with single cycle surgeries to be zero. More precisely: As written in (1) right above Definition 5.21.(1), if  $A_i$  and  $A_j$  are given as in Fact 5.19, then we define  $c[A_i; A_j] = 0$ . Recall Remark 5.22. We can summarize this by saying that the coefficient that corresponds to a single cycle surgery is taken to be zero.

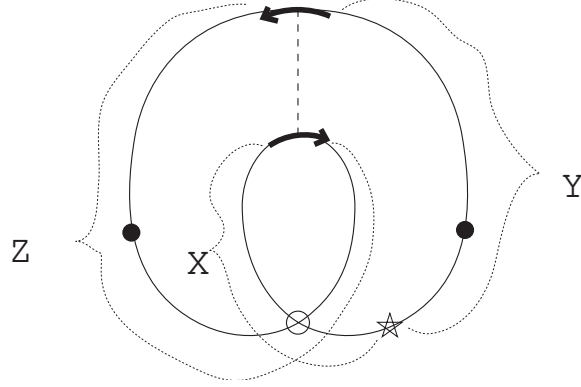


FIGURE 5.16. A resolution configuration with cut loci and a starting star

**Definition 5.21.(3)** The definition of  $\zeta((D_L(u), x), (D_L(v), y))$ . In order to define  $\zeta((D_L(u), x), (D_L(v), y))$ , we need to check only four cases of surgeries along each arc, which are drawn in Figure 5.17. Here,  $\Delta_*$ ,  $\nabla_*$ ,  $M_*$ , and  $W_*$  denote a labeled resolution configuration, and  $\alpha_*$ ,  $\alpha_{\#i}$ ,  $\beta_*$ ,  $\gamma_*$ ,  $\sigma_*$  an immersed circle. We carry out one surgery in each of Figures 5.17.(1)-(4). We define the number  $\xi(\alpha_*)$  (respectively,  $\xi(\alpha_{\#i})$ ,  $\xi(\beta_*)$ ,  $\xi(\gamma_*)$ , and  $\xi(\sigma_*)$ ) for this surgery and an immersed circle  $\alpha_*$  (respectively,  $\alpha_{\#i}$ ,  $\beta_*$ ,  $\gamma_*$ ,  $\sigma_*$ ). We define

$$\begin{aligned} \zeta(\Delta_1, \Delta_2) &= \xi(\alpha_{22}) \\ \zeta(\Delta_1, \Delta_3) &= \xi(\alpha_{31}) \\ \zeta(\nabla_1, \nabla_2) &= \xi(\beta_1) + \xi(\beta_2) + \xi(\beta_3) \\ \zeta(M_1, M_2) &= \xi(\gamma_2) + \xi(\gamma_3) \\ \zeta(W_1, W_2) &= 0. \end{aligned}$$

**Remark.** In the case of Figures 5.17.(1), we have two cases  $\zeta(\Delta_1, \Delta_2)$  and  $\zeta(\Delta_1, \Delta_3)$ . The coefficient is defined for each pair of enhanced Kauffman states.

By an explicit calculation, we have the following.

**Theorem 5.24.** ([37]) For  $\delta$  in Definition 5.21, we have  $\delta \cdot \delta = 0$ . That is, the  $\mathbb{Z}$  coefficient Khovanov homology for virtual links is defined.

Thus Definition 5.21 is well-defined.

This homology of  $L$  is the same as that of  $-L$ .

**Definition 5.25.** Let  $L$  be a virtual link diagram. Take the Khovanov chain complex for  $L$ . The Khovanov chain complex with the differential yields the *Khovanov homology for the virtual link diagram  $L$* . Let  $A_i$  be each resolution configuration made from  $L$

$$(1) \quad \begin{array}{c} \alpha_1 \\ \circ \\ \text{---} \\ \circ \\ \text{---} \\ \text{x}_+ \\ \Delta_1 \end{array} \longrightarrow \begin{array}{c} \left( \begin{array}{cc} \alpha_{21} & \alpha_{22} \\ \circ & \circ \\ \text{x}_+ & \text{x}_- \end{array} \right) + \left( \begin{array}{cc} \alpha_{31} & \alpha_{32} \\ \circ & \circ \\ \text{x}_- & \text{x}_+ \end{array} \right) \\ \Delta_2 \qquad \qquad \qquad \Delta_3 \end{array}$$

$$(2) \quad \begin{array}{c} \beta_1 \\ \circ \\ \text{---} \\ \circ \\ \text{---} \\ \text{x}_- \\ \nabla_1 \end{array} \longrightarrow \begin{array}{c} \left( \begin{array}{cc} \beta_2 & \beta_3 \\ \circ & \circ \\ \text{x}_- & \text{x}_- \end{array} \right) \\ \nabla_2 \end{array}$$

$$(3) \quad \begin{array}{c} \left( \begin{array}{cc} \gamma_1 & \gamma_2 \\ \circ & \circ \\ \text{---} & \text{---} \\ \text{x}_+ & \text{x}_- \end{array} \right) \longrightarrow \begin{array}{c} \gamma_3 \\ \circ \\ \text{x}_- \\ \text{M}_2 \end{array} \\ \text{M}_1 \end{array}$$

$$(4) \quad \begin{array}{c} \left( \begin{array}{cc} \sigma_1 & \sigma_2 \\ \circ & \circ \\ \text{---} & \text{---} \\ \text{x}_+ & \text{x}_+ \end{array} \right) \longrightarrow \begin{array}{c} \sigma_3 \\ \circ \\ \text{x}_+ \\ \text{W}_2 \end{array} \\ \text{W}_1 \end{array}$$

Now  $\left( \begin{array}{cc} \circ & \circ \\ \text{---} & \text{---} \\ \text{x}_- & \text{x}_+ \end{array} \right) \longrightarrow \begin{array}{c} \circ \\ \text{x}_- \end{array}$  is explained by (3).

FIGURE 5.17. We define  $\mathfrak{E}$  by using these figures.

( $i \in \Lambda$ ). Note that  $\Lambda$  is a finite set. Then  $\{A_i\}_{i \in \Lambda}$  is the basis of Khovanov chain complex for  $L$ . We call each  $A_i$  *Khovanov basis element* ( $i \in \Lambda$ ), and  $\{A_i\}_{i \in \Lambda}$  *Khovanov basis*.

Let  $Kh^{q,i}(L)$  (respectively,  $C^{q,i}(L)$ ) denote Khovanov homology (respectively, Khovanov chain complex) with the  $\mathbb{Z}$  coefficient of quantum grading  $q$  and homological grading  $i$  for a virtual link diagram  $L$ . We sometimes omit the words,  $\mathbb{Z}$  coefficient, when it is clear from the context.

By using the Khovanov chain complex  $C^{q,i}(L; \mathbb{Z})$ , we can define the Khovanov chain complex  $C^{q,i}(L; \mathbb{Z}_2)$ , and the Khovanov homology  $Kh^{q,i}(L; \mathbb{Z}_2)$  with  $\mathbb{Z}_2$  coefficients, quantum grading  $q$  and homological grading  $i$  for a virtual link diagram  $L$ .

See [6, 37, 40]. For a fixed virtual link diagram and its associated Khovanov chain complex, Khovanov homology is independent of the placement of the starting star in each immersed circle of each labeled resolution configuration. Khovanov homology for a given virtual link diagram  $L$  does not change by Reidemeister moves on  $L$ . Thus the following is well-defined.

**Definition 5.26.** Let  $\mathcal{L}$  be a virtual link. Let  $L$  be a virtual link diagram which represents  $\mathcal{L}$ . Define Khovanov homology  $Kh^{q,i}(\mathcal{L})$  to be  $Kh^{q,i}(L)$  for  $L$ . We can define  $Kh^{q,i}(\mathcal{L}; \mathbb{Z}_2)$ , as well.

The Jones polynomial of any virtual link  $L$  is a graded Euler characteristic of the  $\mathbb{Z}$ -coefficient Khovanov homology of  $L$ . See [6, 37].

**Definition 5.27.** Take  $L$  and  $\mathcal{L}$  above. Use  $\text{Hom}(C^{q,i}(L; \mathbb{Z}), \mathbb{Z})$ , and  $\langle \partial a, \alpha \rangle = \langle a, \delta \alpha \rangle$  for a dual chain  $a$  and a Khovanov chain  $\alpha$ , where  $\langle, \rangle$  is the Kronecker product as usual. Thus we can define the *dual Khovanov chain complex*  $C_{q,i}(L)$ , and the *homology of the dual Khovanov chain complex*,  $Kh_{q,i}(L)$ . We can define  $Kh_{q,i}(\mathcal{L}; \mathbb{Z}_2)$ , as well. It does not matter if we write  $K_{q,i}(L)$  (respectively,  $C_{q,i}(L)$ ) as  $K_i^q(L)$  (respectively,  $C_i^q(L)$ ).

Let  $A_i$  be each Khovanov basis element for a virtual link diagram  $L$  ( $i \in \Lambda$ , where  $\Lambda$  is a finite set). Let  $a_i$  ( $i \in \Lambda$ ) be each basis element of the dual Khovanov chain complex for  $L$  such that  $\langle A_l, a_k \rangle = \delta_{l,k}$  for two arbitrary elements,  $l$  and  $k$ , in  $\Lambda$ . We call each  $a_i$  the *dual Khovanov basis element* of the dual Khovanov chain complex for  $L$ , and  $\{a_i\}$  *dual Khovanov basis*. We call the dual Khovanov basis element the Khovanov basis element when it is clear from the context what is meant.

Define the homological grading  $\text{gr}_h a_i$  to be  $\text{gr}_h A_i$  for any  $i \in \Lambda$ .

Let  $\{a_*\}_{* \in \Lambda}$  be the dual Khovanov basis. Define a partial order  $\prec$  on the set  $\{a_*\}_{* \in \Lambda}$  as follows: Let  $k, l \in \Lambda$ .  $a_k \prec a_l$  if and only if  $A_l \prec A_k$ .

Define  $c[a_l; a_k]$  to be the coefficient in  $\partial a_k = \sum_{l \in \Lambda} c[a_l; a_k] a_l$ . Note that  $c[a_l; a_k] = c[A_k; A_l]$ .

**Theorem 5.28.** *Let  $\mathcal{L}$  be a classical link. Note that  $\mathcal{L}$  is a virtual link since any classical link is also a virtual link. Then the virtual Khovanov homology for the link  $\mathcal{L}$  is the original Khovanov homology for the link  $\mathcal{L}$  as a classical link.*

**Proof of Theorem 5.28.** Recall  $\mathcal{A}(\alpha^{no}, \beta^{no})$  in Remark 5.22.

Let  $K$  be a classical link diagram. Note that there is no cut loci in any Kauffman state made from  $K$  if we use the rule in Figure 5.4. Hence we do not need  $\mathcal{P}(\ , \ )$  when we define the coefficient. We have the following.

**Claim 5.29.** *Let  $K$  be a classical link diagram. The Khovanov chain complex of  $K$  defined by the coefficients  $\mathcal{A}(\alpha^{no}, \beta^{no})$  is chain isomorphic to that by  $\mathcal{O}(\alpha^{no}, \beta^{no})$ .*

**Proof of Claim 5.29.** If the number of classical crossings of a given virtual link diagram is zero, Claim 5.29 is true.

Let  $K$  be a virtual link diagram with  $m$  classical crossings.

Make all Kauffman states and all enhanced Kauffman states.

Let  $P$  be the poset of all (non-enhanced) Kauffman states made by the natural partial order on the set of the vectors.

Let  $x, y \in P$  satisfy the following condition: Only one component is different, comparing the components of  $x$  with those of  $y$ . Then we give  $+1$  or  $-1$  to the pair  $x, y \in P$  in two ways defined by  $\mathcal{O}(\ , \ )$  and  $\mathcal{A}(\ , \ )$ .

Let  $i, j \in \{1, \dots, n+1\}$ . Let

$$\begin{aligned} v_{00} &= (\dots, v_{i-1}, 0, v_{i+1}, \dots, v_{j-1}, 0, v_{j+1}, \dots) \\ v_{01} &= (\dots, v_{i-1}, 0, v_{i+1}, \dots, v_{j-1}, 1, v_{j+1}, \dots) \\ v_{10} &= (\dots, v_{i-1}, 1, v_{i+1}, \dots, v_{j-1}, 0, v_{j+1}, \dots) \\ v_{11} &= (\dots, v_{i-1}, 1, v_{i+1}, \dots, v_{j-1}, 1, v_{j+1}, \dots). \end{aligned}$$

By the definition of  $\mathcal{A}(\ , \ )$ , we have

$$(5.4) \quad \mathcal{A}(v_{00}, v_{01})\mathcal{A}(v_{01}, v_{11}) = -\mathcal{A}(v_{00}, v_{10})\mathcal{A}(v_{10}, v_{11}).$$

By the definition of  $\mathcal{O}(\ , \ )$ , we have

$$(5.5) \quad \mathcal{O}(v_{00}, v_{01})\mathcal{O}(v_{01}, v_{11}) = -\mathcal{O}(v_{00}, v_{10})\mathcal{O}(v_{10}, v_{11}).$$

Thus we obtain a co-chain complex  $C_{\mathcal{O}}$  (respectively,  $C_{\mathcal{A}}$ ) whose basis is  $P$  which is made by  $\mathcal{O}(\ , \ )$  (respectively,  $\mathcal{A}(\ , \ )$ ).

We assume the following.

**Claim.** *Let  $n \in \mathbb{N}$ . There is a chain isomorphism from  $C_{\mathcal{O}}$  to  $C_{\mathcal{A}}$  if  $m = n$ .*

Therefore Claim 5.29 is valid if  $m = n$ .

We prove that Claim is true if  $m = n + 1$ . Then Claim 5.29 is valid for all  $m \in \{0\} \cup \mathbb{N}$ .

Let  $P'$  (respectively,  $P''$ ) be a subposet of  $P$ , made of all (non-enhanced) Kauffman states with the vector  $v_{n+1} = 0$  (respectively,  $v_{n+1} = 1$ ).

Make cochain complexes  $C_{\mathcal{O}}$ ,  $C_{\mathcal{A}}$ ,  $C'_{\mathcal{O}}$ ,  $C'_{\mathcal{A}}$ ,  $C''_{\mathcal{O}}$ , and  $C''_{\mathcal{A}}$ . Note that  $C'_{\mathcal{O}}$  and  $C''_{\mathcal{O}}$  are sub-cochain complex of  $C_{\mathcal{O}}$ , and that  $C'_{\mathcal{A}}$  and  $C''_{\mathcal{A}}$  are sub-cochain complex of  $C_{\mathcal{A}}$ .

By the assumption of the induction, we have chain isomorphisms  $f' : C'_{\mathcal{O}} \rightarrow C'_{\mathcal{A}}$  and  $f'' : C''_{\mathcal{O}} \rightarrow C''_{\mathcal{A}}$ .

We construct  $f : C_{\mathcal{O}} \rightarrow C_{\mathcal{A}}$  as below.

If  $\mathcal{O}((0, \dots, 0), (0, \dots, 1)) = \mathcal{A}((0, \dots, 0), (0, \dots, 1))$ ,  $f$  is defined by  $f'$  and  $f''$ .

If  $\mathcal{O}((0, \dots, 0), (0, \dots, 1)) = -\mathcal{A}((0, \dots, 0), (0, \dots, 1))$ ,  $f$  is defined by  $f'$  and  $-f''$ .

Then  $f$  is a chain isomorphism by the equations (5.4) and (5.5). □

Let  $K$  be a virtual link diagram. Make  $\mathcal{P}(\alpha, \beta)$  by using the rule in Figure 5.4. We ask a question. Can we define a cochain complex by using  $\mathcal{A}(\alpha^{\text{no}}, \beta^{\text{no}})\mathcal{P}(\alpha, \beta)$ ? If so, is the cochain complex chain isomorphic (or chain homotopy equivalent) to that defined by the coefficients  $\mathcal{O}(\alpha^{\text{no}}, \beta^{\text{no}})\mathcal{P}(\alpha, \beta)$ ? We know that we can use  $\mathcal{A}(\alpha^{\text{no}}, \beta^{\text{no}})$  in the classical case, but in the virtual case we only know at present how to make a consistent definition using  $\mathcal{O}(\alpha^{\text{no}}, \beta^{\text{no}})\mathcal{P}(\alpha, \beta)$ .

## 6. AN EXAMPLE OF KHOVANOV BASIS OF THE KHOVANOV CHAIN COMPLEX FOR A VIRTUAL LINK DIAGRAM

We show an example of Khovanov basis of a Khovanov chain complex for a virtual link diagram in Figures 6.1 and 6.2, and another one in Figures 6.3-6.6. We draw posets of decorated resolution configurations in Figures 6.5 and 6.6.

### Part 3. Khovanov-Lipshitz-Sarkar CW complexes and the second Steenrod square for virtual links

#### 7. FRAMED FLOW CATEGORY: FRAMINGS, MDULIS, AND CW COMPLEXES

As we announced in §2, we will make a CW complex from a Khovanov chain complex for a given virtual link diagram. We assign to a given chain complex, which is not

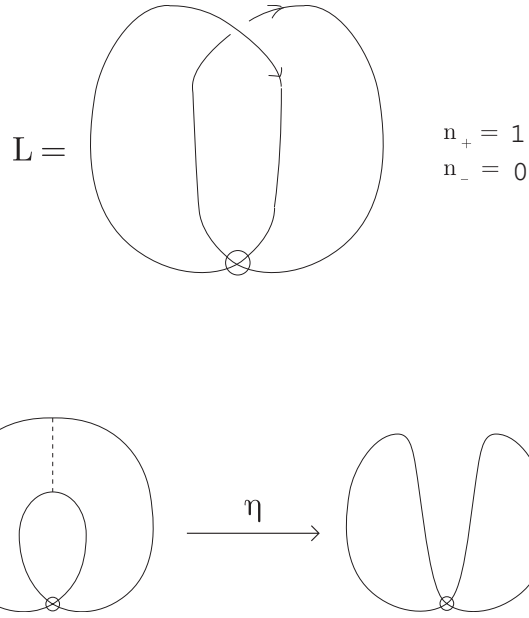


FIGURE 6.1. A virtual link  $L$ , and the relation, which is made by surgeries, among all (non-labeled) resolution configurations made from  $L$ . See Definition 5.17 for the definition of  $n_+$  and  $n_-$ .  $\eta$  denotes a single cycle surgery.

necessarily a Khovanov chain complex, a framed flow category (framings and moduli). For our purpose, we consider a stable homotopy type of CW complexes whose chain complex is a given one.

**Example 7.1.** Both  $\Sigma^k$  (the one point union of  $S^2 \cup S^4$ ) and  $\Sigma^k(\mathbb{C}P^2)$ , where  $\Sigma^k$  denotes the  $k$ -times suspension and  $k$  is large, have a natural CW decomposition (the base point)  $\cup e^{2+k} \cup e^{4+k}$ . Consider a set of moduli spaces associated with  $\Sigma^k$  (the one point union of  $S^2 \cup S^4$ ) (respectively,  $\Sigma^k(\mathbb{C}P^2)$ ). In  $\partial e^{2+k}$ , there is no moduli space. In  $\partial e^{4+k}$ , take an embedded circle. It is a moduli space. Take the normal bundle of the circle in  $\partial e^{4+k}$ , and take the trivial (respectively, nontrivial) framing. It is a framing on the moduli space.

**Example 7.2.** Regard  $D^2$  as a union of the base point, a 1-cell  $e^1$ , and 2-cell  $e^2$ . We can regard  $\Sigma^k(D^2)$  as a union of the base point, a  $(k+1)$ -cell  $e^{k+1}$ , and  $(k+2)$ -cell  $e^{k+2}$ . In  $\partial e^{k+1}$ , there is no moduli. In  $\partial e^{k+2}$ , take one point. It is a moduli space. The framing on the normal bundle of the point in  $\partial e^{k+2}$  is unique after we give an orientation.



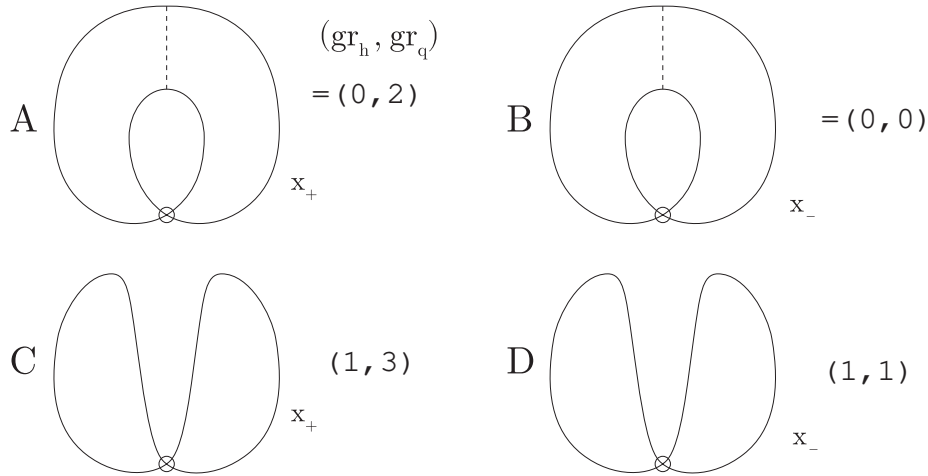


FIGURE 6.2. The Khovanov basis of Khovanov chain complex for the virtual link diagram  $L$  in Figure 6.1: They are all labeled resolution configurations made from  $L$ .  $gr_h$  denotes the homological degree, and  $gr_q$  the quantum one. We have  $\delta(A) = \delta(B) = \delta(C) = \delta(D) = 0$ . Recall Fact 5.19, which is an important comment on a single cycle surgery.

In short, for any given chain complex, once we have moduli spaces in each cell, and framings on them, we have a CW complex by the generalized Pontrjagin-Thom construction. Note that the chain complex may not be a Khovanov chain complex. There is more than one way to associate a framed flow category (See Definition 3.12 of [29] in page 4 of this paper, [29, §3.3 and §4] and [31, §3.3].) to a chain complex in general. The cube moduli in [29, §4] for Khovanov chain complexes of classical links lets Lipshitz and Sarkar choose a specific way to make the framed flow category.

## 8. THE LADYBUG CONFIGURATION FOR CLASSICAL LINK DIAGRAMS

We review the ladybug configuration for classical link diagrams, which is introduced in [29, section 5.4]. Lipshitz and Sarkar introduced it to define a CW complex for any classical link digram. We cite the definition of it, that of the right pair, and that of the left pair associated with it from [29, section 5.4.2].

**Definition 8.1.** ([29, Definition 5.6]). An index 2 basic resolution configuration  $D$  is said to be a ladybug configuration if the following conditions are satisfied (See Figure 8.1.).

- $Z(D)$  consists of a single circle, which we will abbreviate as  $Z$ ;

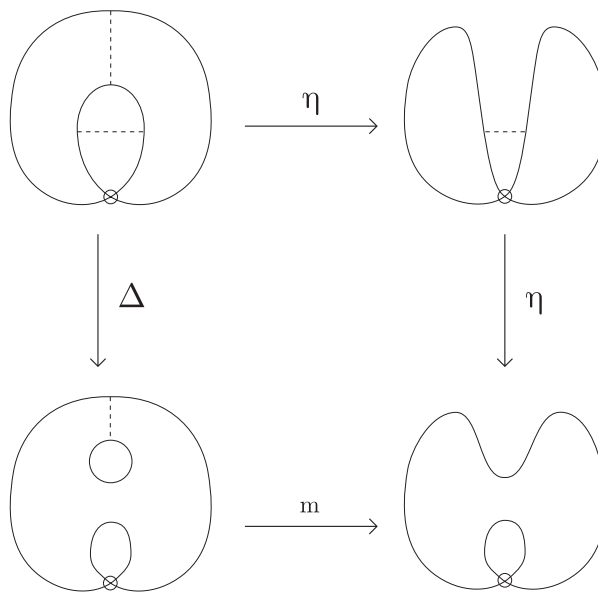
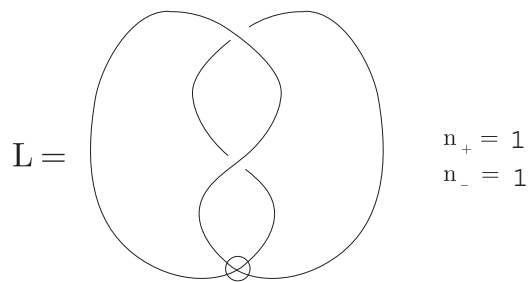


FIGURE 6.3. A virtual link  $L$ , and the relation, which is made by surgeries, among all (non-labeled) resolution configurations made from  $L$ . See Definition 5.17 for the definition of  $n_+$  and  $n_-$ .  $\eta$  denotes a single cycle surgery.

- The endpoints of the two arcs in  $A(D)$ , say  $A_1$  and  $A_2$ , alternate around  $Z$  (that is,  $\partial A_1$  and  $\partial A_2$  are linked in  $Z$ ).

**Definition 8.2.** ([29, section 5.4.2]). Let  $Z$  denote the unique circle in  $Z(D)$ . The surgery  $s_{A_1}(D)$  (respectively,  $s_{A_2}(D)$ ) consists of two circles; denote these  $Z_{1,1}$  and  $Z_{1,2}$  (respectively,  $Z_{2,1}$  and  $Z_{2,2}$ ); that is,  $Z(s_{A_i}(D)) = \{Z_{i,1}, Z_{i,2}\}$ . Our main goal is to find a

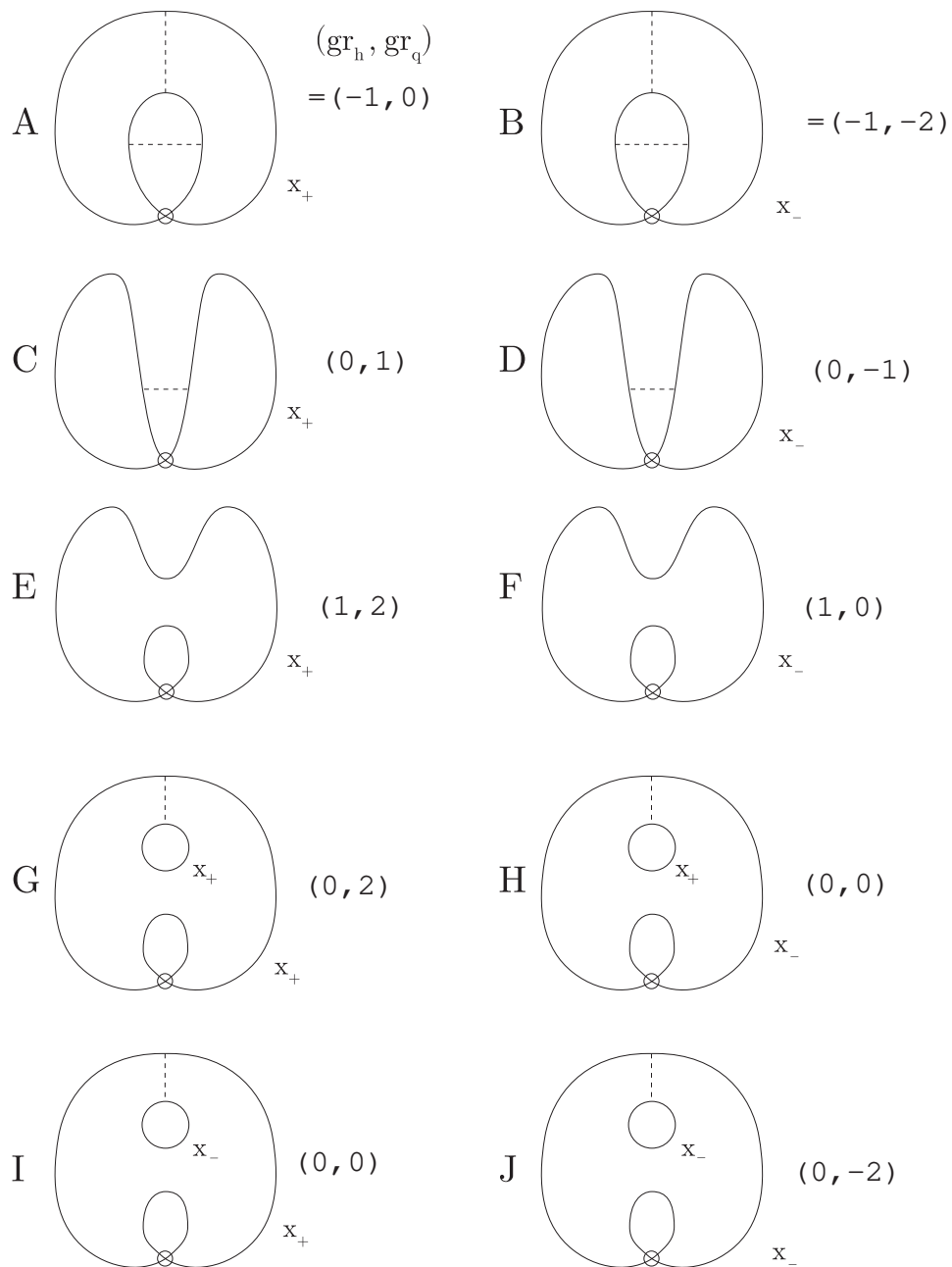


FIGURE 6.4. The Khovanov basis of Khovanov chain complex for the virtual link diagram  $L$  in Figure 6.3: They are all labeled resolution configurations made from  $L$ .  $gr_h$  denotes the homological degree, and  $gr_q$  the quantum one.

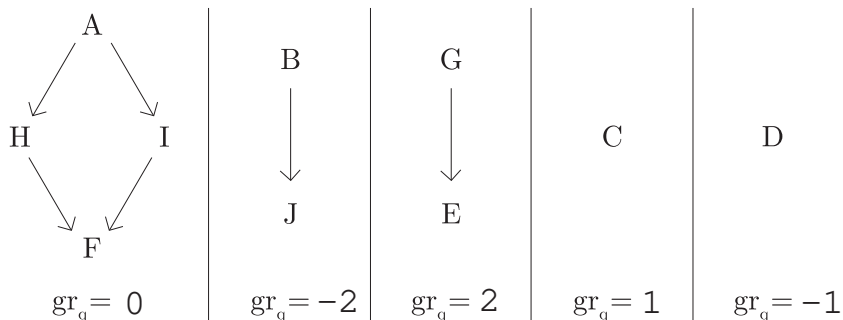


FIGURE 6.5. The relation, which is made by surgeries, among all Khovanov basis elements in Figure 6.3. Let  $P$  and  $Q$  be labeled resolution configurations. If  $c[P; Q] \neq 0$ , we connect  $P$  and  $Q$  by an arrow from  $P$  to  $Q$ . There are five chunks. All Khovanov basis elements in each chunk have the same quantum grading. Note that if  $c[P; Q] \neq 0$ , then  $c[P; Q] = \pm 1$ . Recall that whether  $+1$  or  $-1$  is determined by using starting stars and cut loci. Recall Fact 5.19, which is an important comment on a single cycle surgery.

bijection between  $\{Z_{1,1}, Z_{1,2}\}$  and  $\{Z_{2,1}, Z_{2,2}\}$ ; this bijection will then tell us which points in  $\partial_{\text{exp}}\mathcal{M}(x, y)$  to identify.

As an intermediate step, we distinguish two of the four arcs in  $Z - (\partial A_1 \cup \partial A_2)$ . Assume that the point  $\infty \in S^2$  is not in  $D$ , and view  $D$  as lying in the plane  $S^2 - \{\infty\} \cong \mathbb{R}^2$ . Then one of  $A_1$  or  $A_2$  lies outside  $Z$  (in the plane) while the other lies inside  $Z$ . Let  $A_i$  be the inside arc and  $A_o$  the outside arc. The circle  $Z$  inherits an orientation from the disk it bounds in  $\mathbb{R}^2$ . With respect to this orientation, each component of  $Z - (\partial A_1 \cup \partial A_2)$  either runs from the outside arc  $A_o$  to an inside arc  $A_i$  or vice-versa. The *right pair* is the pair of components of  $Z - (\partial A_1 \cup \partial A_2)$  which run from the outside arc  $A_o$  to the inside arc  $A_i$ . The other pair of components is the *left pair*. See [29, Figure 5.1].

We explain why the ladybug configuration is important, below.

**Proposition 8.3.** *Let  $\mathbf{x}$  (respectively,  $\mathbf{y}$ ) be a labelled resolution configuration of homological grading  $n$  (respectively,  $n + 2$ ). Then the cardinality of the set*

*$\{p | p \text{ is a labelled resolution configuration. } \mathbf{x} \prec p, p \prec \mathbf{y}, p \neq \mathbf{x}, p \neq \mathbf{y}\}$  is 0, 2, or 4, where  $\prec$  is defined in Definition 5.15.*

Let  $D$  be the ladybug configuration. Give  $D$  (respectively,  $s(D)$ ) a labeling  $x_+$  (respectively,  $x_-$ ). We call the resultant labeled resolution configuration  $(D, x)$  (respectively,  $(s(D), y)$ ). The resultant decorated resolution configuration  $(D, y, x)$  is called the *decorated resolution configuration associated with the ladybug configuration  $D$* . We draw the poset of  $(D, y, x)$  in Figure 8.2.

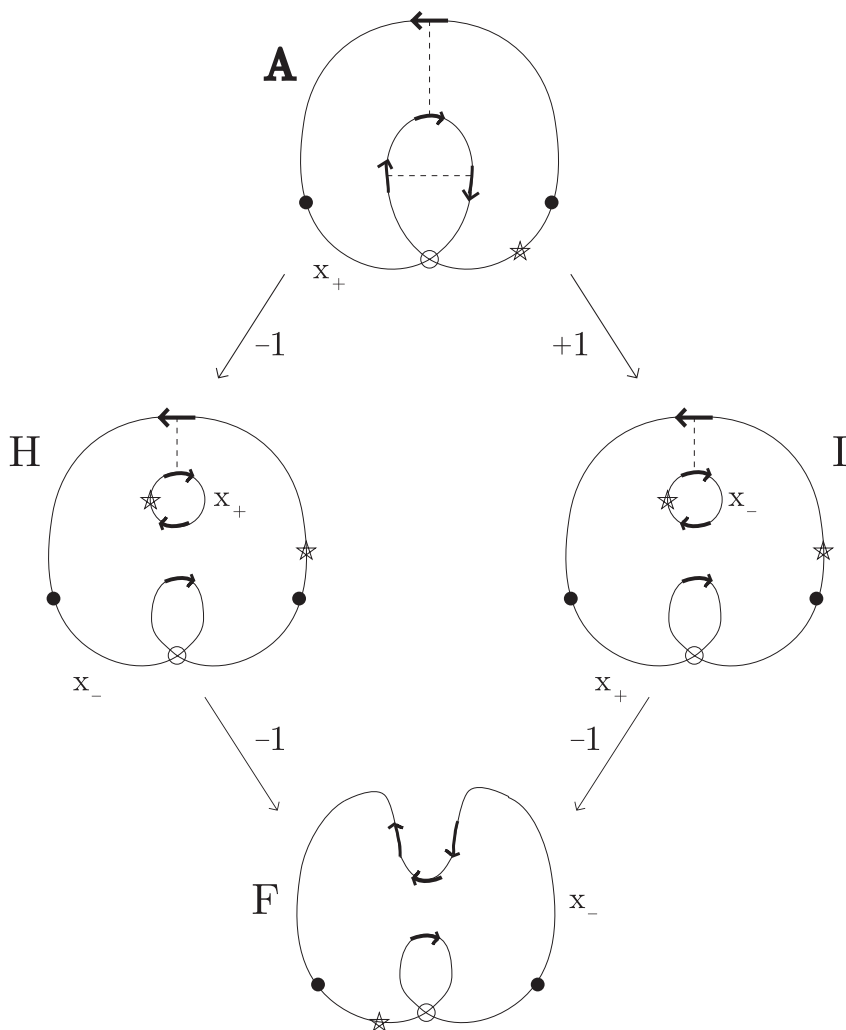


FIGURE 6.6. Examples of starting stars, cut loci, and  $\zeta(\ )$ : By the above calculation, we know that  $\delta \cdot \delta(A) = 0$ .

**Fact 8.4.** *The case of 4 in Proposition 8.3 occurs when we have the decorated resolution configuration associated with the ladybug configuration.*

Fact 8.4 is also explained in [29, section 5.4].

**Proposition 8.5.** ([29, §6].) *The stable homotopy type of the Khovanov-Lipshitz-Sarkar construction for classical link diagrams does not depend on whether we use the right pair or the left pair of each ladybug configuration in the classical link case when we construct Khovanov-Lipshitz-Sarkar CW complexes.*

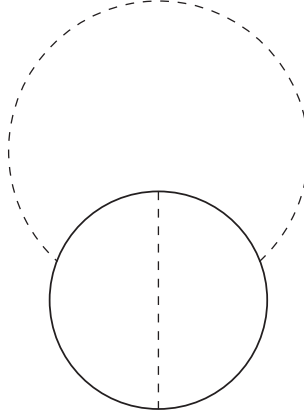


FIGURE 8.1. **The ladybug configuration**

**Proposition 8.6.** (This follows from results in [29]. See the comments below.)  
*The stable homotopy type of the Khovanov-Lipshitz-Sarkar construction for classical link diagrams does not depend on the choice of framing on modulis.*

Of course Proposition 8.6 does not hold in the general case of construction of CW complexes. See Example 7.1: Framings change the stable homotopy types of CW complexes.

However, Proposition 8.6 is true in this case. Example 7.2 is an example of a sub CW complex of a Khovanov CW complex. In Example 7.2, we use a framing when we construct a CW complex, but framings do not play such an important role, comparing Example 7.1.

Proposition 8.6 is the same as [29, (4) in the first part of section six], which is proved in the proof of [29, Proposition 6.1]: In three lines above [31, Definition 3.4], it is written, “all such framings lead to the same Khovanov homotopy type [29, Proposition 6.1]”. See also [29, Lemma 4.13, which is cited in the proof of Proposition 6.1].

It is an outstanding property of the Khovanov chain complex and Khovanov stable homotopy type for classical links that, if  $\mathcal{M}_{\mathcal{C}_K(L)}(\mathbf{x}, \mathbf{y}) \neq \phi$ , each connected component of  $\mathcal{M}_{\mathcal{C}_K(L)}(\mathbf{x}, \mathbf{y})$  is determined only by  $\text{gr}_h \mathbf{x} - \text{gr}_h \mathbf{y}$ . Chain complexes in other cases do not have this property in general.

Recall Remark 3.1. We mix the right pair and the left one.

## 9. LADYBUG CONFIGURATIONS AND QUASI-LADYBUG CONFIGURATIONS FOR VIRTUAL LINK DIAGRAMS

When we introduce the Steenrod square for virtual links, we also have the ladybug configuration. Furthermore, in the case of virtual links, we have quasi-ladybug configurations

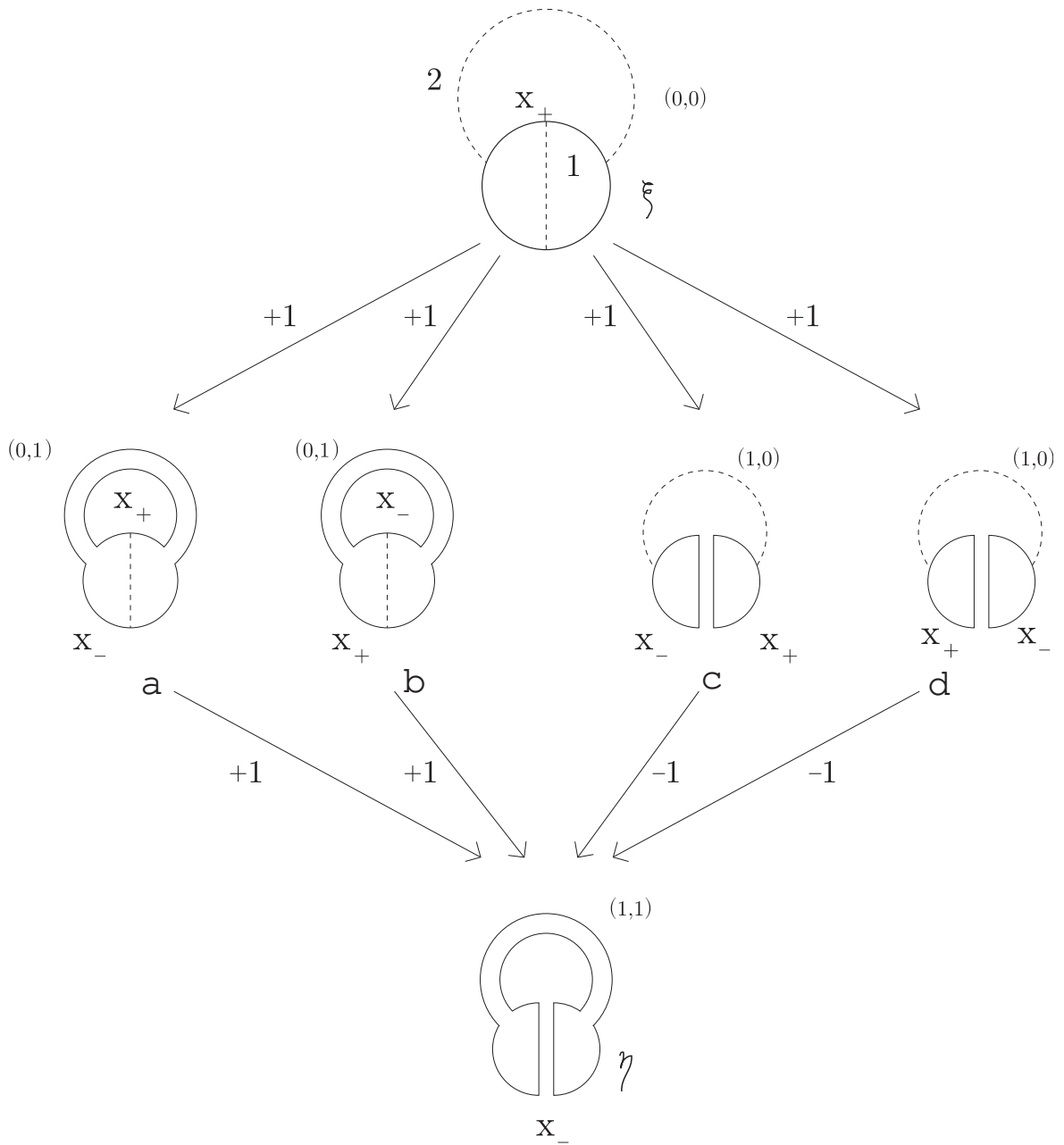


FIGURE 8.2. The boundary operator acting on the ladybug configuration: The notation  $a, b, c,$  and  $d$  are defined in [29, section 5.4.2]. In [29, Definition 2.2 and 2.15],  $(*, \#)$  is defined associated with arcs. The numbers  $+1$  and  $-1$  denote the coefficient [the labeled resolution configuration at the arrowtail; that at the arrowhead].

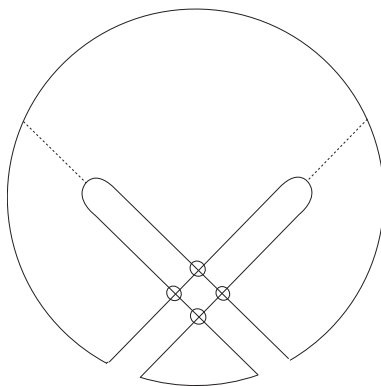


FIGURE 9.1. **A quasi-ladybug configuration**

that is different from the ladybug configuration.

Take a resolution configuration which is made of one immersed circle and two m-arcs.

Stand at a point in the immersed circle where you see an arc to your right. Go ahead along the immersed circle. Go around one time. Assume that you encounter the following pattern: In the order of travel you next touch the other arc. Then you touch the first arc. Then you touch the other arc again. Finally, you came back the point at the beginning.

Since both arcs are m-arcs, both satisfy the following property: At both endpoints of each arc, you see the arc in the same side – either on the right hand side and on the left hand side.

If you see arcs both in the right hand side and in the left hand side (respectively, only in the right hand side) while you go around one time, the resolution configuration is called a *ladybug configuration* (respectively, *quasi-ladybug configuration*).

If a given resolution configuration has no virtual crossing, this definition of ladybug configurations is the same as that in §8.

No quasi-ladybug configuration appears if a given resolution configuration has no virtual crossing. However, a quasi-ladybug configuration may exist if a given resolution configuration has a virtual crossing. An example is drawn in Figure 9.1.

Let  $D$  be a ladybug configuration. Let  $C$  be the only one immersed circle in  $Z(D)$ . Cut  $C$  at the four points where the arcs meet the endpoints. The immersed circle is then divided into four pieces. Recall that, at the beginning point of your trip, you see an arc on the right hand side. The first and third pieces of the four, which you are in while your



trip, is the *right pair*, and call the other two the *left pair*. Note that the orientation of your trip and the place where you stand at the beginning of your trip do not change the right and the left pair. Note also that, if a given resolution configuration does not have a virtual crossing, this definition is the same as that in §8.

It is important that we cannot determine the right and left pair in the case of quasi-ladybug configurations by this method. (We pause to ask a question: Can one find a method to define the right and the left pair for quasi-ladybug configurations, to be compatible with the construction of Khovanov-Lipshitz-Sarkar stable homotopy type?)

Let  $D$  be a ladybug configuration (respectively, quasi-ladybug configuration). Make  $s(D)$ . Give  $D$  (respectively,  $s(D)$ ) a labeling  $x_+$  (respectively,  $x_-$ ). Call the resultant labeled resolution configuration  $(D, x)$  (respectively,  $(s(D), y)$ ). The decorated resolution configuration  $(D, y, x)$  is called the *decorated resolution configuration associated with the ladybug configuration (respectively, quasi-ladybug configuration)  $D$* . We draw the poset of an example in Figure 8.2 (respectively, Figure 9.2).  $P(D, y, x)$  includes four labeled resolution configurations other than  $(D, x)$  and  $(s(D), y)$ . We have two ways to make a 2-dimensional CW complex associated with  $P(D, y, x)$ .

In the case of ladybug configurations, by using the right and left pairs introduced above, we determine the right and left pair of the labeled resolution configurations in the middle row of the poset of the decorated resolution configuration associated with a given ladybug configuration as in [29, Figure 5.1 and its explanation in §5.4.2].

Recall Remark 3.1. In Lipshitz and Sarkar's paper [29] it is important how to assign to the ladybug configuration a moduli. They give all ladybug configurations one of the right and the left pair. That is, all ladybug configurations have the same pair. In our paper, we consider the following situation: Each ladybug configuration may have different pairs. We consider all cases. Therefore we may consider more than one set of moduli for one Khovanov chain complex. We discuss both the condition that Lipshitz and Sarkar[29] discussed and the condition that Lipshitz and Sarkar[29] did not discuss. See also Proposition 8.5 and Remark 13.3.

However, in the case of quasi-ladybug configurations, we cannot distinguish two cases. Therefore we make two CW complexes if there is a quasi-ladybug configuration. This means that we consider a multiplicity of Khovanov homotopy types and take the collection of them as an invariant, as we explain below.

Recall Remark 3.1. We mix the right pair and the left one.

**Remark 9.1.** In both Figures 8.2 and 9.2, we have the following identities of coefficients in the differentials.

$[\xi; a][a; \eta] = [\xi; b][b; \eta] = -[\xi; c][c; \eta] = -[\xi; d][d; \eta]$  and  $[\xi; *], [*; \eta], [\xi; *], [*; \eta] \in \{+1, -1\}$ , where  $*$  =  $a, b, c, d$ .

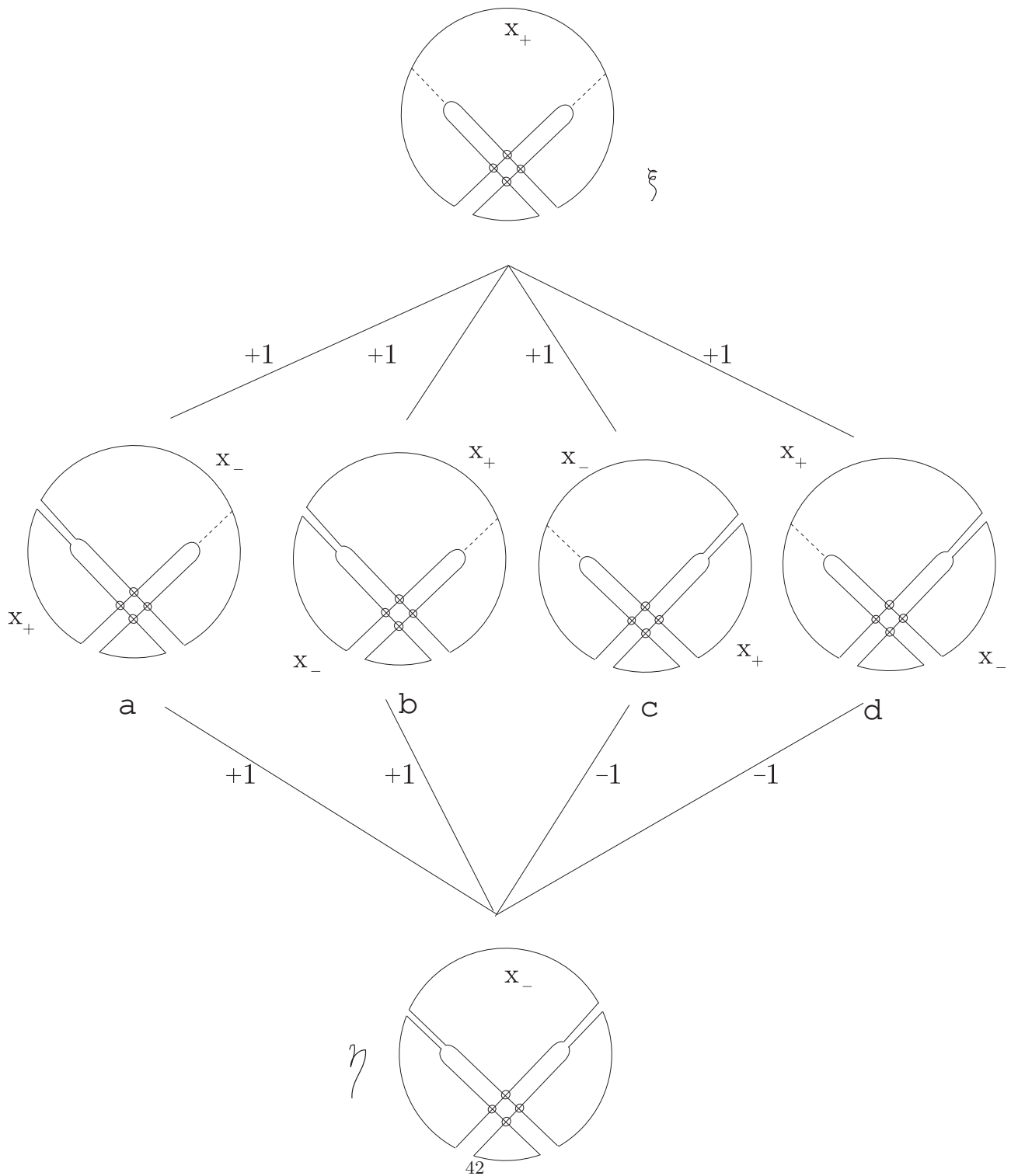


FIGURE 9.2. The decorated resolution configuration associated with a quasi-ladybug configuration

*Reason.* The vector (in Definition 5.3) of  $a$  and that of  $b$  are the same. That of  $c$  and that of  $d$  are the same. That of  $a$  (respectively,  $b$ ) is different from that of  $c$  (respectively  $d$ ).

Therefore the moduli of the decorated resolution configurations in Figures 8.2 and 9.2 is the disjoint union of two segments, and its boundary is  $a \amalg b \amalg c \amalg d$ . We have just two cases.

(i) One segment connects  $a$  and  $c$ , and the other  $b$  and  $d$ .

(ii) One segment connects  $a$  and  $d$ , and the other  $b$  and  $c$ .

We never have the following case: One segment connects  $a$  and  $b$ , and the other  $c$  and  $d$ .

*Reason.* If we choose “ $a \amalg b$ , and  $c \amalg d$ ”, then  $\delta \circ \delta \neq 0$  by the definition of  $\delta$  and therefore  $\partial \circ \partial \neq 0$ , associated with each moduli.

In the case of ladybug configurations, we can distinguish the cases (i) and (ii) above, by using the right and left pairs. However, in the case of quasi-ladybug configurations, we cannot distinguish them. As we wrote above, this means that, in general, we may associate more than one CW complex to a single virtual link diagram. See the following sections.

## 10. WHY IS IT MORE DIFFICULT TO DEFINE KHOVANOV-LIPSHITZ-SARKAR STABLE HOMOTOPY TYPE FOR VIRTUAL LINKS THAN FOR CLASSICAL LINKS?

In the following sections, we will define a second Steenrod square for virtual links that is stronger than Khovanov homology for virtual links. We use a CW complex associated with a dual Khovanov chain complex.

The presence of the single cycle zero map in the virtual Khovanov chain complex and  $\mathcal{P}(\alpha, \beta)$  in the coefficient of the virtual Khovanov chain complex take us out of the cube complex method for defining a framed flow category. For this reason we use a truncated homotopy type for this paper.

In the case of classical link diagrams, for Khovanov basis elements  $\mathbf{x} = (D_L(u), x)$  and  $\mathbf{y} = (D_L(v), y)$ , of the Khovanov chain complex of a classical link diagram  $L$ , we can assign to the moduli space

$$\mathcal{M}_{\mathcal{C}_K(L)}(\mathbf{x}, \mathbf{y}) = \mathcal{M}(D_L(v) - D_L(u), x|, y|),$$

a disjoint union of the  $\text{gr}_h \mathbf{x} - \text{gr}_h \mathbf{y}$  dimensional cube moduli. Here,  $\mathbf{y} \prec \mathbf{x}$ . On the other hand, in the case of virtual link diagrams, we cannot assign to the moduli space  $\mathcal{M}_{\mathcal{C}_K(L)}(\mathbf{x}, \mathbf{y}) = \mathcal{M}(D_L(v) - D_L(u), x|, y|)$  an  $m$ -dimensional cube, in general.

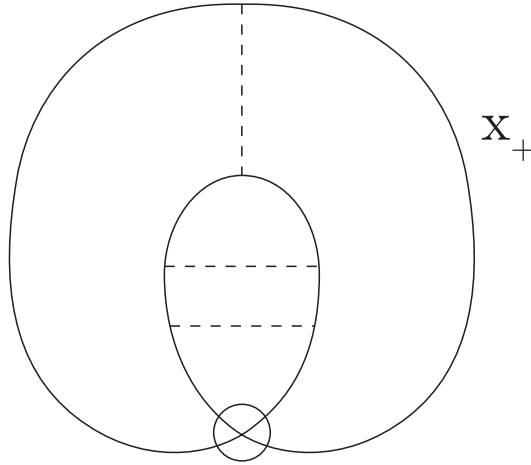


FIGURE 10.1. A labeled resolution configuration

An example is shown in Figures 10.1-10.4. A labeled resolution configuration  $A$  is drawn in Figure 10.1. The sequence of the labeled resolution configurations starting from  $A$  is drawn in Figure 10.2. Of course this sequence is made by surgery along arcs. A decorated resolution configuration associated with  $A$  is drawn in Figure 10.3. The poset of the decorated resolution configuration is drawn in Figure 10.4. Note that Figures 10.2 and 10.4 are different.

In [29, section 5.1] it is proved that, if  $\text{Ind}(D, x, y)=3$ ,  $\mathcal{M}(D, x, y)$  is a disjoint union of the 3-dimensional cube moduli in the case of classical link diagrams. However, Figure 10.4 indicates the following:  $\text{Ind}(D, x, y)=3$  does not imply that  $\mathcal{M}(D, x, y)$  is a disjoint union of the 3-dimensional cube moduli in general. Under this condition, if  $\text{Ind}(D, x, y) > 3$ , the situation would be more difficult. Therefore it is more difficult to define moduli spaces for Khovanov chain complex in the case of virtual links than in that of classical links.

We draw another poset in Figure 10.5: There is not a natural onto map from this poset to  $\mathcal{C}(3)$ . We can associate to this poset a moduli homeomorphic to the 2-disc, but it is not the 3-cube moduli  $\mathcal{M}_{\mathcal{C}(3)}(1, 0)$ .

We have two other reasons: Remark 10.1 and the comment below Remark 10.1.

**Remark 10.1.** See Figure 6.6. In the case of virtual link diagrams with virtual crossing points, we have the following. We have  $[A; H][H; F] = -[A; I][I; F] = 1$ , and we have the vector of  $H$  is the same as  $I$ .

In Figure 6.6, the moduli space  $\mathcal{M}(F, A)$  is one segment. Consider a map from this moduli to the 2-dimensional cube moduli which is written in [29, §5.1], and say  $\pi$ . The image of the boundary, just two points, of  $\mathcal{M}(F, A)$ , by this map is one point because the

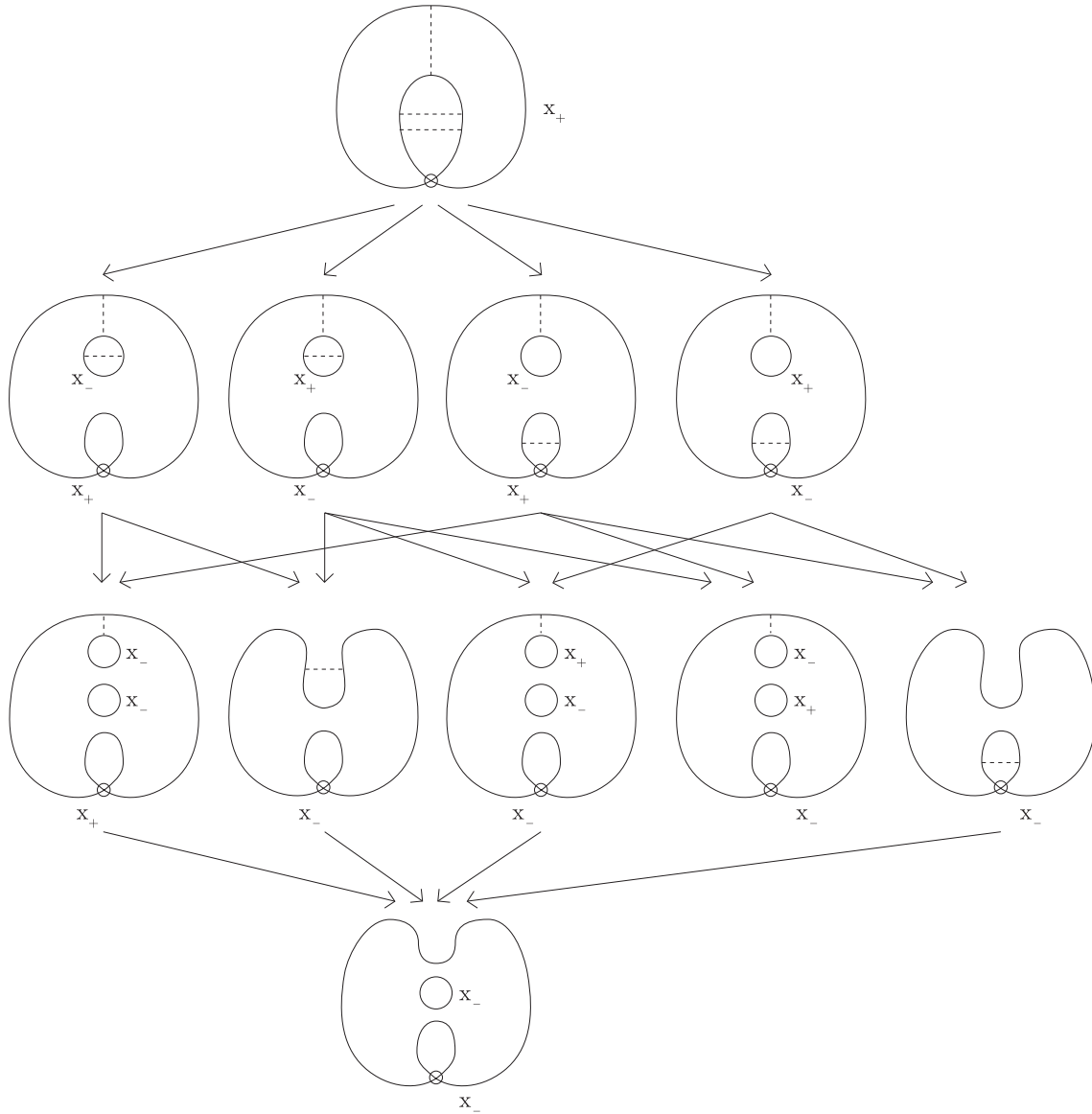


FIGURE 10.2. The sequence of the labeled resolution configurations made from a labeled resolution configuration in Figure 10.1

vector of  $H$  is the same as  $I$ . We do not have this phenomenon in the case of classical link diagrams.

Let  $x, p, q$  and  $y$  be labelled resolution configurations for a virtual link diagram  $D$  of a virtual link  $L$ . Suppose that  $[x; p][p; y] = -[x; q][q; y] = 1$ . If  $D$  does not have a virtual crossing, the vector (in Definition 5.3) of  $p$  is different from that of  $q$ . On the other hand,

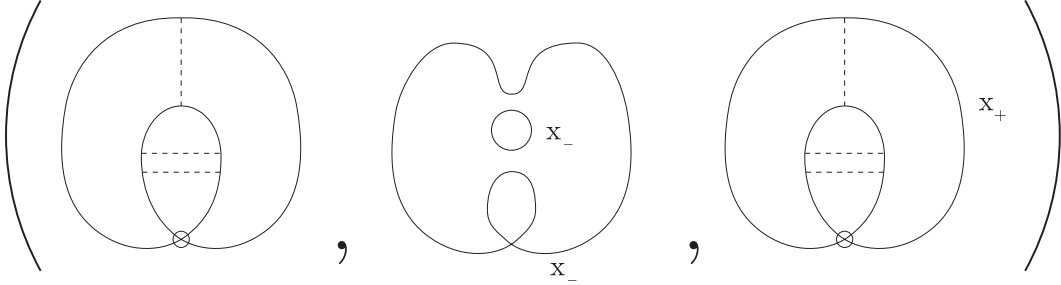


FIGURE 10.3. A decorated resolution configuration

if  $D$  has a virtual crossing, the vector of  $p$  is the same as that of  $q$  in some cases as written right above, and the former is different from the latter in the other cases.

As we stated in §9, we may have a quasi-ladybug configuration in general, in the case of non-classical link diagrams. Then we may associate more than one CW complex to a single virtual link diagram in general.

## 11. OUR STRATEGY OF THE CONSTRUCTION OF THE SECOND STEENROD SQUARE FOR VIRTUAL LINKS

We explain the detail of our strategy that we announced in §3

It is easy to prove that a dual Khovanov chain complex always associates no less than one CW complex (see for example [39, Theorem in Exercise 4, section 39, page 231]). However, we do not know whether we can define the moduli space consistently by only the information of the relations of Khovanov basis elements in general, in the virtual link case.

See [29, Definition 5.5]: Lipshitz and Sarkar use the  $(n - 1)$  cube moduli, which we call the ‘generating moduli’ for a classical link  $n$  crossings and define all moduli spaces and framings consistently for Khovanov chain complex of all classical link diagrams, and define the CW complex. They proved that the stable homotopy type of it is invariant under all Reidemeister moves.

Take a set of all CW complexes which are associated with the dual Khovanov chain complex for an arbitrary virtual link diagram. In fact, this set may be an invariant for virtual links if we can prove the invariance under Reidemeister moves. However, even if so, we do not know whether this invariant is stronger than Khovanov homology, nor whether we can calculate this invariant.

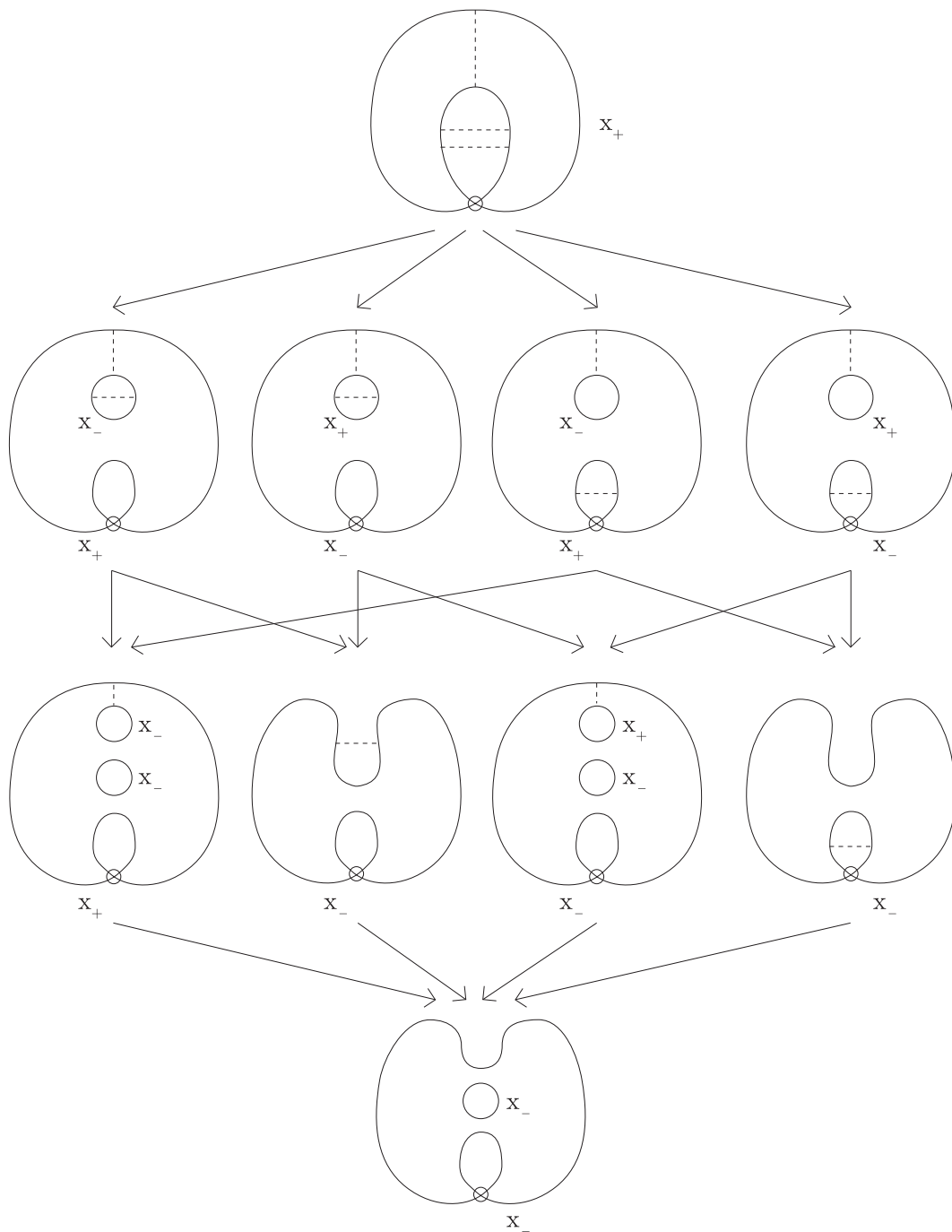


FIGURE 10.4. The poset of the decorated resolution configuration in Figure 10.3

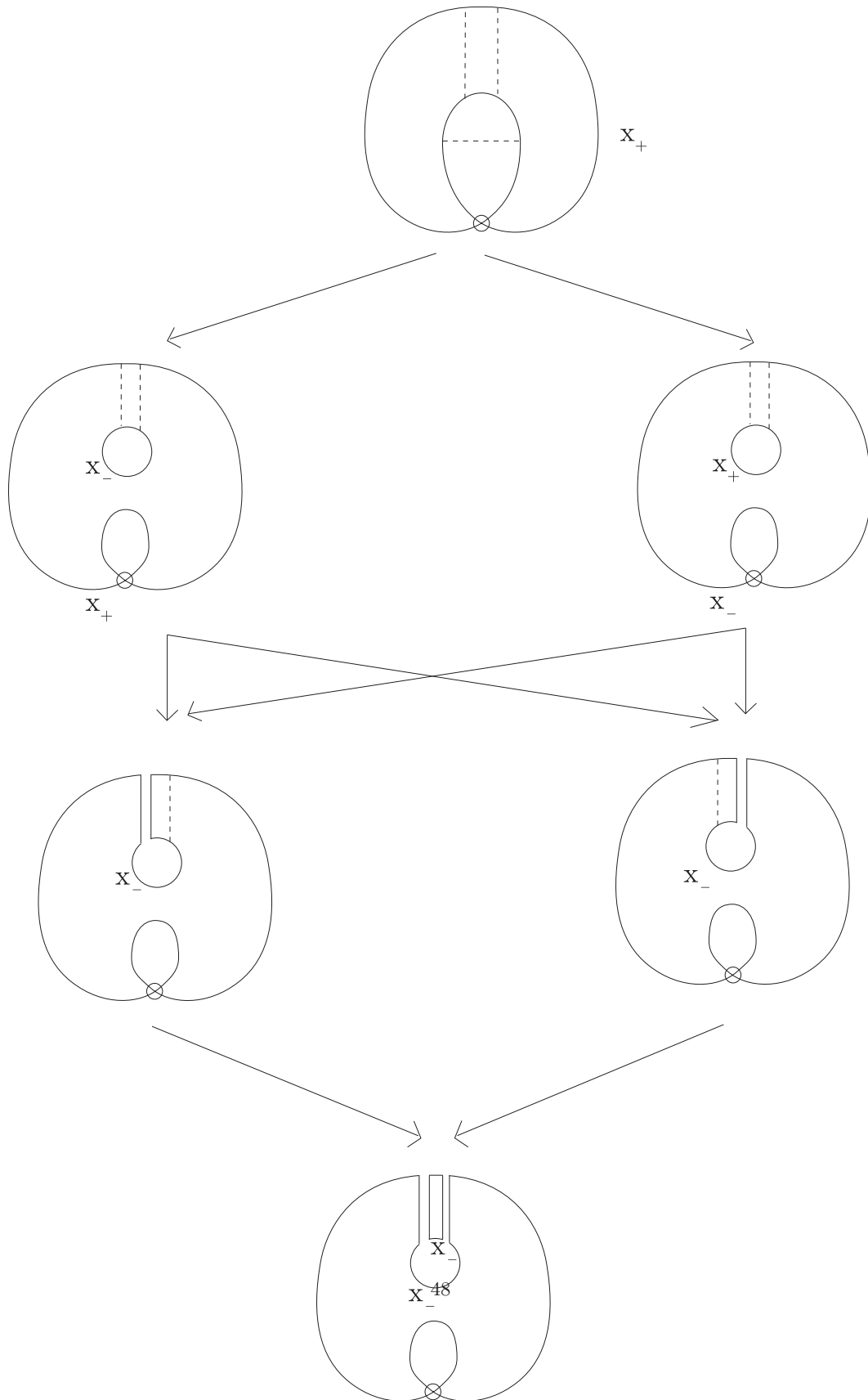


FIGURE 10.5. The poset of the decorated resolution configuration of an index 3 labeled resolution configuration



In the virtual case, it is very complicated to construct a ‘generating moduli’ because of the property of coefficients in the virtual case (Definition 5.21) is different from the classical case. In this paper we show an explicit way to assign to the moduli space  $\mathcal{M}_{\mathcal{C}_K(L)}(\mathbf{x}, \mathbf{y}) = \mathcal{M}(D_L(v) - D_L(u), x|, y|)$ , a compact topological space which admits a CW structure, when  $\text{gr}_h \mathbf{x} - \text{gr}_h \mathbf{y}$  is one, two, and three. We construct a CW complex which consists of only  $(m - 1)$ -cells,  $m$ -cells,  $(m + 1)$ -cells,  $(m + 2)$ -cells, and  $(m + 3)$ -cells, where  $m$  is any integer, for the dual Khovanov chain complex in this case by using these moduli spaces. We prove that the second Steenrod square of the CW complex is invariant under any Reidemeister move although we do not prove whether the stable homotopy type of the CW complex is invariant under any Reidemeister move.

We have not constructed moduli when  $\text{gr}_h \mathbf{x} - \text{gr}_h \mathbf{y} \geq 5$ , to be compatible with those in the case of  $\text{gr}_h \mathbf{x} - \text{gr}_h \mathbf{y} \leq 4$ .

## 12. 0-DIMENSIONAL MODULIS AND FRAMINGS

Let  $\mathcal{L}$  be a virtual link. Let  $L$  be a virtual link diagram which represents  $\mathcal{L}$ . Let  $\mathbf{x} = (D_L(u), x)$  and  $\mathbf{y} = (D_L(v), y)$  be Khovanov basis elements. We will make moduli spaces  $\mathcal{M}_{\mathcal{C}_K(L)}(\mathbf{x}, \mathbf{y}) = \mathcal{M}(D_L(v) - D_L(u), x|, y|)$  when  $\text{gr}_h \mathbf{x} - \text{gr}_h \mathbf{y} = 1, 2, 3, 4$ . In this section we suppose that the moduli are not the empty set. Of course, this discussion includes the case of classical link diagrams because any classical link diagram is a virtual link diagram.

We have the following proposition.

**Proposition 12.1.** *If  $\text{gr}_h \mathbf{x} - \text{gr}_h \mathbf{y} = 1$ , we can assign to the moduli space  $\mathcal{M}_{\mathcal{C}_K(L)}(\mathbf{x}, \mathbf{y})$  a single point.*

**Proof of Proposition 12.1.** The proposition follows because  $c[x : y]$  is  $+1, 0$ , or  $-1$ .  $\square$

**Remark 12.2.** In the case of classical links, Proposition 12.1 is the same as [29, section 5.3].

We give a framing on  $\mathcal{M}_{\mathcal{C}_K(L)}(\mathbf{x}, \mathbf{y})$  so that it satisfies the conditions in [29, Definitions 3.18 and 3.20].

## 13. 1-DIMENSIONAL MODULIS AND FRAMINGS

We have the following.

**Lemma 13.1.** *Let  $\mathbf{a}, \mathbf{b}$  be two dual Khovanov basis elements such that the difference of the homological gradings are two. Let  $\# = \#\{\mathbf{x} | \mathbf{a} \prec \mathbf{x}, \mathbf{x} \prec \mathbf{b}, x \neq a, x \neq b\}$ . If  $\# \neq 0$ , it is two or four.*

**Proof of Lemma 13.1.** If  $\mathbf{a}$  and  $\mathbf{b}$  are (respectively, are not) associated with a ladybug configuration or a quasi-ladybug configuration,  $\#$  is four (respectively, two).  $\square$

It is easy to prove the following proposition.

**Proposition 13.2.** *Let  $\text{gr}_h \mathbf{x} - \text{gr}_h \mathbf{y} = 2$ . Under the conditions of Proposition 12.1, we have just three cases.*

- (1) *We can assign to the moduli space  $\mathcal{M}_{\mathcal{C}_K(L)}(\mathbf{x}, \mathbf{y})$  one closed segment if  $\#$  in Lemma 13.1 is two.*
- (2) *We can assign to the moduli space  $\mathcal{M}_{\mathcal{C}_K(L)}(\mathbf{x}, \mathbf{y})$  two kinds of a disjoint union of two closed segments if  $\#$  in Lemma 13.1 is four.*

**Remark.** In the case of virtual links, we may have both ladybug configurations and quasi-ladybug configurations. Note that quasi-ladybug configurations are different from ladybug configurations. Recall §9. We must note that, in the case of classical links, there is not a quasi-ladybug configuration.

We use Lemma 13.1, and prove Proposition 13.2 as in the case of classical links in [29, section 5.4]. Proposition 13.2 in the case of classical links includes [29, section 5.4]. They are not the same. See the following Remark.

**Remark 13.3.** As we stated in §9, if we have a quasi-ladybug configuration, we may assign to a single virtual link diagram more than one CW complex. As we stated in Remark 3.1, if we have a ladybug configuration, we may also assign to a single virtual link diagram more than one CW complex.

Compare [29, The property associated with (2) in the proof of Proposition 6.5] with the following.

**Fact 13.4.** *Fix a link diagram  $L$ , and let  $L'$  be the result of reflecting  $L$  across the  $y$ -axis, say, and reversing all of the classical crossings. Then  $L$  and  $L'$  do not always represent the same virtual link.*

The boundary of one segment in  $\mathcal{M}_{\mathcal{C}_K(L)}(\mathbf{x}, \mathbf{y})$  is two points. The framings on two points have different orientations. Therefore we can extend the framing on the boundary to  $\mathcal{M}_{\mathcal{C}_K(L)}(\mathbf{x}, \mathbf{y})$ . Take a framing on  $\mathcal{M}_{\mathcal{C}_K(L)}(\mathbf{x}, \mathbf{y})$ . See [29, §4].

## 14. 2-DIMENSIONAL MODULIS AND FRAMINGS

**Review 14.1.** The 3-cube moduli  $\mathcal{M}_{\mathcal{C}(3)}(\bar{1}, \bar{0})$  is a hexagon, and is homeomorphic to the 2-disc. See [29, §4.1].

In Figure 14.1, we draw the partial ordered set  $\mathcal{C}(3)$ , the set of six vertices of the 3-dimensional cube, and cells associated with the six vertices: Here we show an example the

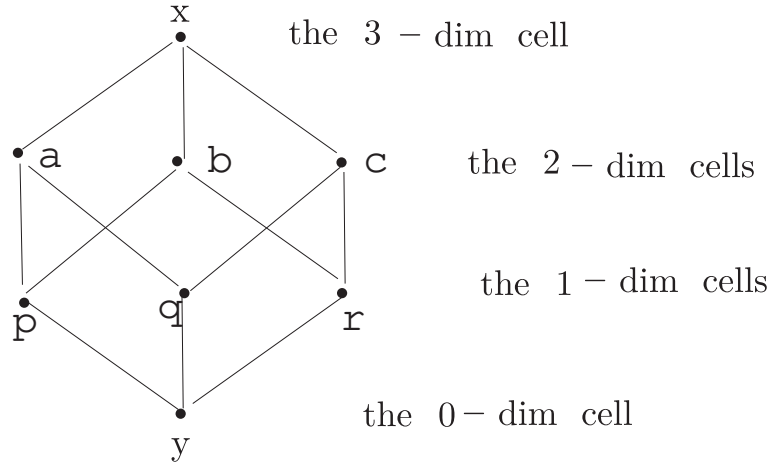


FIGURE 14.1. Cells associated with the partial ordered set  $\mathcal{C}(3)$ , the set of six vertices of the 3-dimensional cube

cells are 3, 2, 1, and 0-dimensional case for convenience. This moduli space  $\mathcal{M}_{\mathcal{C}(3)}(\bar{1}, \bar{0})$  is in the 2-sphere,  $\mathbb{R}^2 \cup \{\infty\}$ , which is the boundary of the 3-cell  $x$ . We draw  $\mathcal{M}_{\mathcal{C}(3)}(\bar{1}, \bar{0})$  and  $\partial\mathcal{M}_{\mathcal{C}(3)}(\bar{1}, \bar{0})$  in this  $\mathbb{R}^2$  in Figures 14.3 and 14.2.

We have the following proposition when  $\text{gr}_h \mathbf{x} - \text{gr}_h \mathbf{y} = 3$ .

**Proposition 14.2.** *Let  $\text{gr}_h \mathbf{x} - \text{gr}_h \mathbf{y} = 3$ . Under the conditions of Propositions 12.1 and 13.2, we can assign to each moduli space  $\mathcal{M}_{\mathcal{C}_K(L)}(\mathbf{x}, \mathbf{y})$ , a space homeomorphic to a finite number of 2-discs.*

**Remark 14.3.** In Proposition 14.2, in the case of virtual links  $\mathcal{M}(D, x, y)$  is not a cube flow category in general as is shown by the example of Figures 10.1-10.4 in §10. Consider  $\mathcal{M}(D, x, y)$  associated with the example of Figures 10.1-10.4. We can check directly that  $\partial\mathcal{M}(D, x, y)$  is homeomorphic to a disjoint union of circles, and can suppose that  $\mathcal{M}(D, x, y)$  is homeomorphic to a disjoint union of 2-discs.

In the case of classical links, Proposition 14.2 is the same as [29, section 5.5].

**Proof of Proposition 14.2.** Make a basic index 3 decorated resolution configuration  $(D, x, y)$  associated with  $\mathbf{x}$  and  $\mathbf{y}$  by the same method of [29, Definition 5.3].  $P(D, x, y)$  has the maximal element  $(D, y)$  and the minimal element  $(s(D), x)$ .

We assign a cell to each element of  $P(D, x, y)$  as drawn in Figure 14.4:  $\mathbf{x}$  (respectively,  $\mathbf{y}$ ) corresponds to  $(s(D), x)$  (respectively,  $(D, y)$ ). Assume that (the homological degree of  $\mathbf{x}$ ) – that of  $\mathbf{y}$  is 3. There are  $N$ -cells  $e_i^N$  and  $(N + 1)$ -cells  $e_j^{N+1}$  between  $\mathbf{x}$  and  $\mathbf{y}$ . Here,  $N$  is a large integer,  $i = 1, \dots, \nu_i$  and  $j = 1, \dots, \nu_j$ .

By the definition,  $\mathbf{y} = (D, y)$  has just three arcs.

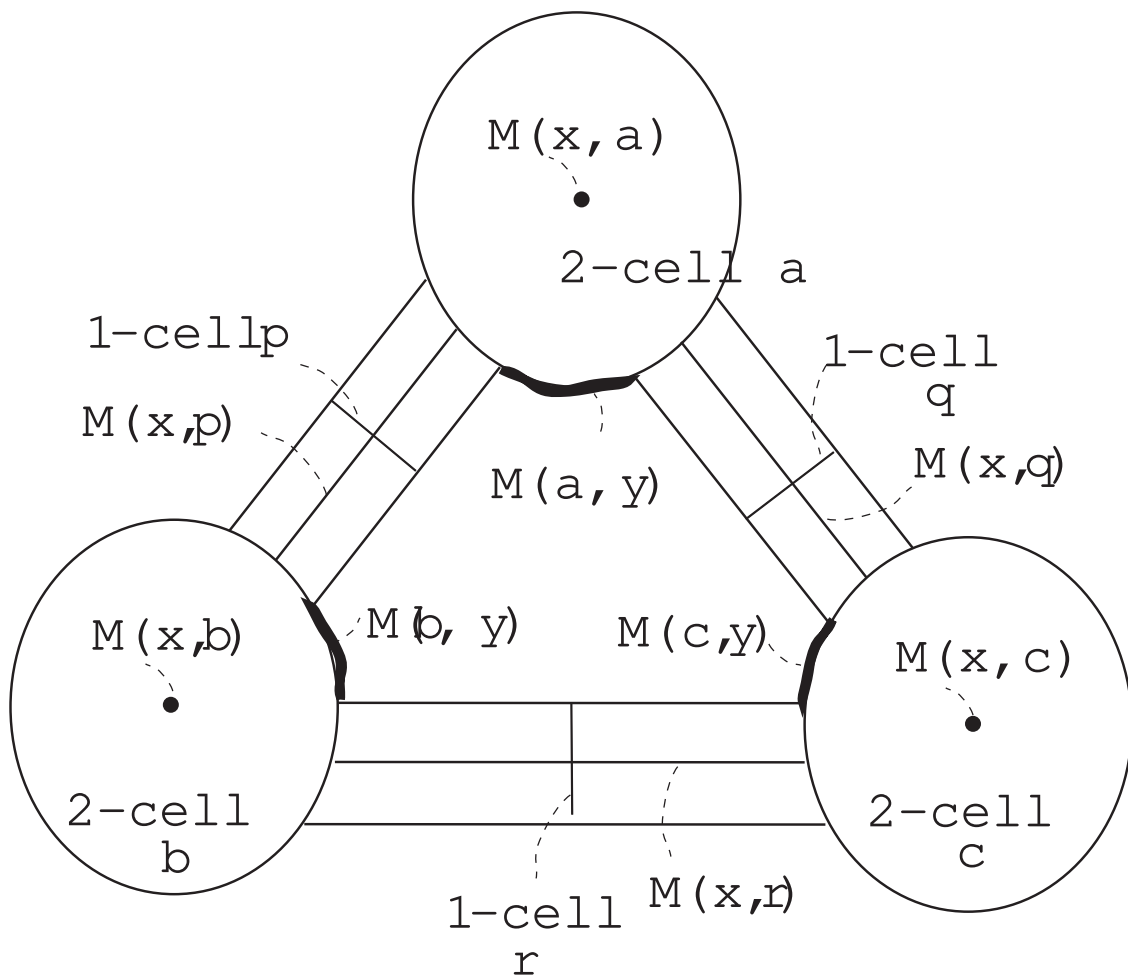


FIGURE 14.2. The 3-dimensional cube moduli. Take only the hexagon  $\mathcal{M}_{C(3)}(1, 0)$  from Figure 14.3.

If all arcs in each labelled resolution configuration of  $P(D, x, y)$  are mc arcs, we have the same results as ones in [29, section 5.5]. In this case Proposition 14.2 holds.

If all arcs in  $(D, y)$  are scs arcs,  $\delta(D, y) = 0$ . However  $(D, y)$  is an element of  $P(D, x, y)$  which is not the empty set. We arrived at a contradiction. Hence this case does not occur.

We prove the other cases.

Note that, even if  $(D, y)$  has only three mc arcs, a labeled resolution configuration  $e_*^{1+N}$  may have a scs arc. See Figure 14.5 for an example.

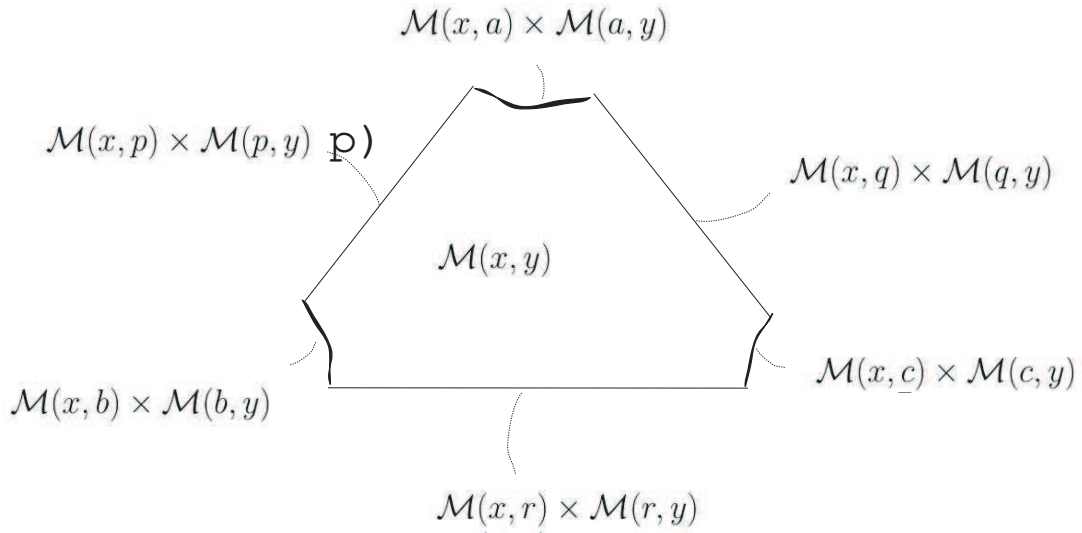
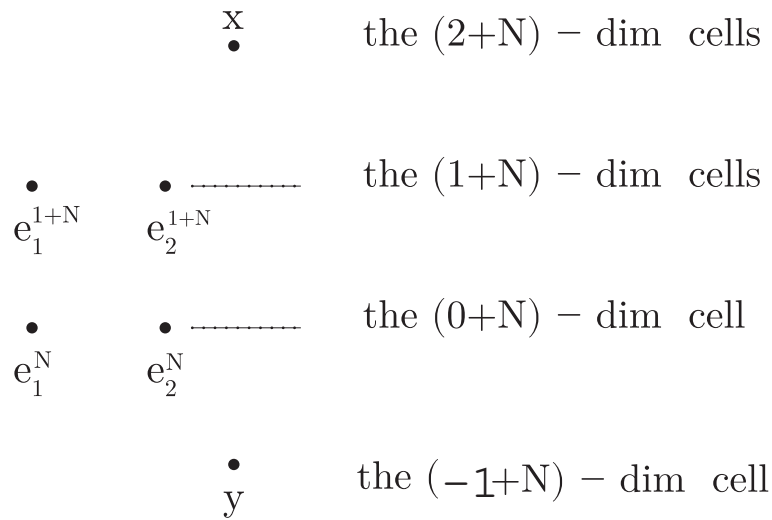


FIGURE 14.3. The 3-dimensional cube moduli. See also Figure 14.2



$$N \in \mathbb{N}$$

FIGURE 14.4. Khovanov basis elements in Proposition 14.2

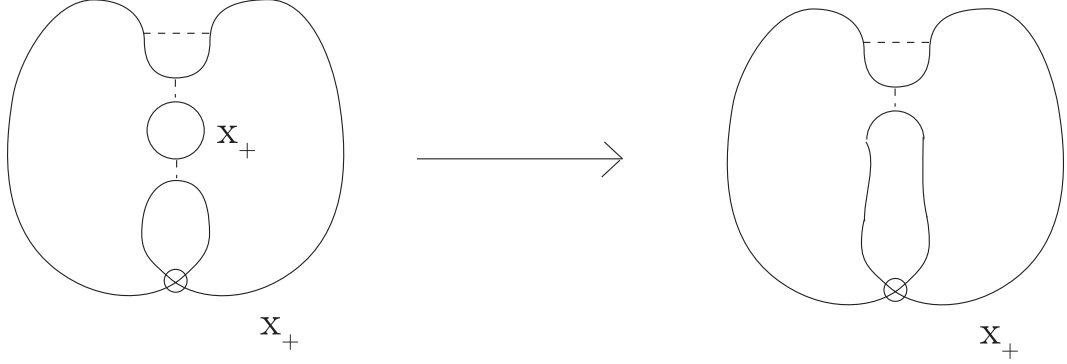


FIGURE 14.5. An example of surgery which changes a labelled resolution configuration with only mc arcs into a labelled resolution configuration with a scs arc.

If we can construct  $\mathcal{M}(\mathbf{x}, \mathbf{y})$ , by [29, Definition 3.12.(M-2)],  $\partial\mathcal{M}(\mathbf{x}, \mathbf{y})$  is a union of

$$\prod_{i=1, \dots, \nu_i} \mathcal{M}(e_i^N, \mathbf{y}) \times \mathcal{M}(\mathbf{x}, e_i^N)$$

$$(\quad = \partial_1 \mathcal{M}(\mathbf{x}, \mathbf{y}))$$

and

$$\prod_{j=1, \dots, \nu_j} \mathcal{M}(e_j^{N+1}, \mathbf{y}) \times \mathcal{M}(\mathbf{x}, e_j^{N+1})$$

$$(\quad = \partial_2 \mathcal{M}(\mathbf{x}, \mathbf{y})).$$

Each of  $\mathcal{M}(e_i^N, \mathbf{y}) \times \mathcal{M}(\mathbf{x}, e_i^N)$  and  $\mathcal{M}(e_j^{N+1}, \mathbf{y}) \times \mathcal{M}(\mathbf{x}, e_j^{N+1})$  is a segment.

We have that the set of the boundary of each segment above is the set of points,  $\mathcal{M}(e_i^{N+1}, e_j^N)$  ( $i = 1, \dots, \nu_i$  and  $j = 1, \dots, \nu_j$ ).

Furthermore, we have the following: Fix  $i$  and  $j$ . There is an only one segment in  $\partial_1 \mathcal{M}(\mathbf{x}, \mathbf{y})$  (respectively,  $\partial_2 \mathcal{M}(\mathbf{x}, \mathbf{y})$ ) which touches a point  $\mathcal{M}(e_i^{N+1}, e_j^N)$ . These two segments touch each other at the point.

Therefore  $\partial\mathcal{M}(\mathbf{x}, \mathbf{y})$  is a disjoint union of circles.

Therefore we can define as follows:  $\mathcal{M}(x, y)$  is a finite disjoint union of CW complexes which are homeomorphic to the 2-ball. This  $\mathcal{M}(x, y)$  is what we call  $\mathcal{M}_{\mathcal{C}_K(L)}(\mathbf{x}, \mathbf{y})$  here.

In all cases of Proposition 14.2, we have defined  $\mathcal{M}_{\mathcal{C}_K(L)}(\mathbf{x}, \mathbf{y})$  to be a finite disjoint union of CW complexes which are homeomorphic to the 2-ball (Each of these CW complexes is a  $< 2 >$ -manifold defined in [29, Definition 3.1].) This completes the proof of

Proposition 14.2. □

**Remark.** Since  $\mathbf{y} = (D, y)$  has just three arcs, the number of  $e_*^{1+N}$  is  $\leq 6$ . *Reason.* One surgery on a labeled resolution configuration makes no greater than two labeled resolution configurations. Recall Definitions 5.15. Furthermore the number of  $e_*^{2+N}$  is  $\leq 6$  by [29, Lemma 2.13].

Suppose that  $y_1, \dots, y_{\nu_{N-1}}$  are all  $(-1 + N)$ -dimensional cells to which the  $(2 + N)$ -dimensional cell  $x$  is attached. Here, we also use  $x$  and  $y_*$  for cells. For each  $i$ ,  $\mathcal{M}(x, y_i)$  is embedded in  $\partial x$ . If  $i \neq j$ , we have  $\mathcal{M}(x, y_i) \cap \mathcal{M}(x, y_j) = \emptyset$ .

Segments  $\mathcal{M}(x, e_{\sharp}^{N+1}) \times \mathcal{M}(e_{\sharp}^{N+1}, y_*)$  have been framed before attaching  $x$ . Note that  $\mathcal{M}(x, e_{\sharp}^{N+1})$  is 0-dimensional and that  $\mathcal{M}(e_{\sharp}^{N+1}, y_*)$  is 1-dimensional. We give framings to segments  $\mathcal{M}(x, e_{\sharp}^N) \times \mathcal{M}(e_{\sharp}^N, y_*)$  so that we can extend a framing on  $\partial \mathcal{M}(x, y_*)$  to  $\mathcal{M}(x, y_*)$ . (A part of [29, Proof Proposition 4.12] explains how we extend a sign assignment. We use the same way written there.)

### 15. 3-DIMENSIONAL MODULIS AND FRAMINGS

A *handle-body* is a compact oriented 3-manifolds with a CW decomposition of one 0-handle and  $g$  1-handles, where  $g \in \mathbb{N} \cup \{0\}$ :  $g$  is called the *genus*.

**Proposition 15.1.** *Let  $\text{gr}_h \mathbf{x} - \text{gr}_h \mathbf{y} = 4$ . Under the conditions of Propositions 12.1, 13.2, and 14.2, we can assign to each moduli space  $\mathcal{M}_{\mathcal{G}_K(L)}(\mathbf{x}, \mathbf{y})$ , a space homeomorphic to a finite number of handle-bodies.*

**Proof of Proposition 15.1.** Assume that  $\mathbf{x}$  (respectively,  $\mathbf{y}$ ) is an  $(m + 3 + N)$ -cell (respectively,  $(m - 1 + N)$ -cell) which corresponds to a Khovanov basis  $(s(D), x)$  (respectively,  $(D, y)$ ) whose homological grading is  $m + 3$  (respectively,  $m - 1$ ). Let  $N$  be a fixed large integer. We define cells to be closed balls, not open balls.

Take  $P(D, x, y)$ . Let  $g_i^m$  (respectively,  $g_j^{m+1}$ ,  $g_k^{m+2}$ ) be all dual Khovanov basis elements other than  $\mathbf{x}$  and  $\mathbf{y}$  in  $P(D, x, y)$ , whose homological gradings are  $m$  (respectively,  $m + 1$ ,  $m + 2$ ). We assign to  $g_i^m$  (respectively,  $g_j^{m+1}$ ,  $g_k^{m+2}$ ) a cell  $e_i^{m+N}$  (respectively,  $e_j^{m+1+N}$ ,  $e_k^{m+2+N}$ ), where the right upper suffix of the notation of cells denote the degree. Note that  $i, j$  and  $k$  run over a fixed finite set of natural numbers.

We assume the following.

**Assumption 15.2.** We can attach  $\mathbf{x}$  to  $\mathbf{y}$  to be compatible with the modulis and the framings in Propositions 12.1, 13.2, and 14.2.

If Assumption 15.2 is true,  $\partial \mathcal{M}(\mathbf{x}, \mathbf{y})$  satisfies [29, Definition 3.12.(M-2)], which is quoted in §14.  $\partial \mathcal{M}(\mathbf{x}, \mathbf{y})$  is made of  $\partial \mathcal{M}(p, q)$ , where  $p$  (respectively,  $q$ ) is one of  $\mathbf{x}, \mathbf{y}$ ,

$e_i^{m+N}$ ,  $e_j^{m+1+N}$ , and  $e_k^{m+2+N}$ , and  $(p, q) \neq (\mathbf{x}, \mathbf{y})$ .

Note the following: Even if Assumption 15.2 does not hold, we can define a surface  $F$  which is  $\partial\mathcal{M}(\mathbf{x}, \mathbf{y})$  if Assumption 15.2 holds.  $F$  is embedded in the  $(m + 2 + N)$ -sphere  $\partial\mathbf{x}$ .

**Claim 15.3.** *The above  $F$  is orientable.*

**Proof of Claim 15.3.** Each  $\mathcal{M}(\mathbf{x}, e_*^{m+N+1}) \times \mathcal{M}(e_*^{m+N+1}, \mathbf{y})$  in  $F$  is a disjoint collection of squares.  $F$  is orientable if and only if

$F$ – (all  $\mathcal{M}(\mathbf{x}, e_*^{m+N+1}) \times \mathcal{M}(e_*^{m+N+1}, \mathbf{y})$ ) is orientable.

Let  $A = (\mathcal{M}(\mathbf{x}, e_{\#}^{m+2+N}) \times \mathcal{M}(e_{\#}^{m+2+N}, \mathbf{y}))$

and  $B = (\mathcal{M}(\mathbf{x}, e_*^{m+N}) \times \mathcal{M}(e_*^{m+N}, \mathbf{y}))$ .

Then  $A \cap B$  is  $C = \mathcal{M}(\mathbf{x}, e_{\#}^{m+2+N}) \times \mathcal{M}(e_{\#}^{m+2+N}, e_*^{m+N}) \times \mathcal{M}(e_*^{m+N}, \mathbf{y})$ . By the rule of [29, Definition 3.18], we have the following fact.

**Fact 15.4.** *The framing on  $A$  and  $C$  are compatible at  $C$ .*

Therefore  $F$  is orientable. This completes the proof of Claim 15.3. □

This completes the proof of Proposition 15.1. □

We prove the following.

**Proposition 15.5.** *Assumption 15.2 is true.*

**Remark.** Since  $\Omega_2^{\text{fr}} = \mathbb{Z}_2$ , only Proposition 15.1 and Fact 15.4 never imply Claim 15.5.

**Proof of Proposition 15.5.** We fix  $l$  and  $h$  and consider  $\mathcal{M}(e_l^{m+N+3}, e_h^{m+N-1})$ . Note that  $\mathbf{x} = e_l^{m+N+3}$  and  $\mathbf{y} = e_h^{m+N-1}$ .

A framing on  $\mathcal{M}(e_l^{m+N+3}, e_k^{m+N+2})$  is determined by the differential operator.

A framing on  $\mathcal{M}(e_l^{m+N+2}, e_j^{m+N-1})$  is determined when we attach  $e_l^{m+N+2}$  to the  $(m + N + 1)$ -skeleton.

Hence a framing on  $\mathcal{M}(e_l^{m+N+3}, e_k^{m+N+2}) \times \mathcal{M}(e_k^{m+N+2}, e_h^{m+N-1})$  in the  $(m + 2 + N)$ -skeleton has been determined. This is a dodecagon or a hexagon.

Here, we consider all possibilities of  $h, i, j$ , and  $k$ . Framings on 0-dimensional modulis

$\mathcal{M}(e_l^{m+N+3}, e_k^{m+N+2}) \times \mathcal{M}(e_k^{m+N+2}, e_j^{m+N+1}) \times \mathcal{M}(e_j^{m+N+1}, e_i^{m+N}) \times \mathcal{M}(e_i^{m+N}, e_h^{m+N-1})$  have been given by the differential operator.

When we attach  $e_l^{m+N+3}$ ,  $\mathcal{M}(e_l^{m+N+3}, e_k^{m+N+2})$  has been framed, and neither  $\mathcal{M}(e_l^{m+N+3}, e_j^{m+N+1})$ ,  $\mathcal{M}(e_l^{m+N+3}, e_i^{m+N})$ , nor  $\mathcal{M}(e_i^{m+N}, e_h^{m+N-1})$  has been framed.



We can change framings on 1-dimensional modulis

$$\mathcal{M}(e_l^{m+3+N}, e_j^{m+1+N}) \times \mathcal{M}(e_j^{m+1+N}, e_i^{m+N}) \times \mathcal{M}(e_i^{m+N}, e_h^{m-1+N})$$

and

$$\mathcal{M}(e_l^{m+3+N}, e_k^{m+2+N}) \times \mathcal{M}(e_k^{m+2+N}, e_i^{m+N}) \times \mathcal{M}(e_i^{m+N}, e_h^{m-1+N}).$$

Recall  $F = \partial\mathcal{M}(e_l^{m+N+3}, e_h^{m+N-1})$ . Suppose that a moduli  $\mathcal{M}$  is embedded in  $F$ . Let  $X = \amalg_{\text{all } l} (\mathcal{M}(e_l^{m+N+3}, e_k^{m+N+2}) \times \mathcal{M}(e_k^{m+N+2}, e_h^{m+N-1}))$ . If  $\text{Int } \mathcal{M}$  is included in  $\text{Int } F - X$ , then  $\text{Int } \mathcal{M}$  has not been framed. We will give framing to it.

Give a framing  $fr$  on  $F$  that extends to  $\mathcal{M}(e_l^{m+N+3}, e_h^{m+N-1})$ . Each pair of  $\mathcal{M}(e_l^{m+N+3}, e_k^{m+N+2}) \times \mathcal{M}(e_k^{m+N+2}, e_h^{m+N-1})$  are disjoint. Each  $\mathcal{M}(e_l^{m+N+3}, e_k^{m+N+2}) \times \mathcal{M}(e_k^{m+N+2}, e_h^{m+N-1})$  is contractible.

All 0-dimensional modulis in  $F$  is in  $X$ .

Using an isotopy of framings, change  $fr$  on  $F$  so that  $fr|_X$  coincides with the framing on  $X$  that we have given already in the lower dimensional skeleton. *Reason:* Each component of  $X$  is contractible. Restrict this new  $fr$  to  $F - X$ .

Take any square moduli. Only two disjoint 1-dimensional modulis, or edges, are in  $X$ . The other part is in  $F - X$ .

For any square moduli  $S$ , we have the following: There is a connected component  $E$ , a segment, of  $\mathcal{M}(e_*^{m+N+3}, e_j^{m+N+1})$  and  $F$  of  $\mathcal{M}(e_*^{m+N+1}, e_h^{m+N-1})$  for a suffix  $*$ . We have  $S = E \times F$ .

Let  $\partial E$  be two points  $P \amalg P'$ . Let  $\partial F$  be two points  $Q \amalg Q'$ . Then  $F \times P$  and  $F \times P'$  are in  $X$ . We have  $\text{Int } E \times Q$  and  $\text{Int } E \times Q'$  are in  $F - X$ .

We must change the framing  $fr$  on  $F$  so that  $fr|_S$  is the product of a framing on  $\mathcal{M}(e_*^{m+N+3}, e_j^{m+N+1})$  and that on  $\mathcal{M}(e_*^{m+N+1}, e_h^{m+N-1})$  (See [29, Definition 3.18]).

We can do it by using an isotopy of framings because  $S$  is contractible.

Restrict  $fr$  to  $F - X - \text{all } S$ . Therefore there is a framing on the 3-dimensional moduli  $\mathcal{M}(e_l^{m+3+N}, e_h^{m-1+N})$  which is compatible with the framing which has been fixed in the  $(m + 2 + N)$ -skeleton. This completes the proof of Proposition 15.5.  $\square$

Now we have constructed 0,1,2, and 3-dimensional modulis and framings on them. We will use these modulis and frmiangs and construct partial Khovanov CW complexes.

## 16. REVIEW OF THE FIRST STEENROD SQUARE OPERATOR $Sq^1$

In [51, 52] the Steenrod square  $Sq^*(*)$  ( $*$   $\in \mathbb{Z}$ ) is defined. Let  $X$  and  $X'$  be compact CW complexes. Let  $\{C_i\}_{i \in \mathbb{Z}}$  be a chain complex. Assume that  $\{C_i\}_{i \in \mathbb{Z}}$  is associated with both a CW decomposition on  $X$  and a CW decomposition on  $X'$ . It is well-known that  $Sq^1(X) = Sq^1(X')$  (see e.g. [31, Introduction]) and that  $Sq^2(X)$  and  $Sq^2(X')$  are different in general (see e.g. [53]).

Therefore  $Sq^1$  is not useful as classical (respectively, virtual) link invariants. We consider  $Sq^2$  below.

## 17. REVIEW OF THE SECOND STEENROD SQUARE OPERATOR $Sq^2$

We review the definition of the second Steenrod square.

**Definition 17.1.** ([51, 52].) Let  $K$  be the Eilenberg–MacLane space  $K(\mathbb{Z}_2, m)$  for any natural number  $m > 1$ . We have that  $K$  is connected. We have that  $\pi_i(K) \cong \mathbb{Z}_2$  (respectively, 0) if  $i = m$  (respectively,  $i \neq m$  and  $i > 1$ ). It is well-known that the homotopy type of  $K$  is unique. It is known that  $H^{m+2}(K; \mathbb{Z}_2) \cong \mathbb{Z}_2$ . Let  $\xi$  be the generator of  $H^{m+2}(K; \mathbb{Z}_2) \cong \mathbb{Z}_2$ .

Let  $X$  be a CW complex. Let  $[X, K]$  be the set of all homotopy classes of continuous maps  $X \rightarrow K$ . It is well-known that  $[X, K] = H^m(X; \mathbb{Z}_2)$ .

For an arbitrary element  $x \in H^m(X; \mathbb{Z}_2)$ , take  $f_x$  by this bijection. Define the second Steenrod square  $Sq^2(x)$  to be  $f_x^*(\xi)$ .

This definition is reviewed and explained very well in [31, section 3.1]. See also [8, The item (4) between Proposition 4L.1 and Theorem 4L.2]. We review an important property of the second Steenrod square operator  $Sq^2$ .

**Proposition 17.2.** (See [51, section 12] and [8, §4.L].) *Let  $Y$  be any compact CW complex. Let  $Y^{(*)}$  be the  $*$ -skeleton of  $Y$  ( $*$   $\in \mathbb{Z}$ ). Then the second Steenrod square  $Sq^2(Y) : H^m(Y; \mathbb{Z}_2) \rightarrow H^{m+2}(Y; \mathbb{Z}_2)$  is determined by the stable homotopy type of  $Y^{(m+2)}/Y^{(m-1)}$ .*

This proposition is reviewed and explained very well in [31, section 3.1].

We explain how we know  $Sq^2(Y)$  from  $Sq^2(Y^{(m+2)}/Y^{(m-1)})$ . There are maps

$$Y \xleftarrow{\text{inclusion}} Y^{(m+2)} \xrightarrow{\text{quotient}} Y^{(m+2)}/Y^{(m-1)}$$

By the CW structure of  $Y$ , that of  $Y^{(m+2)}$  and that of  $Y^{(m+2)}/Y^{(m-1)}$ , we have the following commutative diagram (17.1). Call the homomorphisms as written there.

$$(17.1) \quad \begin{array}{ccccc} H^{m+2}(Y; \mathbb{Z}_2) & \xrightarrow{\text{injective, } g'} & H^{m+2}(Y^{(m+2)}; \mathbb{Z}_2) & \xleftarrow{\text{isomorphism, } f'} & H^{m+2}(Y^{(m+2)}/Y^{(m-1)}; \mathbb{Z}_2) \\ Sq^2 \uparrow & & Sq^2 \uparrow & & Sq^2 \uparrow \\ H^m(Y; \mathbb{Z}_2) & \xrightarrow{\text{isomorphism, } g} & H^m(Y^{(m+2)}; \mathbb{Z}_2) & \xleftarrow{\text{surjective, } f} & H^m(Y^{(m+2)}/Y^{(m-1)}; \mathbb{Z}_2) \end{array}$$

First we explain how we know  $Sq^2$  on  $H^m(Y^{(m+2)}; \mathbb{Z}_2)$  by using  $Sq^2$  on  $H^m(Y^{(m+2)}/Y^{(m-1)}; \mathbb{Z}_2)$ . Take any element  $x \in H^m(Y^{(m+2)}; \mathbb{Z}_2)$ . Take  $y \in H^m(Y^{(m+2)}/Y^{(m-1)}; \mathbb{Z}_2)$  such that  $f(y) = x$ . By the naturality of  $Sq^2$ , we have  $f'(Sq^2(y)) = Sq^2(f(y))$ . So we can know that  $Sq^2(x)$  is  $f'(Sq^2(y))$ . Here, note the following fact: Suppose that there is an element  $\tilde{y} \in H^m(Y^{(m+2)}/Y^{(m-1)}; \mathbb{Z}_2)$  such that  $f(\tilde{y}) = x$  and such that  $y \neq \tilde{y}$ . Then  $f'(Sq^2(y)) = f'(Sq^2(\tilde{y}))$  although  $y \neq \tilde{y}$ .

Second we explain how we know  $Sq^2$  on  $H^m(Y; \mathbb{Z}_2)$  by using  $Sq^2$  on  $H^m(Y^{(m+2)}; \mathbb{Z}_2)$ . Take any element  $z \in H^m(Y; \mathbb{Z}_2)$ . By the naturality of  $Sq^2$ , we have  $g'(Sq^2(z)) = Sq^2(g(z))$ . Note that  $g'$  is injective. We can know that  $Sq^2(z)$  is  $g'^{-1}(Sq^2(g(z)))$ .

Last we explain how we know  $Sq^2$  on  $H^m(Y; \mathbb{Z}_2)$  by using  $Sq^2$  on  $H^m(Y^{(m+2)}/Y^{(m-1)}; \mathbb{Z}_2)$ . Take any element  $z \in H^m(Y; \mathbb{Z}_2)$ . Take  $y \in H^m(Y^{(m+2)}/Y^{(m-1)}; \mathbb{Z}_2)$  such that  $f(y) = g(z)$ . So we can know that  $Sq^2(z)$  is  $g'^{-1}(f'(Sq^2(y)))$ . Here, note the following fact.

**Fact 17.3.** *Take any element  $z \in H^m(Y; \mathbb{Z}_2)$ . Take  $y$  in the previous paragraph. Suppose that there is an element  $\tilde{y} \in H^m(Y^{(m+2)}/Y^{(m-1)}; \mathbb{Z}_2)$  such that  $f(\tilde{y}) = g(z)$  and such that  $y \neq \tilde{y}$ . Then  $g'^{-1}(f'(Sq^2(y))) = g'^{-1}(f'(Sq^2(\tilde{y})))$  although  $y \neq \tilde{y}$ .*

*We also have that  $Sq^2(\{f^{-1}(g(z))\})$  has only one element.*

## 18. THE SECOND STEENROD SQUARE OPERATOR FOR VIRTUAL LINKS

**Definition 18.1.** Let  $\mathcal{L}$  be a virtual link. Let  $L$  be a virtual link diagram which represents  $\mathcal{L}$ . We define a CW complex  $Z(L)$  for  $L$  below.

Let  $\{a_p\}_{p \in \Lambda}$  be the dual Khovanov basis for  $L$ . Note that  $\Lambda$  is a finite set.

Let  $\{a_p\}_{p \in \Lambda}$  be the dual Khovanov basis for  $L$ . Note that  $\Lambda$  is a finite set. Take an element  $a$  in  $\{a_p\}_{p \in \Lambda}$ . If  $\text{gr}_h a$  is less than  $m$ , we assign a base point. If  $\text{gr}_h a$  is greater than  $m + 4$ , we assign nothing.

Let  $g_h^{m-1}$  (respectively,  $g_i^m, g_j^{m+1}, g_k^{m+2}, g_l^{m+3}$ ) be all dual Khovanov basis elements whose homological gradings are  $m - 1$  (respectively,  $m, m + 1, m + 2, m + 3$ ) in  $\{a_p\}_{p \in \Lambda}$ . We assign to  $g_h^{m-1}$  (respectively,  $g_i^m, g_j^{m+1}, g_k^{m+2}, g_l^{m+3}$ ) a cell  $e_h^{m-1+N}$  (respectively,  $e_i^{m+N},$

$e_j^{m+1+N}, e_k^{m+2+N}, e_l^{m+3+N}$ ), where the right upper suffix of the notation of cells denote the degree and  $N$  is a large integer. Fix  $N$ .

We attach the cells,  $e_h^{m-1+N}, e_i^{m+N}, e_j^{m+1+N}, e_k^{m+2+N}$ , and  $e_l^{m+3+N}$ : We use the moduli spaces and the framings defined in §12-§15. The result is  $Z(L)$ .

**Remark.** We consider all possibilities of modulis and framings. We may assign to a single virtual link diagram, more than one CW complexes if there is a ladybug or a quasi-ladybug configuration. See Remark 13.3.

Construct  $Z(L)$  for each set of modulis and framings. We have the following commutative diagram (18.1). The left column is Khovanov chain complex for  $L$ . The middle column is made as follows: Remove  $C^*(L; \mathbb{Z}_2)$  ( $* > m + 4$ ) from the left one. Put 0 instead. Let  $C^{m+4}(L; \mathbb{Z}_2) \rightarrow 0$ .

The right column is a cochain complex associated with each CW complex  $Z(L)$ .

$$\begin{array}{ccccccc}
& & \cdot & & & & \\
& & \cdot & & & & \\
& & \cdot & & & & \\
& \delta \uparrow & & & & & \\
C^{m+4}(L; \mathbb{Z}_2) & \longrightarrow & 0 & \longleftarrow & 0 & & \\
& \delta \uparrow & & & \delta \uparrow & & \delta \uparrow \\
C^{m+3}(L; \mathbb{Z}_2) & \xrightarrow{\text{isomorphism}} & C^{m+3}(L; \mathbb{Z}_2) & \xleftarrow{\text{isomorphism}} & C^{m+3+N}(Z(L); \mathbb{Z}_2) & & \\
& \delta \uparrow & & & \delta \uparrow & & \delta \uparrow \\
C^{m+2}(L; \mathbb{Z}_2) & \xrightarrow{\text{isomorphism}} & C^{m+2}(L; \mathbb{Z}_2) & \xleftarrow{\text{isomorphism}} & C^{m+2+N}(Z(L); \mathbb{Z}_2) & & \\
& \delta \uparrow & & & \delta \uparrow & & \delta \uparrow \\
(18.1) \quad C^{m+1}(L; \mathbb{Z}_2) & \xrightarrow{\text{isomorphism}} & C^{m+1}(L; \mathbb{Z}_2) & \xleftarrow{\text{isomorphism}} & C^{m+1+N}(Z(L); \mathbb{Z}_2) & & \\
& \delta \uparrow & & & \delta \uparrow & & \delta \uparrow \\
C^m(L; \mathbb{Z}_2) & \xrightarrow{\text{isomorphism}} & C^m(L; \mathbb{Z}_2) & \xleftarrow{\text{isomorphism}} & C^{m+N}(Z(L); \mathbb{Z}_2) & & \\
& \delta \uparrow & & & \delta \uparrow & & \delta \uparrow \\
C^{m-1}(L; \mathbb{Z}_2) & \xrightarrow{\text{isomorphism}} & C^{m-1}(L; \mathbb{Z}_2) & \longleftarrow & C^{m-1+N}(Z(L); \mathbb{Z}_2) & & \\
& \delta \uparrow & & & \delta \uparrow & & \delta \uparrow \\
C^{m-2}(L; \mathbb{Z}_2) & \xrightarrow{\text{isomorphism}} & C^{m-2}(L; \mathbb{Z}_2) & \longleftarrow & 0 & & \\
& \delta \uparrow & & & \delta \uparrow & & \\
& \cdot & \longrightarrow & & \cdot & & \\
& \cdot & \longrightarrow & & \cdot & & \\
& \cdot & \longrightarrow & & \cdot & & 
\end{array}$$

We define the second Steenrod square for virtual link diagrams.  
In the following definition, recall that there may be many choices of a set of modulis.

**Definition 18.2.** Let  $L$  be a virtual link diagram. Fix a quantum grading. Let  $x$  be any element in  $Kh^m(L; \mathbb{Z}_2)$ . Define the second Steenrod square  $Sq^2(x) \in Kh^{m+2}(L; \mathbb{Z}_2)$  to be  $\kappa^{-1}(Sq^2(\{\pi^{-1}(x)\}))$  for each  $Z(L)$ , where  $Z(L)$  is defined above and  $\pi$  and  $\kappa$  are defined below.

By the commutative diagram (18.1) we have two natural isomorphisms

$$\pi : H^{m+N}(Z(L); \mathbb{Z}_2) \rightarrow Kh^m(L; \mathbb{Z}_2)$$

and

$$\kappa : Kh^{m+2}(L; \mathbb{Z}_2) \rightarrow H^{m+2+N}(Z(L); \mathbb{Z}_2).$$

for each  $Z(L)$ .

**Remark.** For each  $m$ ,  $Z(L)$  is a CW complex. Hence  $Z(L)$  has the second Steenrod square  $Sq^2$ . By using  $Sq^2$  for each  $Z(L)$ , and these two homomorphisms, we define the second Steenrod square  $Sq^2$  for  $L$  as above.

## 19. OUR SECOND STEENROD SQUARE DOES NOT DEPEND ON MODULIS OR FRAMINGS

We have the following.

**Theorem 19.1.**  *$Sq^2$  for  $L$  in Definition 18.2 is independent of the choice of modulis and framings.*

**Proof of Theorem 19.1.** The second Steenrod square of  $Z(L)$  is determined by  $Z^{(m+2+N)}(L)/Z^{(m-1+N)}(L)$  (See [31, §3.1]).

$Z^{(m+2+N)}(L)/Z^{(m-1+N)}(L)$  are made of the cells  $e_i^{m+N}$ ,  $e_j^{m+1+N}$ , and  $e_k^{m+2+N}$  ( Recall Definition 18.1.)

See the part of [29, Proof of Proposition 6.1] corresponding to the following discussion. Consider the link diagram  $L'$  obtained by taking the disjoint union of  $L$  with a 1-crossing unknot  $U$ , drawn so that the 0-resolution of  $U$  consists of two circles (and hence the 1-resolution of  $U$  consists of a single circle). Make two (resepctively, one) component enhanced Kauffman state  $\tau$  (respectively,  $o$ ) from  $U$  as in Figure 19.1.

Let  $P$  be a poset of all  $e_i^{m+N}$ ,  $e_j^{m+1+N}$ , and  $e_k^{m+2+N}$  of  $Z^{(m+2+N)}(L)/Z^{(m-1+N)}(L)$ .

Let  $\xi$  be a cell of  $P$ . Hence  $\xi$  corresponds to an enhanced Kauffman state. Make posets  $T = \{\xi \amalg \tau\}$ ,  $O = \{\xi \amalg o\}$ , and  $Q = T \cup O$ .

Note the following.  $[\delta(\tau); o] = 1$ .

$$[\delta(\xi \amalg \tau); \xi \amalg o] = 1.$$

$$gr_h(\xi \amalg \tau) = gr_h(\xi \amalg o) + 1.$$

$$gr_q(\xi \amalg \tau) = gr_q(\xi \amalg o).$$

There is an order preserving one-to-one map from  $P$  to  $O$  (respectively,  $T$ ).

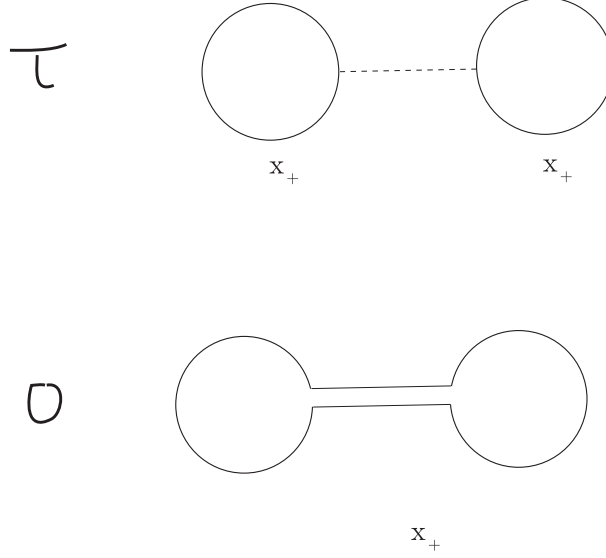


FIGURE 19.1. **Two (respectively, one) component enhanced Kauffman state  $\tau$  (respectively,  $o$ )**

Consider a set  $\mathcal{S}$  (respectively,  $\hat{\mathcal{S}}$ ) of pairs  $(\mathcal{M}(\xi, \xi'), fr)$  (respectively,  $(\hat{\mathcal{M}}(\xi, \xi'), \hat{fr})$ ) of moduli and framings for  $P$ . Construct a CW complex  $W$  (respectively,  $\hat{W}$ ).

For  $\xi \amalg \tau \in T$ , let  $(\mathcal{M}(\xi \amalg \tau, \xi' \amalg \tau), fr) = (\mathcal{M}(\xi, \xi'), fr)$ . Make a CW complex  $W_o$  from  $O$ .

For  $\hat{\xi} \amalg o \in O$ , let  $(\hat{\mathcal{M}}(\hat{\xi} \amalg o, \hat{\xi}' \amalg o), \hat{fr}) = (\hat{\mathcal{M}}(\xi, \xi'), \hat{fr})$ .

Let  $\xi \amalg \tau \in T$  and  $\hat{\xi} \amalg o \in O$ . Note  $\xi \amalg \tau \in T, \hat{\xi} \amalg o \in O \in T \cup O = Q$ . Make a moduli  $\mathcal{M}(\xi \amalg \tau, \hat{\xi} \amalg o)$  as in §12-§15. We can extend framings on this moduli  $\mathcal{M}(\xi \amalg \tau, \hat{\xi} \amalg o)$  to be compatible with those two ones  $(\mathcal{M}(\xi \amalg \tau, \xi' \amalg \tau), fr)$  and  $(\hat{\mathcal{M}}(\hat{\xi} \amalg o, \hat{\xi}' \amalg o), \hat{fr})$ . *Reason:* Let  $e \in T$  and  $f \in O$ . Let  $g \in P(e, f)$ . Let  $\text{gr}_h(e)_h^{\text{gr}}(f) = 3$  and  $\text{gr}_h(e)_h^{\text{gr}}(g) = 2$ . Then  $\mathcal{M}(e, g) \subset \partial\mathcal{M}(e, f)$  has not been framed when we attach  $\mathcal{M}(e, f)$ . We give a framing on each  $\mathcal{M}(e, g)$  so that the framings on  $\partial\mathcal{M}(e, f)$  extends to  $\mathcal{M}(e, f)$ .

Make a CW complex  $W_Q$  from  $Q$ .

By the same discussion of the part of [29, Proof of Proposition 6.1], we have the following: We have  $W_Q/W_O = \Sigma\hat{W}$  by the construction of these CW complexes. By Puppe theorem which is cited in [29, Lemma3.32.(3)],  $W_Q/W_O$  is stable homotopy type equivalent to  $\Sigma\hat{W}$ .

Therefore  $Z^{(m+2+N)}(L)/Z^{(m-1+N)}(L)$  does not depend on which moduli and which framings we use.  $\square$

**Remark 19.2.** If we give a framing to moduli of  $Z^{(m+2)}(L)/Z^{(m-1)}(L)$  different from the framing defined in Definition 18.1,  $Sq^2$  does not change (Theorem 19.1).

Although the second Steenrod square of  $Z(L)$  is determined by  $Z^{(m+2+N)}(L)/Z^{(m-1+N)}(L)$  (Proposition 17.2), we do not have  $H^{m+N}(Z^{(m+2+N)}(L)/Z^{(m-1+N)}(L); \mathbb{Z}_2) \cong Kh^m(L; \mathbb{Z}_2)$  and  $Kh^{m+2}(L; \mathbb{Z}_2) \cong H^{m+2+N}(Z^{(m+2+N)}(L)/Z^{(m-1+N)}(L); \mathbb{Z}_2)$  in general (see (18.1)). Therefore we need to let  $\rho \geq 4$  to define  $Sq^2$ , where  $\rho$  is the difference between the largest degree of chain groups and the smallest degree of them in the right column in (18.1).

For  $Z(L)$ , we make a commutative diagram (17.1). We can check maps in (17.1) explicitly by using the commutative diagram (18.1). Hence we can apply Proposition 17.2 well. We can also apply Fact 17.3.

Furthermore, therefore, we have the following. Suppose that  $Z(L)$  and  $Z^\bullet(L)$  are not homotopy type equivalent. Assume that  $Z^{(m+2)}(L)/Z^{(m-1)}(L)$  and  $(Z^\bullet(L))^{(m+2)}/(Z^\bullet(L))^{(m-1)}$  are homotopy type equivalent. Then  $Z(L)$  and  $Z^\bullet(L)$  determine the same  $Sq^2$  for  $L$ .

**Remark.** There may be many choices of  $Z(L)$ . Let  $Z(L)$  and  $Z^\bullet(L)$  be such ones. Although  $Z(L)$  and  $Z^\bullet(L)$  may not be homotopy type equivalent, there is a natural chain isomorphism between  $C^*(Z(L); \mathbb{Z}_2)$  and  $C^*(Z^\bullet(L); \mathbb{Z}_2)$  by the commutative diagram (18.1). However there is no continuous map between  $Z(L)$  and  $Z^\bullet(L)$  that induces this natural chain isomorphism, in general.

Take  $f$  (respectively,  $f', g, g'$ ) for  $Z(L)$  in the commutative diagram (17.1), and call one for  $Z^\bullet(L)$ ,  $f^\bullet$  (respectively,  $f^{\bullet'}, g^\bullet, g^{\bullet'}$ ). There are two commutative diagrams below.

$$(19.1) \quad \begin{array}{ccccc} H^m(Z(L); \mathbb{Z}_2) & \xrightarrow{\text{isomorphism, } g} & H^m((Z(L))^{(m+2)}; \mathbb{Z}_2) & \xleftarrow{\text{surjective, } f} & H^m((Z(L))^{(m+2)}/(Z(L))^{(m-1)}; \mathbb{Z}_2) \\ \text{isomorphism } \uparrow & & \text{isomorphism } \uparrow & & \text{isomorphism } \uparrow \\ H^m(Z^\bullet(L); \mathbb{Z}_2) & \xrightarrow{\text{isomorphism, } g^\bullet} & H^m((Z^\bullet(L))^{(m+2)}; \mathbb{Z}_2) & \xleftarrow{\text{surjective, } f^\bullet} & H^m((Z^\bullet(L))^{(m+2)}/(Z^\bullet(L))^{(m-1)}; \mathbb{Z}_2) \end{array}$$

$$(19.2) \quad \begin{array}{ccccc} H^{m+2}(Z(L); \mathbb{Z}_2) & \xrightarrow{\text{injective, } g'} & H^{m+2}(Z(L)^{(m+2)}; \mathbb{Z}_2) & \xleftarrow{\text{isomorphism, } f'} & H^{m+2}(Z(L)^{(m+2)}/Z(L)^{(m-1)}; \mathbb{Z}_2) \\ \text{isomorphism } \uparrow & & \text{isomorphism } \uparrow & & \text{isomorphism } \uparrow \\ H^{m+2}(Z^\bullet(L); \mathbb{Z}_2) & \xrightarrow{\text{injective, } g^{\bullet'}} & H^{m+2}((Z^\bullet(L))^{(m+2)}; \mathbb{Z}_2) & \xleftarrow{\text{isomorphism, } f^{\bullet'}} & H^{m+2}((Z^\bullet(L))^{(m+2)}/(Z^\bullet(L))^{(m-1)}; \mathbb{Z}_2) \end{array}$$

There is no continuous map between  $Z(L)$  and  $Z^\bullet(L)$  that induces the vertical isomorphisms in (19.1) and (19.2), in general.

Make  $Sq^2$  by using each of  $Z(L)$  and  $Z^\bullet(L)$  according to Definition 18.2. By the commutative diagrams (19.1) and (19.2), the difference of each  $Sq^2$  occurs by the the most right-handed vertical homomorphism in the commutative diagrams (17.1) for  $Z(L)$  and  $Z^\bullet(L)$ :



$$\begin{array}{ccc}
H^{m+2}((Z(L))^{(m+2)}/(Z(L))^{(m-1)}; \mathbb{Z}_2) & & H^{m+2}((Z(L)^\bullet)^{(m+2)}/(Z(L)^\bullet)^{(m-1)}; \mathbb{Z}_2) \\
\uparrow Sq^2 & \text{and} & \uparrow Sq^2 \\
H^m((Z(L))^{(m+2)}/(Z(L))^{(m-1)}; \mathbb{Z}_2) & & H^m((Z(L)^\bullet)^{(m+2)}/(Z(L)^\bullet)^{(m-1)}; \mathbb{Z}_2).
\end{array}$$

## 20. REIDEMEISTER MOVES DO NOT CHANGE OUR SECOND STEENROD SQUARE

Although the homotopy type of each  $Z(L)$  may change by Reidemeister moves on  $L$ , we have the following. It is a main result of this paper.

**Theorem 20.1.** *Let  $L$  and  $L'$  be virtual link diagrams which represent the same virtual link. Note that  $Kh^m(L; \mathbb{Z}_2) \cong Kh^m(L'; \mathbb{Z}_2)$ . Then the second Steenrod square  $Sq^2(L)$  is the same as  $Sq^2(L')$ .*

**Proof of Theorem 20.1.** We have the following.

**Fact 20.2.** *It is enough to prove the case where  $L$  is changed into  $L'$  by a single Reidemeister move. The Reidemeister moves are shown in Figure 4.3.*

Fix a quantum grading. Let  $\{C^*(L)\}$  (respectively,  $\{C^*(L')\}$ ) be Khovanov chain complex for the virtual link diagram  $L$  (respectively,  $L'$ ), and  $\{C_\#(L)\}$  (respectively,  $\{C_\#(L')\}$ ) the dual Khovanov chain complex for  $L$  (respectively,  $L'$ ).

**The case of non-classical Reidemeister moves.** Assuming that the Reidemeister move is non-classical, then there is a bijective map from Khovanov basis of  $L$  to that of  $L'$  such that the homological and quantum gradings are kept and such that the partial order of the dual Khovanov basis are kept. (See §5.). This identity map induces a chain identity map  $C_\#(L) \rightarrow C_\#(L')$ .

By using the dual Khovanov basis of  $L$  (respectively,  $L'$ ) and the moduli spaces, construct each  $Z(L)$  (respectively,  $Z(L')$ ) as in Definition 18.1. By using the above bijection from the dual Khovanov basis of  $L$  to that of  $L'$ , we can make a homeomorphism from a disjoint union of all  $Z(L)$  to that of all  $Z(L')$ , where we give appropriate orders to the components of the disjoint unions.

By this homeomorphism map, Theorem 20.1 holds in this case.

**The case of classical Reidemeister moves.** If the Reidemeister move is the classical Reidemeister move  $I$  or  $II$ , we can prove, by the same way as the one in [29, section 6], that there is an injective map from Khovanov basis (respectively, the dual Khovanov basis) of one of  $L$  and  $L'$  to that of the other, such that the homological and quantum gradings are kept and such that the partial order of Khovanov basis (respectively, the

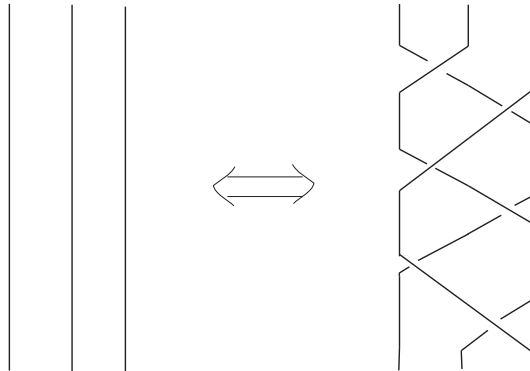


FIGURE 20.1. **The classical braid-like Reidemeister move III**

dual Khovanov basis) are kept. Without loss of generality, we can assume that this injective map is from that of  $L$  to that of  $L'$ . Furthermore, this injective map induces injective chain homotopy equivalence maps,  $C^*(L') \rightarrow C^*(L)$  and  $C_{\#}(L) \rightarrow C_{\#}(L')$ .

Suppose that the Reidemeister move is the classical Reidemeister move *III*. Note that both [5, section 3.5.5] and [29, section 6] proved that there is a chain homotopy equivalence map  $C^*(L) \rightarrow C^*(L')$  or  $C^*(L') \rightarrow C^*(L)$  if  $L$  and  $L'$  are classical links and if  $L$  is changed into  $L'$  by one classical Reidemeister *III* move. The result from [29, section 6] improves on the result in [5, section 3.5.5].

By the same method of [29, section 6], we can prove the following. Let  $\mathbb{N}$  be the set of natural numbers. For  $L$  and  $L'$  above, there are virtual link diagrams,  $M_1, \dots, M_{\mu}$  ( $\mu \in \mathbb{N} - \{1\}$ ), with the following properties:  $M_1$  is one of  $L$  and  $L'$ , and  $M_{\mu}$  the other. If  $1 \leq i \leq \mu - 1$ ,  $M_i$  is made into  $M_{i+1}$  by one classical Reidemeister *II* or one classical braid-like Reidemeister move *III* in [29, Figure 6.1] and in [3, section 7.3]. The classical braid-like Reidemeister move *III* is shown in Figure 20.1.

Let  $M$  be obtained from  $M'$  by one classical braid-like Reidemeister move *III*. Then there is an injective map from Khovanov basis (respectively, the dual Khovanov basis) of one of  $M$  and  $M'$  to that of the other such that the homological and quantum gradings are kept and such that the partial order of Khovanov basis (respectively, the dual Khovanov basis) are kept.

So we interpret Fact 20.2 as follows.

**Fact 20.3.** *It is enough to prove Theorem 20.1 in the case where  $L$  is changed into  $L'$  by a single move. The single move is each of the classical braid-like Reidemeister*

move III shown in Figure 20.1 and all other Reidemeister moves except for the classical Reidemeister move III shown in Figure 4.3.

From here, we use the notations  $\{C^*(L)\}$ ,  $\{C^*(L')\}$ ,  $\{C_{\#}(L)\}$ , and  $\{C_{\#}(L')\}$  for  $L$  and  $L'$  in Fact 20.3.

We proved the case of non-classical Reidemeister moves in the first part of this proof.

We prove the case of classical Reidemeister moves below.

In all classical cases of Fact 20.3, we can assume, by the discussion right above, that we have injective maps from the dual Khovanov set (repectively, Khovanov set) of  $L$  to that of  $L'$ , and injective chain homotopy equivalence maps  $\alpha : C_{\#}(L) \rightarrow C_{\#}(L')$  (respectively,  $\beta : C^*(L) \rightarrow C^*(L')$ ).

We can prove the following by the same method of [29].

**Claim 20.4.** *Let  $\mathbf{x} = (D_L(u), x)$  (respectively,  $\mathbf{y} = (D_L(v), y)$ ) correspond to  $\mathbf{x}' = (D_{L'}(u'), x')$  (respectively,  $\mathbf{y}' = (D_{L'}(v'), y')$ ) by this map. Then we have the following facts.*

*Let  $B$  be a 2-dics where the Reidemeister move is carried out. After we remove arcs in  $B$  from  $\mathbf{x}'$  (respectively,  $\mathbf{y}'$ ),  $\mathbf{x}$  and  $\mathbf{x}'$  (respectively,  $\mathbf{y}$  and  $\mathbf{y}'$ ) are the same. See [29, Figure 6.2-6.4]: In these figures, dotted arcs (their red arcs) are omitted.*

*$(D_L(u) - D_L(v), x)$  (respectively,  $(D_L(v) - D_L(u), y)$ ) is the same as  $(D_{L'}(u') - D_{L'}(v'), x')$  (respectively,  $(D_{L'}(v') - D_{L'}(u'), y')$ ).*

*There is a map from  $P(D_L(v) - D_L(u), x, y)$  to  $P(D_{L'}(v') - D_{L'}(u'), x', y')$  preserving the homological degree and the quantum one.*

*The set of all possible  $\mathcal{M}(\mathbf{x}, \mathbf{y})$  is the same as that of all possible  $\mathcal{M}(\mathbf{x}', \mathbf{y}')$ .*

**Remark.** For a fixed pair of  $\mathbf{x}$  and  $\mathbf{y}$ , there are no more than one  $\mathcal{M}(\mathbf{x}, \mathbf{y})$  in general. When we make modulis in Proposition 14.2, there may be many choices by the existence of quasi-ladybug configurations. When we make modulis in Proposition 15.1, there may be many choices of homeomorphisms of the boudary of handle bodies.

We use the above injective maps between the dual Khovanov basis (not Khovanov basis), and  $\alpha : C_{\#}(L) \rightarrow C_{\#}(L')$  (not  $\beta : C^*(L) \rightarrow C^*(L')$ ). Note that this injective chain homotopy equivalence map  $\alpha : C_{\#}(L) \rightarrow C_{\#}(L')$  induces a chain homotopy equivalence map  $\varphi : C^*(L') \rightarrow C^*(L)$  by using the usual ‘‘Hom’’ duality. Note that  $\varphi : C^*(L') \rightarrow C^*(L)$  is not  $\beta : C^*(L) \rightarrow C^*(L')$ , and that  $\varphi$  is not necessarily injective, in general.

## 21. SUB CW COMPLEXES

We are now in a position to construct the needed CW complexes, as we explain below. We define each  $Z(L)$  (respectively,  $Z(L')$ ) for  $L$  (respectively  $L'$ ) by using the moduli spaces above. There may be more than one  $Z(L)$  (respectively,  $Z(L')$ ). By the definition of  $\alpha$  and Claim 20.4, we have the following.

**Claim 21.1.** *Each  $Z(L)$  is a sub CW complex of one  $Z(L')$  and the inclusion map is obtained by using  $\alpha$ . For Each  $Z(L')$ , there is one  $Z(L)$  which is a sub CW complex of the  $Z(L')$ , and the inclusion map is obtained by using  $\alpha$ .*

This inclusion map  $Z(L) \rightarrow Z(L')$  is important for our proof.

We want to prove that  $Sq^2$  for  $Z(L)$  and  $Sq^2$  for  $Z(L')$  are the same.

Let  $f_{\sharp}^*$  be a cell in  $Z(L')$ . Then we have only two cases:  $\text{Int}f_{\sharp}^*$  is in  $Z(L)$ .  $\text{Int}f_{\sharp}^*$  is out  $Z(L)$ .

When we attach  $f_{\sharp}^*$ , framings in the lower dimensional skeleton and in  $Z(L)$  are determined. Note that this situation is the same as the following situation: When we attach  $f_{\sharp}^*$ , framings in the lower dimensional skeleton are determined.

We proved that we can attach  $f_{\sharp}^*$  in this situation. Therefore we can define framings on modulis so that we can construct  $Z(L')$ .

Since  $\wp : C^*(L') \rightarrow C^*(L)$  is a chain homotopy equivalence map, we have two isomorphisms

$$Kh^*(L') \rightarrow Kh^*(L)$$

and

$$\rho : Kh^*(L'; \mathbb{Z}_2) \rightarrow Kh^*(L; \mathbb{Z}_2)$$

for all  $*$ .

By using the dual Khovanov basis elements of  $L'$  and the moduli spaces, construct  $Z(L')$  as in Definition 18.1. By using the above injective map from the dual Khovanov basis of  $L$  to that of  $L'$ , we can let one  $Z(L)$  be a sub-CW complex of one  $Z(L')$  as written above. Hence there is an inclusion map  $Z(L) \rightarrow Z(L')$ .

By the diagram (18.1) we have the following two commutative diagrams.

$$\begin{array}{ccc}
C^{m+4}(L; \mathbb{Z}_2) & \longleftarrow & 0 \\
\delta \uparrow & & \delta \uparrow \\
C^{m+3}(L; \mathbb{Z}_2) & \xleftarrow{\text{isomorphism}} & C^{m+3+N}(Z(L); \mathbb{Z}_2) \\
\delta \uparrow & & \delta \uparrow \\
C^{m+2}(L; \mathbb{Z}_2) & \xleftarrow{\text{isomorphism}} & C^{m+2+N}(Z(L); \mathbb{Z}_2) \\
\delta \uparrow & & \delta \uparrow \\
C^{m+1}(L; \mathbb{Z}_2) & \xleftarrow{\text{isomorphism}} & C^{m+1+N}(Z(L); \mathbb{Z}_2) \\
\delta \uparrow & & \delta \uparrow \\
C^m(L; \mathbb{Z}_2) & \xleftarrow{\text{isomorphism}} & C^{m+N}(Z(L); \mathbb{Z}_2) \\
\delta \uparrow & & \delta \uparrow \\
C^{m-1}(L; \mathbb{Z}_2) & \xleftarrow{\text{isomorphism}} & C^{m-1+N}(Z(L); \mathbb{Z}_2) \\
\delta \uparrow & & \delta \uparrow \\
C^{m-2}(L; \mathbb{Z}_2) & \longleftarrow & 0
\end{array}$$

(21.1)

$$\begin{array}{ccc}
C^{m+4}(L'; \mathbb{Z}_2) & \longleftarrow & 0 \\
\delta \uparrow & & \delta \uparrow \\
C^{m+3}(L'; \mathbb{Z}_2) & \xleftarrow{\text{isomorphism}} & C^{m+3+N}(Z(L'); \mathbb{Z}_2) \\
\delta \uparrow & & \delta \uparrow \\
C^{m+2}(L'; \mathbb{Z}_2) & \xleftarrow{\text{isomorphism}} & C^{m+2+N}(Z(L'); \mathbb{Z}_2) \\
\delta \uparrow & & \delta \uparrow \\
C^{m+1}(L'; \mathbb{Z}_2) & \xleftarrow{\text{isomorphism}} & C^{m+1+N}(Z(L'); \mathbb{Z}_2) \\
\delta \uparrow & & \delta \uparrow \\
C^m(L'; \mathbb{Z}_2) & \xleftarrow{\text{isomorphism}} & C^{m+N}(Z(L'); \mathbb{Z}_2) \\
\delta \uparrow & & \delta \uparrow \\
C^{m-1}(L'; \mathbb{Z}_2) & \xleftarrow{\text{isomorphism}} & C^{m-1+N}(Z(L'); \mathbb{Z}_2) \\
\delta \uparrow & & \delta \uparrow \\
C^{m-2}(L'; \mathbb{Z}_2) & \longleftarrow & 0
\end{array}$$

(21.2)

The following is a part of the chain homotopy equivalence map  $\varphi : C^*(L') \rightarrow C^*(L)$ .

$$\begin{array}{ccc}
 C^{m+3}(L'; \mathbb{Z}_2) & \longrightarrow & C^{m+3}(L; \mathbb{Z}_2) \\
 \delta \uparrow & & \delta \uparrow \\
 C^{m+2}(L'; \mathbb{Z}_2) & \longrightarrow & C^{m+2}(L; \mathbb{Z}_2) \\
 \delta \uparrow & & \delta \uparrow \\
 C^{m+1}(L'; \mathbb{Z}_2) & \longrightarrow & C^{m+1}(L; \mathbb{Z}_2) \\
 \delta \uparrow & & \delta \uparrow \\
 C^m(L'; \mathbb{Z}_2) & \longrightarrow & C^m(L; \mathbb{Z}_2) \\
 \delta \uparrow & & \delta \uparrow \\
 C^{m-1}(L'; \mathbb{Z}_2) & \longrightarrow & C^{m-1}(L; \mathbb{Z}_2) \\
 \delta \uparrow & & \delta \uparrow \\
 C^{m-2}(L'; \mathbb{Z}_2) & \longrightarrow & C^{m-2}(L; \mathbb{Z}_2)
 \end{array}
 \tag{21.3}$$

By using the commutative diagrams (21.2)-(21.3), we make the following

$$\begin{array}{ccc}
0 & \longrightarrow & 0 \\
\delta \uparrow & & \delta \uparrow \\
C^{m+3+N}(Z(L'); \mathbb{Z}_2) & \longrightarrow & C^{m+3+N}(Z(L); \mathbb{Z}_2) \\
\delta \uparrow & & \delta \uparrow \\
C^{m+2+N}(Z(L'); \mathbb{Z}_2) & \longrightarrow & C^{m+2+N}(Z(L); \mathbb{Z}_2) \\
\delta \uparrow & & \delta \uparrow \\
C^{m+1+N}(Z(L'); \mathbb{Z}_2) & \longrightarrow & C^{m+1+N}(Z(L); \mathbb{Z}_2) \\
\delta \uparrow & & \delta \uparrow \\
C^{m+N}(Z(L'); \mathbb{Z}_2) & \longrightarrow & C^{m+N}(Z(L); \mathbb{Z}_2) \\
\delta \uparrow & & \delta \uparrow \\
C^{m-1+N}(Z(L'); \mathbb{Z}_2) & \longrightarrow & C^{m-1+N}(Z(L); \mathbb{Z}_2) \\
\delta \uparrow & & \delta \uparrow \\
0 & \longrightarrow & 0
\end{array}
\tag{21.4}$$

that induces two isomorphisms

$$\zeta : H^{m+N}(Z(L'); \mathbb{Z}_2) \rightarrow H^{m+N}(Z(L); \mathbb{Z}_2)$$

and

$$\theta : H^{m+2+N}(Z(L'); \mathbb{Z}_2) \rightarrow H^{m+2+N}(Z(L); \mathbb{Z}_2).$$

We have the following two commutative diagrams by the construction of  $Z(L)$ , that of  $Z(L')$ , the definition of  $\varphi$ , and the commutative diagrams (18.1) and (21.2)-(21.4).

The homomorphism  $H^{m+N}(Z(L'); \mathbb{Z}_2) \rightarrow H^{m+N}(Z(L); \mathbb{Z}_2)$  is an epimorphism by the construction of  $Z(L)$  and that of  $Z(L')$ .

$$\begin{array}{ccc}
Kh^m(L'; \mathbb{Z}_2) & \xrightarrow{\text{isomorphism, } \rho} & Kh^m(L; \mathbb{Z}_2) \\
\text{isomorphism, } \pi \uparrow & & \text{isomorphism, } \pi \uparrow \\
H^{m+N}(Z(L'); \mathbb{Z}_2) & \xrightarrow{\text{isomorphism, } \zeta} & H^{m+N}(Z(L); \mathbb{Z}_2)
\end{array}$$



$$\begin{array}{ccc}
H^{m+2+N}(Z(L'); \mathbb{Z}_2) & \xrightarrow{\text{isomorphism, } \theta} & H^{m+2+N}(Z(L); \mathbb{Z}_2) \\
\text{isomorphism, } \kappa \uparrow & & \text{isomorphism, } \kappa \uparrow \\
Kh^{m+2}(L'; \mathbb{Z}_2) & \xrightarrow{\text{isomorphism, } \rho} & Kh^{m+2}(L; \mathbb{Z}_2)
\end{array}$$

The naturality of Steenrod squares makes the following commutative diagram.

$$\begin{array}{ccc}
H^{m+N}(Z(L'); \mathbb{Z}_2) & \xrightarrow{\text{isomorphism, } \zeta} & H^{m+N}(Z(L); \mathbb{Z}_2) \\
Sq^2 \downarrow & & Sq^2 \downarrow \\
H^{m+2+N}(Z(L'); \mathbb{Z}_2) & \xrightarrow{\text{isomorphism, } \theta} & H^{m+2+N}(Z(L); \mathbb{Z}_2)
\end{array}$$

Combine these three commutative diagrams to obtain a commutative diagram below.

$$\begin{array}{ccc}
Kh^m(L'; \mathbb{Z}_2) & \xrightarrow{\text{isomorphism, } \rho} & Kh^m(L; \mathbb{Z}_2) \\
\text{isomorphism, } \pi \uparrow & & \text{isomorphism, } \pi \uparrow \\
H^{m+N}(Z(L'); \mathbb{Z}_2) & \xrightarrow{\text{isomorphism, } \zeta} & H^{m+N}(Z(L); \mathbb{Z}_2) \\
Sq^2 \downarrow & & Sq^2 \downarrow \\
H^{m+2+N}(Z(L'); \mathbb{Z}_2) & \xrightarrow{\text{isomorphism, } \theta} & H^{m+2+N}(Z(L); \mathbb{Z}_2) \\
\text{isomorphism, } \kappa \uparrow & & \text{isomorphism, } \kappa \uparrow \\
Kh^{m+2}(L'; \mathbb{Z}_2) & \xrightarrow{\text{isomorphism, } \rho} & Kh^{m+2}(L; \mathbb{Z}_2)
\end{array}$$

By this diagram, Theorem 20.1 holds. □

By Theorem 20.1, the following is well-defined.

**Definition 21.2.** Let  $\mathcal{L}$  be a virtual link. Let  $L$  be a virtual link diagram which represents  $\mathcal{L}$ . We define the second Steenrod square  $Sq^2$  for  $\mathcal{L}$  to be that on  $Sq^2$  for  $L$ .

The following is a main result of this paper.

**Theorem 21.3.** *If  $\mathcal{L}$  is a classical link, the second Steenrod square  $Sq^2$  specifies the second Steenrod square in the case of classical links which is defined in [31].*

**Proof of Theorem 21.3.** By Theorem 19.1 and the definition of the second Steenrod square of classical links in [29].  $\square$

Note that Theorem 20.1 includes Theorem 21.3. Note Remark 3.1.

In the case of classical links, in [31] Lipshitz and Sarkar showed a way to calculate  $Sq^2$  by using classical link diagrams. We must consider whether the method can be extended to the case of virtual links.

Recall Theorem 5.1: There are classical links  $K_1$  and  $K_2$  such that Khovanov homology of  $K_1$  is the same as that of  $K_2$ , but that the second Steenrod square of  $K_1$  is different from that of  $K_2$ .

Note that all classical links are virtual links by the definition. Therefore, by Theorem 5.1, there are virtual links  $K_1$  and  $K_2$  such that Khovanov homology of  $K_1$  is the same as that of  $K_2$ , but that the second Steenrod square of  $K_1$  is different from that of  $K_2$ .

It is very natural to ask whether there is a pair of non-classical, virtual links which have different second Steenrod squares and which have the same Khovanov homology. We answer this question below. This is a main result of this paper.

**Theorem 21.4.** *In the case of non-classical, virtual links, our second Steenrod square  $Sq^2$  is stronger than Khovanov homology. That is, there is a pair of non-classical, virtual links which have different second Steenrod squares and which have the same Khovanov homology.*

**Proof of Theorem 21.4.** Let us consider the example in Figure 21.1. Let  $K$  be any classical link diagram. Then this represents a non-classical, virtual link. *Reason.* The virtual link diagram in Figure 21.1 has only one virtual crossing point. No Reidemeister move changes the parity of virtual crossing points which are made by two different components of a virtual link diagram.

In this case, we do not have a quasi-ladybug configuration. The right pair and the left one of ladybug situations give the same Steenrod second square by explicit calculus which uses that about the classical link diagram  $K$ . (Note that the Steenrod square is only one element in this case.)

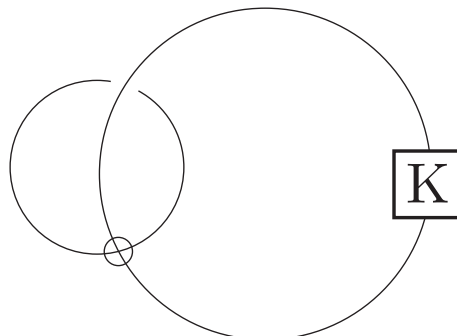


FIGURE 21.1. If  $K$  is any classical link diagram, this virtual link diagram represents a non-classical, virtual link.

Take  $K_1$  and  $K_2$  in Theorem 5.1, cited above. Let  $K$  be  $K_1$  (respectively,  $K_2$ ). These two cases have different Steenrod squares and the same Khovanov homology. Recall that Seed used Lipshitz and Sarkar's work to produce two classical knots  $K_1$  and  $K_2$  with same Khovanov homology that are distinguished by using the Steenrod square. We observe that, by using  $K_1$  and  $K_2$  in our virtual examples, we can achieve the same phenomenon.

**An alternative proof:** The operation flanking (See [6]) of each of Seed's pair of classical knots [53] makes infinitely many pair that satisfy the condition of Theorem 21.4. (Two operations, flanking and virtualization, are different although they are very related. See [6, 50].)  $\square$

The above examples are just the beginning of many possible applications of the result in this paper. Further applications require deeper computations of the virtual Khovanov homology and will be the subject of a subsequent paper.

In [50], Rushworth gives another way to construct a Khovanov homology for virtual links, called the doubled Khovanov Homology. It is natural to ask whether we can make a CW complex and Steenrod squares for the doubled Khovanov chain complex. We hope to answer this question in later work.

## 22. OPEN PROBLEMS

One reason why virtual knots and links are introduced is as follows: The definition of the Alexander polynomial and those of many other invariants for links in  $S^3$  are extended into the case of links in any 3-manifold other than  $S^3$  consistently. It is very natural to ask the following question.

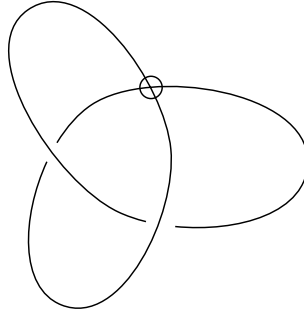


FIGURE 22.1. **The Jones polynomial of this virtual knot is not that of any classical knot.**

**Question 22.1.** Can we generalize the definition of the Jones polynomial for classical links in  $S^3$  to the case of any 3-manifold?

A significant partial answer to this question is given by using virtual knot theory, for the case of manifolds of the form of a thickened surface. The Jones polynomial for virtual knots is defined in [15, 16, 17]. This fact means that, by using virtual 1-knots, we can define the Jones polynomial for links in  $(\text{the closed oriented surface}) \times [-1, 1]$ . The case of knots in the 3-ball  $B^3$  and that in the 3-space  $\mathbb{R}^3$  are trivially the same as that in  $S^3$ . We omit comments about these cases and such similar other trivial cases ( $\mathbb{R}^3$ —(an open 3-balls), etc.). Furthermore see Remark 22.2 below (see also [22]).

Note also that for knots and links in thickened surfaces, taken up to handle stabilization, virtual knot theory has a fully diagrammatic formulation, and it can be studied by using the minimal embedding genus for the virtual knot or link. This gives the theory a flexibility that has led to the discovery of many new invariants of virtual links and relationships with classical knot theory. One finds that by using the generalization of classical knot theory to virtual knot theory, there are infinitely many non-trivial virtual knots with unit Jones polynomial, all occurring in higher genus surfaces so far (see [6]). Virtual knot theory is a context for studying the conjecture that the Jones polynomial detects the classical unknot. (Recall the following facts. Let  $K$  be a classical knot diagram for a classical knot. In [9], Haken introduced an algorithm which detects whether  $K$  represents the classical unknot or not. After that, in [25], Kronheimer and Mrowka proved the Khovanov homology for classical knots can detect that. After that, in [45], Ozsváth and Szabó proved that their introduced knot Floer homology can detect that.)

There is a virtual 1-knot whose Jones polynomial is not that of any classical knot. An example is shown in Figure 22.1. Therefore there is a knot in a thickened surface whose Jones polynomial is not that of any knot in  $S^3$ . We can say that the Jones polynomial

of knots in a thickened surface defined by using virtual knots is not that of knots made by the following way (i) nor that by (ii).

(i) Let  $K$  be a knot in a thickened surface  $F \times [-1, 1]$ . Make  $K$  into  $K'$ : Embed  $F \times [-1, 1]$  in  $S^3$ , for example, in the standard position. We obtain a new knot  $K'$  in  $S^3$ .

(ii) Let  $K$  be a knot in a thickened surface  $F \times [-1, 1]$ . Make  $K$  into  $K'$ : Take the universal covering space, which is  $\mathbb{R}^2 \times [-1, 1]$ , of  $F \times [-1, 1]$ . Lift  $K$  to the universal covering space. Note that the lift of  $K$  has many components in general. Take one of them if there are many. Thus we obtain  $S^1$  or  $\mathbb{R}$  embedded in  $\mathbb{R}^2 \times [-1, 1]$ . We let it be made into a new knot  $K'$  in  $S^3$ .

**Remark 22.2.** In [49, Theorem 3.3.3, page 560] there are defined invariants for links in a closed oriented 3-manifold  $M$ . These invariants depend on the use of the colored Jones polynomials at roots of unity and the use of the Kirby calculus (see the last paragraph of this note). We are interested in more direct constructions for invariants of links in three manifolds, and we believe that the formulation of virtual knot theory is a step in this direction. Similarly in [56] Witten formulated his functional integral for any link in  $S^3$  at physics level. This gives a heuristic three dimensional definition of specializations of the Jones polynomial. However, Question 22.1 is open even in physics-level. Witten's path integral has not been calculated explicitly in the case of links in all 3-manifolds. Another aim for combinatorial topology is to find rigorous combinatorial definitions for invariants such as the Jones polynomial. Here we do not claim that new insight is gained from virtual knot theory. But now we can further ask for fully three dimensional definitions of the extension of the Jones polynomial that we have defined in the virtual theory.

Let  $L$  be a link in  $S^3$ . Let  $RT(L)$  denote all invariants defined in [49, Theorem 3.3.3, page 560]. Note that we consider the case  $M = S^3$ . It is an open question that which is stronger,  $RT(L)$  or the Jones polynomial of  $L$ . Furthermore, even if  $RT(L)$  is no weaker than the Jones polynomial of  $L$ , then do we know the Jones polynomial explicitly by a finite times of algorithm which uses a piece of information of  $RT(L)$ ?

We also have very natural outstanding open questions below.

**Question 22.3.** (1) Can we generalize the definition of the Khovanov homology for links in  $S^3$  to the case of any 3-manifold?

(2) Can we generalize the definition of the second Steenrod square operator on the Khovanov homology for links in  $S^3$  to the case of any 3-manifold?

(3) Can we generalize the definition of the Khovanov stable homotopy type for links in  $S^3$  to the case of any 3-manifold?

In [1], Asaeda, Przytycki, and Sikora gave a partial answer to Question 22.3.(1): It is given in the case of links in thickened surfaces.

In [37], Manturov introduced the Khovanov homology for virtual links. It is a partial answer to Question 22.3.(1): It is the case of links in thickened surfaces by using virtual knot theory.

In [50], Rushworth introduced the Khovanov homology for virtual links in a different way from that in [37]. It is a partial answer to Question 22.3.(1): It is the case of links in thickened surfaces by using virtual knot theory.

See also Tubbenhauer [54] and Viro [55].

In [38], Manturov and Nikonov made an alternative definition of that in [1], and obtained a new result by using it.

In [6], Dye, Kaestner, and Kauffman gave an alternative definition of that of [37], and obtained a new result by using it.

In [40], Nikonov described an alternative definition of integral virtual Khovanov homology of [37]. Nikonov's definition is written elegantly and explicitly.

In this paper we define the second Steenrod square operator on the Khovanov homology for virtual links. Therefore we can define the second Steenrod square operator on the Khovanov homology for links in  $(\text{the closed oriented surface}) \times [-1, 1]$ , and give a partial answer to Question 22.3.(2). This is only one consistent partial answer to Question 22.3.(2), for now. This is the main result of this paper (Main theorem 1.1).

We do not give an answer to Question 22.3.(3) in this paper. We give the partial solution to Question 22.3.(2) toward answering Question 22.3.(3) in the future.

There are found many relations between the Khovanov homology for knots in  $S^3$  and knot Floer homology for knots in  $S^3$ . See [32, 47, 44, 48] for knot Floer homology. See [42, 43] for the Heegaard Floer homology, from which knot Floer homology is made. See [3, 4, 33] and [47, section 1.4] etc. for their relations.

Since we extended the definition of the Jones polynomial for knots in  $S^3$ , that of the Khovanov homology for them, and that of the Steenrod square acting on the Khovanov homology for them to the case of thickened surfaces, it is very natural to ask questions below.

**Question 22.4.** (1) Can we extend knot Floer homology for knots in  $S^3$  to the case of thickened surfaces? Is there an invariant for knots in thickened surfaces which is made from knot Floer homology or which is much related to knot Floer homology?

(2) If we can make an invariant in the question right above, is there a relation between the new invariant and the Khovanov homology for knots in thickened surfaces?

(3) If we can make an invariant in the above question (1), is it virtual knot invariant?

Note that, by using virtual knot theory, we can define the Alexander-Conway polynomial for knots in thickened surfaces even if knots are non-vanishing cycles in thickened surfaces ([15, 16, 17]).

**Remark 22.5.** An observation to Question 22.4. The following is an invariant for knots in thickened surfaces, which is made by using knot Floer homology. Let  $F$  be a closed oriented surface. Let  $i = 1, 2$ . Let  $K_i$  be a null-homologous 1-knot in  $F \times [-1, 1]$ . Regard  $F \times S^1$  as the double of  $F \times [-1, 1]$ . Note that  $K_i \subset F \times [-1, 1] \subset F \times S^1$ , and call this knot in  $F \times S^1$ ,  $K'_i$ . If  $K_1 \subset F \times [-1, 1]$  is obtained from  $K_2 \subset F \times [-1, 1]$  by (a diffeomorphism of  $F$ ) $\times$ (the identity map of  $[-1, 1]$ ),  $K'_1 \subset F \times S^1$  is obtained from  $K'_2 \subset F \times S^1$  by (a diffeomorphism of  $F$ ) $\times$ (the identity map of  $S^1$ ). If  $K_1 \subset F \times [-1, 1]$  is obtained from  $K_2 \subset F \times [-1, 1]$  by a classical move,  $K'_1 \subset F \times S^1$  is obtained from  $K'_2 \subset F \times S^1$  by a classical move.

It is important that knot Floer homology of null-homologous knots in  $F \times S^1$  is defined in [44]. Knot Floer homology of  $K'_i \subset F \times S^1$  gives an invariant of  $K_i \subset F \times [-1, 1]$ .

We could prove that, by using [45, Theorem 1.1], not all invariant of this kind is a virtual knot invariant.

For 3-manifolds with non-vacuous boundary, some Floer homologies are defined: bordered Heegaard Floer homology in [27, 28] and sutured Floer homology in [12]. Can we obtain an invariant of links in thickened surfaces by using them?

**Remark.** It is trivial that there is a meaningful map from the set  $KI$  of knots in  $F \times [-1, 1]$  to that  $KS$  of ones in  $F \times S^1$ , but that it is very difficult to make a ‘meaningful’ map from  $KS$  to  $KI$ . So we can obtain an invariant of knots in  $F \times [-1, 1]$  by using knot Floer homology for null-homologous knots in  $F \times S^1$ . We know the Jones polynomial (resp. the Khovanov homology, the Steenrod square) for knots in  $F \times [-1, 1]$ , but have not known that of knots in  $F \times S^1$  (Recall Questions 22.1 and 22.3.).

**Remark 22.6.** (1) After submitting this paper to arXiv, and before publishing this paper in this journal, Kauffman, Nikonov, and Ogasa [19, 20] constructed the Khovanov homotopy type for links in thickened surfaces. It is the first partial consistent answer to Question 22.3.(3) and the second partial consistent answer to Question 22.3.(2).

(2) Virtual links are not only generalizations of a classical links, but also Virtual links introduce new topological quantum invariants of links in the 3-sphere, that is, classical links. See Kauffman and Ogasa’s paper [21]. In the paper, they also defined new topological quantum invariants of 3-manifolds with non-vacuous boundary. Dye, Kauffman, and Ogasa’s paper [7] is a sequel of [21].

(3) After submitting this paper to arXiv, and before publishing this paper in this journal, Juhász, Kauffman, and Ogasa [13] generalized an idea in 22.5 and introduced a Floer homology for all knots (not only null-homologous knots but also knots that are non-vanishing cycles) in thickened surfaces and all virtual knots.

**Acknowledgment.** The authors would like to thank Igor Mikhailovich Nikonov for the valuable discussion.

Kauffman’s work was supported by the Laboratory of Topology and Dynamics, Novosibirsk State University (contract no. 14.Y26.31.0025 with the Ministry of Education and Science of the Russian Federation.)

#### REFERENCES

- [1] M. M. Asaeda, J. H. Przytycki, and A. S. Sikora; Categorification of the Kauffman bracket skein module of I -bundles over surfaces *Algebraic & Geometric Topology* 4 (2004) 1177–1210 ATG
- [2] D. M. Austin and P. J. Braam: Morse-Bott theory and equivariant cohomology, *The Floer memorial volume, Progr. Math., vol. 133, Birkh user, Basel* (1995) 123–183.
- [3] J. A. Baldwin: On the spectral sequence from Khovanov homology to Heegaard Floer homology, *Int. Math. Res. Not.* 15 (2011) 3426–3470.
- [4] J. A. Baldwin, A. S. Levine and S. Sarkar: Khovanov homology and knot Floer homology for pointed links *Journal of Knot Theory and Its Ramifications* Vol. 26 No. 02 (2017) 1740004.
- [5] D. Bar-Natan: On Khovanov’s categorification of the Jones polynomial, *Algebr. Geom. Topol.* 2(2002), 337–370 (electronic). MR 1917056 (2003h:57014).
- [6] H A Dye, A Kaestner, and L H Kauffman: Khovanov Homology, Lee Homology and a Rasmussen Invariant for Virtual Knots, *Journal of Knot Theory and Its Ramifications* 26 (2017).
- [7] H. A. Dye, L. H. Kauffman and E. Ogasa: Quantum Invariants of Links and 3-Manifolds with Boundary defined via Virtual Links: Calculation of some examples, arXiv:2203.12797 [math.GT]
- [8] A. Hatcher: Algebraic Topology, *Cambridge University Press* (2001)
- [9] W. Haken: Theorie der Normalfl achen *Acta Mathematica* 105 (1961) 245–375.
- [10] D. Ilyutko and V. Manturov, , Virtual Knots: The State of the Art. Series on Knots and Everything. World Scientific Publishing Co, Hackensack, 2013.
- [11] D.P. Ilyutko, V.O. Manturov, I.M. Nikonov, Parity in knot theory and graph links, *J. Math. Sci.* 193 (2013), no. 6, 809–965
- [12] A. Juhász: Holomorphic discs and sutured manifolds, *Algebr. Geom. Topol.* 6(3): 1429-1457 (2006). DOI: 10.2140/agt.2006.6.1429
- [13] A. Juhász, L.HjKauffman, and E. Ogasa: New Invariants via Spanning Surfaces for Virtual Knots arXiv mathGT
- [14] L. H. Kauffman: State models and the Jones polynomial, *Topology* 26 (1987) 395-407.
- [15] L. H. Kauffman: Talks at MSRI Meeting in January 1997, AMS Meeting at University of Maryland, College Park in March 1997, Isaac Newton Institute Lecture in November 1997, Knots in Hellas Meeting in Delphi, Greece in July 1998, APCTP-NANKAI Symposium on Yang-Baxter Systems, Non-Linear Models and Applications at Seoul, Korea in October 1998
- [16] L. H. Kauffman: Virtual Knot Theory, *Europ. J. Combinatorics* (1999) 20, 663–691, *Article No. eujc.1999.0314, Available online at* <http://www.idealibrary.com/math/9811028> [math.GT].



- [17] L. H. Kauffman: Introduction to virtual knot theory, *J. Knot Theory Ramifications* 21 (2012), no. 13, 1240007, 37 pp.
- [18] L. H. Kauffman: Knots and physics, Second Edition. *World Scientific Publishing* 1994.
- [19] L. H. Kauffman, I. M. Nikonov, and E. Ogasa: Khovanov-Lipshitz-Sarkar homotopy type for links in thickened higher genus surfaces *Journal of knot theory and its ramifications*, <https://doi.org/10.1142/S0218216521500528>, arXiv: 2007.09241[math.GT].
- [20] L. H. Kauffman, I. M. Nikonov, and E. Ogasa: Khovanov-Lipshitz-Sarkar homotopy type for links in thickened surfaces and those in  $S^3$  with new modulis, arXiv:2109.09245 [math.GT].
- [21] L. H. Kauffman and E. Ogasa: Quantum Invariants of Links and 3-Manifolds with Boundary defined via Virtual Links, arXiv:2108.13547[math.GT].
- [22] L. H. Kauffman, E. Ogasa, and J. Schneider A spinning construction for virtual 1-knots and 2-knots, and the fiberwise and welded equivalence of virtual 1-knots, arXiv:1808.03023.
- [23] M. Khovanov: A categorification of the Jones polynomial *Duke Math. J.* 101 (2000), no. 3, 359–426. MR 1740682 (2002j:57025).
- [24] R. Kirby: The topology of 4-manifolds *Lecture Notes in Math (Springer Verlag)* vol. 1374, 1989
- [25] P. B. Kronheimer and T. S. Mrowka: Khovanov homology is an unknot-detector *Publications mathématiques de l’IHÉS* 113 (2011) 97–208.
- [26] G. Kuperberg: What is a virtual link? *Algebr. Geom. Topol.* 3 (2003) 587-591.
- [27] R. Lipshitz, P. S. Ozsvath and D. P. Thurston: Bordered Heegaard Floer homology: Invariance and pairing, arXiv:0810.0687 [Math GT].
- [28] R. Lipshitz, P. S. Ozsvath and D. P. Thurston: Bordered Heegaard Floer homology, *Memoirs of the American Mathematical Society* (2018) Volume 254, Number 1216.
- [29] R. Lipshitz and S. Sarkar: A Khovanov stable homotopy type, *J. Amer. Math. Soc.* 27 (2014), no. 4, 983–1042. MR 3230817
- [30] R. Lipshitz and S. Sarkar: A refinement of Rasmussen’s s-invariant, *Duke Math. J.* 163 (2014), no. 5, 923–952. MR 3189434
- [31] R. Lipshitz and S. Sarkar: A Steenrod square on Khovanov homology, *J. Topol.* 7 (2014), no. 3, 817–848. MR 3252965
- [32] C. Manolescu, P. S. Ozsváth, Z. Szabó, and D. Thurston: On combinatorial link Floer homology, *Geom. Topol.*, 11 (2007) 2339–2412.
- [33] C. Manolescu, P. S. Ozsvath: On the Khovanov and knot Floer homologies of quasi-alternating links arXiv:0708.3249[math.GT]
- [34] V.O. Manturov, Bifurcations, atoms and knots, *Moscow Univ. Math. Bull.* 55 (2000), no. 1, 1–7
- [35] V.O. Manturov, On Invariants of Virtual Links, *Acta Applicandae Mathematicae*, Vol. 72, no. 3 (2002), pp. 295–309.
- [36] V.O. Manturov, Multivariable polynomial invariants for virtual knots and links, *Journal of Knot Theory and Its Ramifications*, Vol. 12 ,no. 8 (2003) pp. 1131-1144
- [37] V O Manturov: Khovanov homology for virtual links with arbitrary coefficients, *Journal of Knot Theory and Its Ramifications* 16 (2007), arXiv:math/0601152.
- [38] V. O. Manturov and I. M. Nikonov: Homotopical Khovanov homology *Journal of Knot Theory and Its Ramifications* 24 (2015) 1541003.
- [39] J. R. Munkres: Elements Of Algebraic Topology, *Westview Press* (1996).
- [40] I. M. Nikonov: Virtual index cocycles and invariants of virtual links, arXiv:2011.00248

- [41] P. S. Ozsváth and Z. Szabó: Heegaard Floer homology and alternating knots, *Geom. Topol.* 7 (2003) 225–254.
- [42] P. S. Ozsváth and Z. Szabó: Holomorphic disks and topological invariants for closed three-manifolds, *Ann. of Math.* (2), 159(3) (2004) 1027–1158.
- [43] P. S. Ozsváth and Z. Szabó: Holomorphic disks and three-manifold invariants: properties and applications, *Ann. of Math.* (2), 159(3) (2004) 1159–1245.
- [44] P. S. Ozsváth and Z. Szabó: Holomorphic disks and knot invariants. *Adv. Math.*, (2004) 186(1) 58–116.
- [45] P. S. Ozsváth and Z. Szabó: Holomorphic disks and genus bounds, *Geom. Topol.* Volume 8, Number 1 (2004), 311–334.
- [46] P. S. Ozsváth and Z. Szabó: Kauffman states, bordered algebras, and a bigraded knot invariant, arXiv:1603.06559v3 [math.GT].
- [47] P. S. Ozsváth, A. I. Stipsicz and Z. Szabó: Grid homology for knots and links, (*Mathematical Surveys and Monographs*) American mathematical society 2015.
- [48] J. Rasmussen: Floer homology and knot complements *PhD thesis, Harvard University*, 2003.
- [49] N. Reshetikhin and V. G. Turaev: Invariants of 3-manifolds via link polynomials and quantum groups, *Inventiones mathematicae* 103 (1991) 547–597.
- [50] W. Rushworth: Doubled Khovanov Homology, *Can. J. Math.* 70 (2018) 1130–1172.
- [51] N. E. Steenrod: Cohomology operations, and obstructions to extending continuous functions, *Advances in Math.* 8 (1972) 371–416.
- [52] N. E. Steenrod (Author) and D. B. A. Epstein (Editor): Cohomology Operations, *Annals of Mathematics Studies, Princeton University Press* (1962).
- [53] C. Seed: Computations of the Lipshitz-Sarkar Steenrod square on Khovanov homology, arXiv:1210.1882.
- [54] D. Tubbenhauer: Virtual Khovanov homology using cobordisms, *J. Knot Theory Ramifications* 23 (2014), no. 9, 1450046, 91 pp.
- [55] Viro: Khovanov homology of Signed diagrams 2006 (an unpublished note).
- [56] E. Witten: Quantum field theory and the Jones polynomial *Comm. Math. Phys.* 121 (1989) 351–399.

Louis H. Kauffman  
Department of Mathematics, Statistics and Computer Science  
University of Illinois at Chicago  
851 South Morgan Street  
Chicago, Illinois 60607-7045  
USA  
and  
Department of Mechanics and Mathematics  
Novosibirsk State University  
Novosibirsk  
Russia  
kauffman@uic.edu

Eiji Ogasa  
Meijigakuin University, Computer Science  
Yokohama, Kanagawa, 244-8539  
Japan  
pqr100pqr100@yahoo.co.jp  
ogasa@mail1.meijigakuin.ac.jp